Effects of compounds on

C. elegans DMD model health

Rebecca A Ellwood

BSc. (2016), MSc. (2017)

This thesis is submitted to the University of
Nottingham for the degree of Doctor of Philosophy

October 2021

Abstract

Duchenne muscular dystrophy (DMD) is an X-linked recessive disorder caused by mutations in the dystrophin gene. The dystrophin gene encodes a cytoskeletal protein with the same name that is responsible for ensuring the strength, stability, and functionality of myofibers. In DMD the dystrophin protein is either absent or there are insufficient levels of functional dystrophin resulting in progressive muscular damage and degeneration. This results in muscular weakness, motor delays, loss of ambulation, and a shortened life expectancy due to respiratory impairment and cardiomyopathy. Treatment options are limited and mainly focused on alleviating symptoms; they are not a cure. The main therapeutic treatment used are glucocorticoids, these can be used for a couple of years, but treatment is often ceased due to undesirable side effects. An emerging therapy is the use of exon-skipping but currently these can only be used for patients amenable to skipping of exons 45, 51, and 53 (approximately 30% of patients). There is therefore a great need for alternative therapies.

This thesis uses *C. elegans* as a model for DMD. We demonstrate throughout that the *C. elegans* DMD model has clinical relevance as it shares some of the underlying pathophysiology that are also displayed in patients, including mitochondrial dysfunction and calcium dysregulation. It also has several clinically relevant phenotypes that can be exploited including movement and strength decline and changes in gait. Finally, the current standard treatment used to treat patients with

DMD, prednisone, has also been identified as being beneficial in the DMD *C. elegans* model as well.

Hydrogen sulfide (H_2S) compounds were trialled as a potential treatment for DMD in this thesis. The rationale behind this was that H_2S compounds had been demonstrated previously to improve lifespan in ageing animals. There are some similarities between ageing and DMD muscle, the former being associated with sarcopenia and the latter with progressive muscle degeneration. It therefore seemed reasonable to expect an improvement in the DMD animals given there was one in ageing animals. In Chapter 3, we started by trialling a non-targeted H_2S compound sodium GYY4137 (NaGYY) and showed that this compound does improve movement, strength, and gait in the DMD model. The basis of this improvement was likely mitochondrial, and the mechanism of action was like that of prednisone.

In Chapter 4, to confirm the basis of this we then used a mitochondrially targeted H_2S compound, AP39, and demonstrated that this compound was also able to improve movement and strength in DMD animals. This provided further evidence to suggest that at least part of the mechanism of NaGYY was through improvements in mitochondrial dysfunction. We then further probed the mechanism of action of AP39 in the mitochondria and established that AP39 is likely donating electrons to complex III of the electron transport chain (ETC) and thus causing an increase in ATP content.

In Chapter 5, we show that there is a decline in the gene expression of enzymes responsible for sulfur metabolism that are resulting in a H_2S deficit. We also demonstrate that supplementing sulfur in a different way (via sulfur containing amino acids) is also beneficial in the *C. elegans* DMD model. This highlights a potential novel underlying pathophysiology of DMD in a defective sulfur metabolism pathway and the potential of using H_2S as a biomarker for disease progression.

To conclude we have shown that supplementing H_2S compounds and sulfur containing amino acids are potential treatments for DMD and potential alternatives to prednisone. We have also demonstrated that manipulation of the sulfur metabolism pathway warrants further study in DMD. Future work includes trialling these therapies in the DMD mouse model and beyond and identifying whether the defective sulfur metabolism pathway and H_2S deficit corresponds with higher organisms.

Publications

Ellwood, RA., Slade, L., Lewis, J., Torregrossa, R., Sudevan, S., Etheridge, T., Whiteman, M., Piasecki, M., Szewczyk, NJ. Sulfur amino acid supplementation improves *C. elegans* DMD animal health via correction of a sulfur metabolism defect. Invited resubmission to Communications Biology. (2022).

Sudevan, S., Muto, K., Higashitani, N., Hashizume, T., Higashibata, A., **Ellwood, RA**., Deane, CS., Rahman, M., Vanapalli, SA., Etheridge, T., Szewczyk, NJ., Higashitani, A. Loss of physical contact in space alters dopamine system in *C. elegans*. *iScience,* **25**, 1-12, (2022).

Hewitt, JE., Laranjeira, R., Norouzi, M., **Ellwood, RA**., Antebi, A., Szewczyk, NJ., Driscoll, M., Vanapalli, SA. Multi-environment phenotyping of *C. elegans* for robust evaluation of physical performance. Invited resubmission to PLOS ONE. (2021).

Ellwood, RA., Piasecki, M., Szewczyk, NJ. *Caenorhabditis elegans* as a Model System for Duchenne Muscular Dystrophy. *IJMS*, **22**, 1-19, (2021).

Ellwood, RA., Hewitt, JE., Torregrossa, R., Philp, AM., Hardee, JP., Hughes, S., van de Klashorst, D., Gharadaghi, N., Anupom, T., Slade,

L., Deane, CS., Cooke, M., Etheridge, T., Piasecki, M., Antebi, A., Lynch, GS., Philp, A., Vanapalli, SA., Whiteman, M., Szewczyk, NJ. Mitochondrial hydrogen sulfide supplementation improves health in the *C. elegans* Duchenne muscular dystrophy model. *PNAS*, **118**, 1-12, (2021).

Pollard, AK., Gaffney, CJ., Deane, CS., Balsamo, M., Cooke, M., **Ellwood, RA**., Hewitt, JE., Mierzwa, BE., Mariani, A., Vanapalli, SA., Etheridge, T., Szewczyk, NJ. Molecular Muscle Experiment: Hardware and Operational Lessons for Future Astrobiology Space Experiments. *Astrobiology*, **20**, 935-943, (2020).

Sudevan, S., Takiura, M., Kubota, Y., Higashitani, N., Cooke, M., **Ellwood, RA**., Etheridge, T., Szewczyk, NJ., Higashitani, A. Mitochondrial dysfunction causes Ca^{2+} overload and ECM degradation–mediated muscle damage in *C. elegans*. *FASEBJ,* **33**, 9540-9550 (2019).

Presentations

Papers

Gaffney, CJ., Torregrossa, R., Deane, CS., Whiteman, M., Etheridge, T., Nartallo, R., Neri, G., Zolesi, D., **<u>Ellwood, RA</u>**., Cooke, M., Gharadaghi, N., Piasecki, M., Phillips, B., Szewczyk, NJ. Commercial access for UK/ESA student experiments on board the ISS. 3rd Symposium on Space Education Activities, Leicester, UK. (2019).

Oral Presentations

<u>Ellwood, RA.</u>, Hewitt, JE., Etheridge, T., Piasecki, M., Vanapalli, SA., Whiteman, M., Szewczyk, NJ. Exogenous hydrogen sulfide improves mitochondrial dysfunction in a *C. elegans* DMD model. International Mitochondrial Medicine Conference. University of Cambridge, UK. (2019).

<u>Ellwood, RA.</u>, Hewitt, JE., Etheridge, T., Piasecki, M., Vanapalli, SA., Whiteman, M., Szewczyk, NJ. Exogenous hydrogen sulfide improves dystrophic muscle in a similar but distinct manner to Prednisone. UK Worm Conference. Imperial College London, UK. (2019).

Poster Presentations

<u>Ellwood, RA.</u>, Hewitt, JE., Torregrossa, R., Etheridge, T., Piasecki, M., Vanapalli, SA., Whiteman, M., Szewczyk, NJ. Exogenous hydrogen sulfide improves mitochondrial dysfunction in a *C. elegans* DMD model. European Worm Conference. Virtual Conference. (2020).

<u>Ellwood, RA.</u>, Hewitt, JE., Deane, CS., Etheridge, T., Piasecki, M., Vanapalli, SA., Whiteman, M., Szewczyk, NJ. Prednisone improves mitochondrial function but not excitation contraction coupling in *dys-1*. International Worm Conference. University of California, Los Angeles, USA. (2019).

Scientific Prizes

2019 Travel grant to attend International Mitochondrial Medicine Conference.

Other achievements

2019 Achieved the status of Associate Fellow of The Higher Education Academy

Acknowledgements

Declaration

The data in this thesis was collected and analysed by myself unless otherwise acknowledged below.

In Chapter 3 and 4 I had technical assistance from Dr Jennifer Hewitt for the strength and CeleST assays. The lifespan assays from Chapter 3 and 4 were completed by Mr Luke Slade and the EPG recordings were carried out by Dr Samantha Hughes lab. I also had technical assistance from Dr Nima Gharahdaghi for the western blot experiments in Chapter 4.

I declare that this thesis has been constructed by myself and that all the data presented are my own work unless otherwise stated. All published literature within this thesis has been appropriately referenced. None of the data presented in this thesis has been submitted towards the assessment of a higher degree previously.

Rebecca Ellwood

October 2021

List of abbreviations

αKG	alpha-ketoglutarate
Ach	acetylcholine
ADP	adenosine diphosphate
AHCY	s-adenosylhomocysteine hydrolase
ATP	adenosine triphosphate
AzMC	7-Azido-4-Methylcoumarin
BMD	Becker muscular dystrophy
BSA	bovine serum albumin
CAT	cysteine aminotransferase
cDMD	dystrophin deficient dogs
CDO	cysteine dioxygenase
C. elegans	Caenorhabditis elegans
CeleST	*C. elegans* swim test
CGC	Caenorhabditis Genetics Center
CO	carbon monoxide
CBS	cystathionine-β-synthase
CS	citrate synthase
CSE	cystathionine gamma-lyase
DGC	dystrophin glycoprotein complex

DMD	Duchenne muscular dystrophy
DMSO	dimethyl sulfoxide
DNA	deoxyribonucleic acid
ECG	electrocardiogram
E.coli	*Escherichia coli*
ECM	extracellular matrix
EGF	epidermal growth factor
EPG	electropharyngeogram
ETC	electron transport chain
FADH	flavin adenine dinucleotide
FDA	U.S. Food and Drug Administration
FOXO	forkhead box transcription factors
GFP	green fluorescent protein
GM	glutamate + malate
GRMD	golden retriever model of muscular dystrophy
GS	glutamate + succinate
GST	glutathione S-transferase
H_2S	hydrogen sulfide
HRP	horseradish peroxidase
IGF	insulin-like growth factor

MAPK	mitogen-activated protein kinase
MAPR	mitochondrial ATP production rate
METR	methionine synthase
mPTP	mitochondrial transition pore
NAC	N-acetyl cysteine
NADH/+	nicotinamide adenine dinucleotide
NaGYY	sodium GYY4137
NGM	nematode growth medium
NMJ	neuromuscular junction
nNOS	neuronal nitric oxide synthase
NO	nitric oxide
OCR	oxygen consumption rate
PalM	palmitoyl-l-cartinate + malate
PDMS	polydimethyl siloxane
PRMT	methyl transferase
PVDF	polyvinylidene difluoride
PyM	pyruvate + malate
RCF	relative centrifugal force
RMP	remethylation pathway
ROS	reactive oxygen species

RPM	rounds per minute
S	succinate
SAA	sulfur containing amino acids
SAH	S- adenosyl homocysteine
SAMS	S- adenosyl methionine
SAPK	stress-activated protein kinases
TALENs	transcription activator like effector nucleases
TBST	tris-buffered saline
TEM	transmission electron microscopy
TMP	transmethylation pathway
TSP	transsulfuration pathway
TPP	triphenylphosphonium
WT	wild type
Y2H	yeast two-hybrid
3-MST	3-mercaptopyruvate transferase
$\Delta\Psi m$	mitochondrial membrane potential

Table of contents

Chapter 1: Introduction

1.1 Summary of the dystrophin protein and Duchenne muscular dystrophy

1.1.1 The role of dystrophin in muscle

Dystrophin is an important protein found predominantly in muscle, but small amounts are also present in neuronal cells. It forms part of the dystrophin-glycoprotein complex (DGC) at the muscle sarcolemma where it connects the cytoskeleton to the extracellular matrix (ECM). The dystrophin protein is vital for maintaining muscle integrity and also has signalling roles, but the precise function still remains unknown [1]. In humans the dystrophin protein in encoded by the dystrophin gene, which is the largest known human gene, containing 79 exons and spans approximately 2200 kb [2]. The dystrophin gene has a high mutation rate, and these mutations result in muscular dystrophies, specifically Duchenne muscular dystrophy (DMD) and the less severe form Becker muscular dystrophy (BMD). DMD is usually caused by frameshift or nonsense mutations whereas BMD is caused by missense or in-frame mutations. [3].

DMD is generally thought to be an X-linked recessive genetic disorder, meaning affected males usually inherit the faulty gene from their "carrier" mother. However, ~30% of cases are not inherited and are caused by spontaneous or *de novo* mutations. The most common type of mutation are large deletions of one or more exons (~70%), large duplications (~7%) and other mutations including point mutations (~20%). These usually occur in so called hot spots in the gene, for

example exons 44-55 are hotspots for deletions [3]. In DMD, these mutations alter the structure and/or function of dystrophin or prevent any functional dystrophin from being produced.

The primary known function of dystrophin is to stabilise the plasma membrane through its connection with the DGC. In the absence of dystrophin, the DGC becomes destabilised which leads to progressive fibre damage and membrane leakage [1]. Eccentric contractions induce stress on the sarcolemma which can provoke microlesions in the fibre membrane [4]. These tears inevitably result in a high influx of extracellular calcium, which dysregulates calcium homeostasis in the muscle [5]. There is also an increase in inter-mitochondrial calcium levels which causes prolonged opening of the mitochondrial transition pore (mPTP). This can cause the mitochondria to swell and cell death occurs [6]–[8]. Other changes in DMD include altered regeneration, inflammation, apoptosis, vascular adaptation, and fibrosis [6].

1.1.2 DMD: symptoms, diagnosis, and management

DMD is the most common of the muscular dystrophies, affecting 1 in 3500 live male births [9]. It usually presents between the age of 3-5 with delayed motor milestones including setbacks in walking independently and standing up. Proximal weakness causes a waddling gait and difficulty climbing stairs. Children are usually wheelchair dependent by age 12 years and cardiomyopathy occurs in most individuals with DMD after age 18 years. Respiratory complications and progressive

cardiomyopathy results in premature death by their late twenties or early thirties [10].

The management of DMD can be quite complex and it was not until 2010 that a consensus document was published [11]. A multidisciplinary approach is required in the management of DMD, requiring input from neuromuscular, endocrine, gastrointestinal, respiratory, and cardiac teams, to name but a few. It is also necessary to monitor disease progression and potential complications when it comes to thinking about managing the disease. Common management will include physical therapy, occupational therapy, assistive devices, and surgery when needed. Pharmacological therapies are also often given, the main one being corticosteroids.

The most prescribed corticosteroid is prednisone, although deflazacort is also used in some countries. Steroids have been shown to improve muscle function and strength in several studies, however the best dosage and frequency of use has not been fully determined [12]. Long-term corticosteroid treatment (> 3 years) has been demonstrated to extend the time to loss of ambulation and to increase life expectancy (in children up to 11 years of age) [13]. However, prolonged use is associated with side effects such as weight gain, osteoporosis, high blood pressure, and behaviour changes. In some patients, prolonged use has led to muscle weakness and atrophy, going against the intended benefits of the treatment [14]. Given that corticosteroids are not a cure for the disease and are associated with many undesirable side effects, there

is a big push in research to find a cure and/or to identify alternate therapies to corticosteroids.

1.1.3 DMD: current research projects

Current research is focused on complementary therapies that could either replace dystrophin, protect the muscle from injury, and/or promote muscle repair and regrowth [15]. There is an increased interest in exon-skipping therapies, to make the disease more closely resemble BMD than DMD. In exon skipping, small pieces of DNA called antisense oligonucleotides or 'molecular patches' are used to skip over the exon, which allows the rest of the dystrophin gene to be read. The result is a slightly smaller but functional dystrophin protein [16]. Eteplirsen (Exondys 51) was the first antisense oligonucleotide-based therapy that has received accelerated approval from the U.S. Food and Drug Administration (FDA), it is injected intravenously. This could be used in ~13% of patients who have a mutation in the dystrophin gene that is amenable to exon 51 skipping [17]. In clinical trials, eteplirsen-treated patients showed an increase in exon-skipping and increased levels in dystrophin protein compared to baseline. This corresponded with an attenuation of decline on the 6-minute walk test and significant attenuation of percent predicted forced vital capacity annual decline [18]. Due to the success of eteplirsen, two other exon-skipping therapies have received FDA approval: Vyondys 53 (golodirsen) [19] and Amondys 45 (casimersen) [20]. The former is for patients amenable to exon 53 skipping and the latter for exon 45 skipping. In total this equates to around 30%

of patients who may be eligible for exon skipping therapies. The full effect of these treatments in the long-term is still to be determined as they are only being trialled for 6-48 months and rely on the patient being mobile.

Another molecular-based therapy that is being trialled is for DMD patients who have nonsense mutations (~13% of reported cases). The aim of this therapy is to read through premature stop codons [21]. There are two main compounds that have been tested: gentamicin and atalyuren. Despite promising results in the *mdx* mouse model [22], gentamicin failed to hold up in clinical trials [23]. Ataluren has also shown early promise in the *mdx* mouse model [24] and has shown some potential in early clinical trials [25]. Other research has been focused on gene therapy, where the aim of this treatment is to deliver a replacement copy of the dystrophin gene into the patient. However, the current clinical trials, which have used an adeno-associated virus-based delivery method, have been somewhat disappointing with therapies failing to exert notable benefits in clinical trials despite promising results in animal models [26]. This work continues to be ongoing with several new treatments entering into clinical trials.

To summarise, DMD is a very complex disease resulting from mutations in the dystrophin gene. Despite huge advances in the field a cure remains elusive and the precise mechanisms underpinning the disease are still not fully understood. There is a great deal of ongoing research looking into new treatments for the disease and hopefully eventually a cure. A lot of this work would not be possible without the use of animal models which will be discussed in the next section.

1.2 Overview of animal models for researching Duchenne muscular dystrophy

Numerous animal models have been developed for studying DMD, ranging from invertebrate models to large mammalian models. There are over 60 different animal models for studying DMD and some of the key ones will be covered briefly and summarised in Table 1.1.

The most used animal model for DMD research is the *mdx* mouse. This model was identified in the 1980s due to it showing elevated creatine kinase levels (a marker of muscle damage) [27]. A nonsense mutation in exon 23 prevents full length dystrophin from being transcribed [28]. It is a good biochemical model but fails to show any obvious clinical signs of DMD until the mice are much older. To improve the mouse model, sensitising backgrounds have been introduced to manifest clinical symptoms such as muscle wasting. However, how these additional mutations influence data interpretation remain unclear [29].

Dystrophin deficient dogs (cDMD) display a more severe phenotype than the *mdx* mouse and are regarded as the nearest pathological counterpart of DMD in humans. cDMD animals show similar clinical progression to DMD patients. They show muscle weakness and exercise intolerance early in life and have a shortened life span [29]. Dystrophin deficiency has been seen in ~20 different dog breeds but the most common breed used is the golden retriever (GRMD) [30]. Unsurprisingly, there are many ethical concerns when it comes to using

large mammals such as canines, hence why the mouse model is more favourable.

Other mammalian models that are available but not as commonly used are rabbits, rats, pigs, and felines. The rabbit model has a mutation in exon 51 induced by CRISPR-Cas9. Many of the dystrophic rabbits die early but those that do survive long enough do show reduced mobility and pathological histology [31]. Rat models are available with mutations in exon 23, 3, or 16, induced by TALENs or CRISPR [32],[33]. These rat models have some similar phenotypes showing reduced activity levels and strength. The pig model has a deletion in exon 52 and shows muscle weakness and reduced mobility [34]. The feline model is not often used as the animals get hypertrophy of the tongue which means they struggle to eat and drink. They do, however show muscle fibre necrosis and have signs of cardiomyopathy [35].

Invertebrate models have also been utilised in the study of DMD, these models can be very insightful and often used due to the lack of animal welfare concerns. One animal that has been widely used is the zebrafish. These animals have a high skeletal muscle content and express orthologues for most of the members of the human DGC [36]. The DMD model of the zebrafish is referred to as the *sapje* mutant, these animals resemble the human condition in severity and progression [37]. *Drosophila melanogaster* (the fruit fly) [38],[39] have also been used to study DMD, they show muscle degeneration and reduced motility when dystrophin is mutated. The final model that will be explored and extensively reviewed here is the *Caenorhabditis elegans* DMD model.

Table 1.1. Comparison of the most used animal models in the study of DMD.

Model Type	Benefits	Similarities to DMD in Humans	Limitations
Mdx mouse	One of the easier mammalian models to house and care for with a relatively short lifespan. High genetic similarity to humans including a DGC [28].	Genetic and biochemical homologue of disease in humans. Displays ECG abnormalities and cardiomyopathy [40].	Minimal clinical symptoms (no loss of ambulation and muscle weakness is not displayed until ~15 months) and lifespan is not majorly reduced [29].
Dystrophin deficient dogs	Higher genetic similarity to humans compared to other mammalian models. Case reports showing that DMD occurs naturally in these animals as well.	Extensive homology in pathogenesis. Pathogenesis manifests *in utero* and extensive muscle necrosis can be seen and is progressive. They also have a shortened life span frequently dying from cardiac and respiratory failure [41].	Expensive to maintain, not easily genetically manipulable and many ethical concerns.
Dystrophin deficient rabbits	Good genetic, physiological, and anatomical similarity to humans, and relatively short gestational period.	Reduced survival and mobility [31].	Not well studied as a model for DMD and no therapies have been tested.
Dystrophin deficient rats	A convenient size as they are larger than mice allowing for studies with high statistical power but still relatively easy to house and care for. High genetic similarity including a DGC [32].	Muscles showed severe fibrosis, muscle weakness and reduced activity [32],[33].	Not a well-established model and characterisation is still ongoing.
Dystrophin deficient pigs	Good genetic, physiological, and anatomical similarity to humans.	Muscle weakness and reduced mobility. Have a shortened lifespan [34].	Very early mortality prevents breeding and further study, long gestational period, expensive to maintain and house.
Dystrophin deficient felines	Felines experience many diseases in a similar way to humans.	Display hypertrophy and cardiomyopathy [35].	Large, sentient and emotive animals with limited pathological similarities to DMD.
Zebrafish	Easy to house and care for, high throughput experiments possible. High skeletal muscle content and expresses orthologues of most human DGC proteins [42].	Changes in gait and lower activity [36].	Missing several mammalian organs, are ectothermic and are influenced heavily by their environment.
Drosophila melanogaster (fruit fly)	Has potential to be used for forward genetic screening	Display muscle and neuronal defects and	Anatomy is very different to humans and respond

	and high-throughput screening methods.	reduced mobility [38],[39].	differently to drug therapies.
C. elegans	Easy and cheap to maintain, short lifespan, high throughput experiments possible. Similar muscle structure and has orthologues for most human DGC proteins [43].	Display movement and strength decline [44], altered gait [45] and shortened lifespan [46].	Have a very simple body plan and non-conventional circulatory system [47]. Are unable to regenerate muscle as they lack satellite cells and do not have a conventional inflammatory system [48].

1.3 *Caenorhabditis elegans* as a model organism

1.3.1 Advantages of using *C. elegans*

C. elegans has proved itself useful for the study of several human diseases including DMD [49]. *C. elegans* have a relatively short life span (~2/3 weeks) and can be maintained easily and cheaply on agar plates with an *E. coli* bacterial lawn. The nematodes are either males or hermaphrodites. The hermaphrodites can breed with the males, but they are also self-fertilising, meaning populations are very easy to maintain and in large numbers as each hermaphrodite can produce ~100 eggs per day. *C. elegans* have a fully sequenced genome and contain a similar number of genes as humans [50]. Many of these genes have functional counterparts in humans which makes them particularly useful for modelling human diseases.

1.3.2 Cellular composition of *C. elegans*

C. elegans have a simple body plan which consists of 1000 somatic cells. They have a cylindrical body shape which is made up of two concentric tubes separated by the pseudocoelomic space. The outer tube (body wall) is covered by the extracellular cuticle, which is produced by the underlying hypodermis. This outer tube also consists of the excretory system, nervous system, and muscles. The main features of the inner tube are the muscular pharynx and the intestine. In adult worms, the gonad is also found in the inner tube [51].

C. elegans has a similar muscle structure and contractile apparatus as human skeletal muscle. They have 95 striated muscles and

50 non-striated muscles. The basic functional unit of both *C. elegans* and human striated/skeletal muscle is the sarcomere. The sarcomere is composed of myosin, the thick filaments associated with an M line, and actin, the thin filaments associated with a Z-disk (dense body in *C. elegans*). The myosin binds to actin and ATP, and the pulling of the actin filaments generates a force which is then transduced outside the muscle cell to allow for movement. The M-lines and dense bodies attach the sarcomere to the muscle membrane and fibrous organelles link the muscles to the exoskeleton of the animal, which allows movement of the whole animal [48]. *C. elegans* have several human orthologues for muscle proteins which will be discussed in greater detail later.

The nematode mitochondria are very similar to mammalian, implying mitochondria have a conserved function across organisms [52]. The nuclear encoded mitochondrial genes are also highly conserved but the mitochondrial DNA is smaller than its human counterpart and has a different gene organisation and transcriptional pattern [53]. The *C. elegans* model has been crucial in increasing our understanding of mitochondrial function.

1.3.3 Limitations of using *C. elegans*

Like any model, *C. elegans* is not perfect and it does have some limitations that make it a less-than-ideal model for studying human diseases. Firstly, *C. elegans* have a simple body plan, and lack many defined organs/tissues including a brain, blood, defined fat cells, and internal organs. They are evolutionarily distant from humans and despite

many genes in the nematode having human orthologues there are also many that have no homologues. In addition, although they have similar protein networks to humans, the exact nature of the interactions are different due to the varying levels of homology between genes [54]. Biochemistry is quite difficult to do in worms due to their small size, therefore large numbers are usually required for analysis and the animals will likely be at mixed ages. There are issues in studying muscle disorders in *C. elegans* as well. *C. elegans* muscles lack satellite cells and therefore are unable to regenerate and repair muscles as in humans. However, this is also a useful characteristic for research as it allows for obvious identification of muscle damage and it is possible to track the entire degeneration process in the muscle [48]. They also lack a conventional inflammatory system.

1.4 *C. elegans* as a model for DMD

1.4.1 Dystrophin and the dystrophin glycoprotein complex

In *C. elegans* the homologue for mammalian dystrophin is *dys-1*, which encodes for a dystrophin-like protein called DYS-1. In *C. elegans* there are two known isoforms of DYS-1: DYS-1A and DYS-1B. Whilst DYS-1A is almost analogous to human dystrophin, DYS-1B only corresponds to the last 237 amino acids of isoform A [48]. DYS-1 has been shown to be expressed in the body wall, head, pharyngeal, and vulva muscles [55].

The structure of human dystrophin and *C. elegans* share extensive sequence similarities (Figure 1.1). Introducing mutations into *C. elegans* *dys-1*, gives clinically relevant phenotypes (Table 1.2). The main models used are *dys-1(cx18), dys-1(cx18;hlh-1)* and *dys-1(eg33)*, the position of
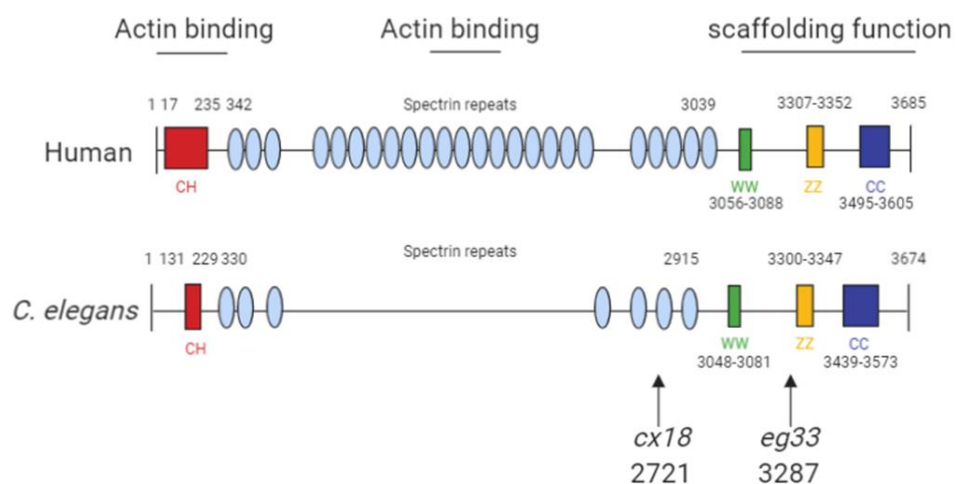
Figure 1.1. Structure of human and C. elegans dystrophin proteins.

The structures of human dystrophin and *C. elegans* DYS-1. The size of human and *C. elegans* dystrophin is almost equivalent. They also share similarities in key motifs: CC, coiled coil domain; CH, calponin homology domain ("actin-binding" domain); WW, domain with two conserved W residue; ZZ, zinc finger domain. The arrows indicate the amino acid positions of the mutation sites for the commonly used mutants: *cx18* and *eg33* alleles, which are both nonsense mutations. Adapted from Oh and Kim (2013) [46] and Gieseler et al. (2017) [48]. Created with biorender.com.

these mutations can be seen in Figure 1.1. To further support the usefulness of this model, the introduction of human dystrophin cDNA is able to rescue these phenotypes [46].

One of the roles of dystrophin is to link the cytoskeleton, the sarcolemma, and the ECM by binding cortical F-actin via its N-terminus and DGC proteins via its C-terminus. The DGC is a monomeric complex that is composed of at least 10 different proteins including dystroglycans, sarcoglycans, sarcospan, dystrobrevins and syntrophin (reviewed by Blake *et al.* 2015 [1]). There is significant evidence of conserved homologues for the other components of the DGC in *C. elegans,* further
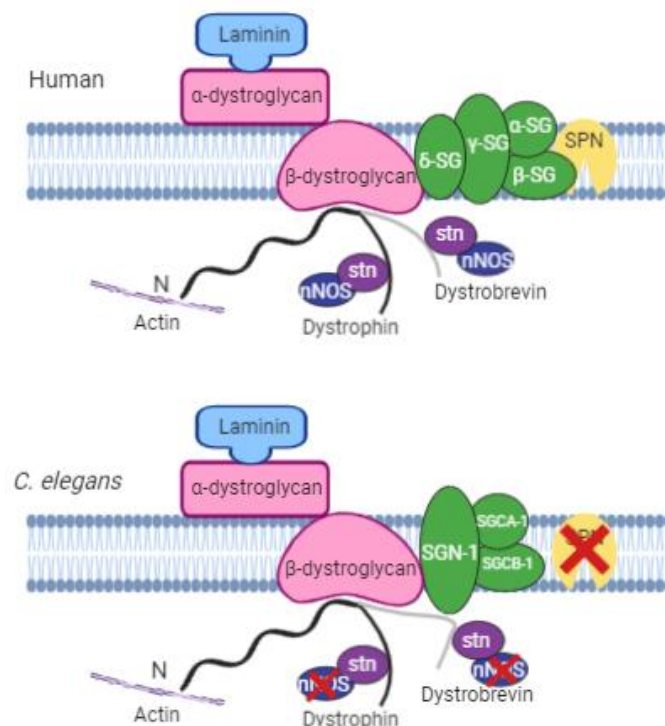
Figure 1.2. Basic structure of human and C. elegans dystrophin glycoprotein complex.

Most of the proteins in the mammalian model are found in *C. elegans* apart from sarcospan (SPN) and nitric oxide synthase (nNOS). SG, sarcoglycans, stn, syntrophin. Adapted from Grisoni et al. (2002) [43]. Created with biorender.com.

highlighting the usefulness of *C. elegans* in the study of DMD (Figure 1.2).

Despite the proven usefulness of the *C. elegans model*, it is not without its limitations as discussed earlier. Although it is acknowledged that there are some limitations to using *C. elegans* as a model for DMD, this model has been extensively utilised and has provided us with useful insights into this complex disease. As there has not been a dedicated review in almost two decades [56],[57] there is a need to reconcile the literature and collate the key findings associated with this model.

1.4.2 Phenotypes observed in *C. elegans* DMD mutants
1.4.2.1 The dys-1 single mutant

The dystrophin homologue in *C. elegans*, *dys-1*, was identified over 20 years ago. Loss-of-function mutations of the *dys-1* gene (*dys-1(cx18/cx26/cx35/cx40/ad538))* gave animals with a distinct phenotype. This consisted of hyperactive locomotion, an "overbent" phenotype when they bend the anterior part of their body and their head more than wild-type (WT), and a tendency to hyper contract when moving backwards [55]. *dys-1(cx18)* have been shown to have decreased swim frequency, speed, and power, as well as increased curvature [58]. They are also defective in burrowing and have a short life span compared to WT animals [46],[59],[60]. Additionally, the *dys-1* mutants were found to be hypersensitive to acetylcholine (Ach) and to the acetylcholinesterase inhibitor aldicarb, suggesting that *dys-1* mutations affect cholinergic transmission [55]. They were also found to be resistant to levamisole [44].

Interestingly, these mutants appeared to have normal muscle cells. Moving forwards the worm mutant *dys-1(cx18)* which has a nonsense mutation at amino acid 2721 (Figure 1.1) was predominantly used as its phenotypes could not be distinguished from carboxy-terminal deletions of the gene [55].

1.4.2.2 Enhancing the phenotype of dys-1 mutants

In patients with DMD, severe muscle degeneration is a well-recognised phenotype. As mutations in *dys-1* did not result in muscle degeneration as would be expected, it was hypothesised that this was due to the short lifespan of the animals as this phenotype can take a long time to become present in mammals [55]. The *mdx* mouse model, akin to the *dys-1* single mutant, has a mild phenotype and thus is not the best model for human DMD. To improve the mouse model, double knockout mice were generated lacking dystrophin and MyoD which display severe muscle degeneration [61], and so it was thought combining a mutation in *hlh-1* (*C. elegans* homologue of MyoD) with *dys-1* would give a time dependent muscle degeneration that was lacking in the original single mutant. This led to the generation of *dys-1(cx18);hlh-1(cc561ts)* mutant [62]. This double mutant shared similar phenotypes to its predecessor but in addition it had severe muscle degeneration and an egg laying defect [62]. Additionally, they also have an exaggerated head-bending phenotype, a slower swim speed, increased curvature [63] and, mitochondrial fragmentation is also seen [64]. This double mutant has been used widely; however, the lack of understanding of the mechanism

of these enhanced muscular degeneration effects may impact upon its translational importance.

1.4.2.3 Novel mutation in dys-1

More recently a newer mutation has been discovered which has a nonsense mutation at position 3287 ((*dys-1(eg33)*)). It is apparent that this model may be the most clinically relevant currently, as unlike prior models carrying mutations in *dys-1*, this mutant does show muscle degeneration without the need for a sensitised background [46]. Furthermore, it has been shown to have similar locomotory defects to the previous two models but with increased severity. It has also been shown to be burrowing deficient, resistant to levamisole, and have altered swimming parameters similar to those of ageing worms [44],[59],[60],[65]. To support that *dys-1(eg33)* is a more clinically relevant model, a recent study compared *dys-1(eg33)* and *dys-1(cx18)* [44]. *dys-1(eg33)* was found to be weaker, to exhibit a more severe decline in locomotion, and have severe mitochondrial fragmentation compared to *dys-1(cx18)* and WT animals. However, unlike *dys-1(cx18)* it also has an elevated basal oxygen consumption rate (OCR) and has no spare respiratory capacity [44]. Table 1.2 shows all the known phenotypes associated with each of the models discussed.

Table 1.2 Known phenotypes associated with the most common dys-1 models.

Class of phenotype	dys-1(cx18)	dys-1(cx18;hlh-1)	dys-1(eg33)
Locomotion	Exaggerated body bends, hyperactive, hypercontracted, overbent, swimming defective and burrowing defective [44],[55],[58]–[60].	Exaggerated body bends, hyperactive, hypercontracted, overbent and swimming defective [62],[63].	Exaggerated body bends, hyperactive, hypercontracted, overbent, swimming defective and burrowing defective [44],[59],[60].
Muscle structure	Very little muscle degeneration [55].	Severe muscle degeneration [62].	Severe muscle degeneration [46].
Response to neuromuscular agents	Aldicarb hypersensitive, levamisole resistant [44],[55].	NT.	Levamisole resistant [44].
Mitochondria structure and function	Minor fragmentation of the mitochondria network, moderate depolarisation of mitochondrial membrane, no change in basal oxygen consumption rate [44].	Severe fragmentation of the mitochondria network [64].	Severe fragmentation of the mitochondria network, severe depolarisation of the mitochondrial membrane, elevated basal oxygen consumption rate [44].
Life span	Shortened life span [46],[66].	NT.	Shortened life span [46],[66].
Egg laying	No defect noted [55].	Egg laying defect [62].	NT.
Strength	Not detectably weaker than WT [44].	NT.	Significant weakness detected compared to WT [44].

1.4.3 Effects of *dys-1* on gene expression

The first gene expression profiling study was conducted by Towers *et al. (*2006) [67] on *dys-1(cx18)* and *dys-1(cx35)* compared to WT using DNA microarray technology. Gene expression profiling identified 44 upregulated and 71 downregulated probe sets. Of these genes, only 10 had human orthologues but the categories of regulated genes were akin to those from DMD patients. The most prominent of upregulated

genes was "cell surface and extracellular matrix", and collagen genes especially were highly upregulated. This is consistent with patients, as damaged muscle cells are gradually replaced by collagen-rich, fibrous tissue [67],[68]. For downregulated genes it was "intracellular signalling and cell-cell communication" (particularly neuropeptide-like proteins), this is inconsistent with human muscle biopsies where "energy metabolism and mitochondria function" was the largest represented group [67]. This discrepancy may be explained by the fact that in humans, muscles go through a cycle of degeneration and regeneration which requires energy. As *C. elegans* lack satellite cells they're unable to regenerate muscle [69]. Other groups that were similar in *C. elegans* and in patients were the upregulation of the immune response, downregulation of development and growth genes, and the downregulation of muscle proteins (particularly UNC-89 in *C. elegans*) [67].

More recently Hrach *et al.* (2020) [66] have looked at transcriptome changes in *dys-1(eg33)* and *dys-1(cx18)*, specifically from the body wall muscles and at different stages of disease progression. The gene expression patterns from these two strains had distinct differences and *dys-1(eg33)* showed aberrant splicing events (*dys-1(cx18)* was not tested). In their pre symptomatic group (embryo to L2), they identified enrichment in genes associated with locomotion and larval development which is consistent with the locomotion defects that are detected in later life. There was also an abundance of genes involved in mitochondrial function, implying mitochondrial dysfunction occurs in early stages of

disease. At later stages, the most abundant group of genes identified were related to myofibrillar assembly [66].

1.4.4 Physical protein interactions with DYS-1
1.4.4.1 DGC associated proteins

The dystrophin protein plays a structural role as part of the DGC and as discussed earlier many of the components of the mammalian DGC have been identified in *C. elegans* (Figure 1.2). The nature of the interactions between DYS-1 and other relevant proteins will be discussed further in this section.

Following the initial finding of DYS-1 in 1998 a handful of other proteins have been found to interact directly or indirectly with it. DYS-1 was found to interact directly with dystrobrevin (DYB-1) and syntrophins (STN-1 and -2), using the GST fusion protein technique and coimmunoprecipitation, providing the first evidence that a DGC may exist in *C. elegans* [43],[54],[70]. Orthologues were also found for other DGC members including, δ/γ-sarcoglycan (SGN-1), α- and β-sarcoglycans (SGCA-1 and SGCB-1), and dystroglycan (DGN-1), although the nature of these interactions is currently unknown [43]. There is some controversy regarding DGN-1, initially it was thought to associate with DYS-1 based of its homology with its human counterpart [43]. However, a subsequent study showed that it was found in the neurones and not the muscle, and that it functioned independently of DYS-1, implying that the initial proposed DGC structure shown in Figure 1.2 was incorrect [71]. More recent transcriptome studies have repeatedly identified *dgn-1* in their *C.*

elegans muscle transcriptome, suggesting that there could be small amounts of DGN-1 in *C. elegans* muscle after all [40],[66],[72]. Other proteins found to interact directly with DYS-1 via yeast two hybrid (Y2H) assay include the G protein GPA-13 [73], the cytoskeletal protein CTN-1 [74], and the dense body protein DEB-1 (vinculin) [75],[76].

Further proteins have been shown to have indirect relationships with DYS-1 by connecting with proteins that have direct associations with DYS-1. For example, STN-1 has been found to associate with DYB-1 as well as DYS-1, and also SNF-6 which encodes an acetylcholine/choline transporter [77]. STN-2 acts as a linker molecule to associate DYS-1 and SAX-7 (a homologue of the L1 family of cell adhesion molecules) to ensure the maintenance of neural integrity [78]. CTN-1 also associates with DYB-1, this interaction is important for localisation at the dense body [74]. This demonstrates that dystrophin has an important structural role in the DGC and likely a number of other roles due to its extensive interactions with other proteins, this will be discussed further.

1.4.4.2 Dense body signalling proteins

In vertebrates, dystrophin is localised at costameres (consisting of the focal adhesion complex, the DGC, and a spectrin-based filament network), at the sarcolemma and at the neuromuscular junction (NMJ). Costameres link the sarcomeres to the sarcolemma through an interaction with Z-disks [1]. In *C. elegans* dense bodies are the functional equivalent of Z-disks and costameres. As previously mentioned, DYS-1

interacts with DEB-1 (vinculin), and is localised at the base of the dense bodies [76]. The ZYX-1 zyxin protein is localised at and interacts with DEB-1, as does ATN-1 (α-actin). ZYX-1 and ATN-1 also have a direct interaction and it has been shown that the localisation of ZYX-1 at the dense bodies is ATN-1 dependent [75]. ZYX-1 also interacts with DYC-1 (a CAPON related protein) resulting in the localisation of DYC-1 to the dense bodies as well [79]. This can be seen in Figure 1.4.

1.4.4.3 Calcium homeostasis associated proteins

Another important group of proteins that have an indirect association with DYS-1 are those that have a role in controlling and maintaining calcium homeostasis. Dysregulation of calcium homeostasis is commonly seen in DMD models including *C. elegans* [80],[81]. SLO-1 is a large conductance potassium channel activated by intracellular calcium and voltage fluctuations. It is present in both neurones, where is helps to regulate neurotransmitter release, and in muscles where it is localised at both the M-line and the dense bodies, close to the L-type calcium channel EGL-19. SLO-1 has been found to be mis localised in *dys-1* mutants, its localisation is thought also to depend on CTN-1 [82]–[84]. ISLO-1 is a DGC interacting gene, it acts as an adapter molecule and physically interacts with SLO-1 and STN-1, connecting it to the DGC. SLO-1 channels are stimulated by calcium entry and are often localised to calcium rich areas. The corresponding mediated potassium efflux is thought to attenuate calcium-dependent activation of muscle and prevent hyper-excitation and hyper-contraction of muscle in response to large

calcium increases, thus involving DYS-1 and the DGC in the control of calcium homeostasis [83]. The nature of these interactions are displayed in Figure 1.3 and 1.4.

1.4.5 Genetic interactions with *dys-1*

The dystrophin gene was first identified in *C. elegans* using a forward genetics approach [55]. Humans have three dystrophin genes (dystrophin, utrophin, DRP2) whereas *C. elegans* only have one. *dys-1* was mapped to the right arm of chromosome I and is made of 46 exons spanning 13 kb. A list of phenotypes associated with these early mutants can be found in Table 1.2. To test whether the *dys-1* gene was functionally like human dystrophin, *dys-1* mutants were given a transgene carrying the putative regulatory regions of the *dys-1* gene fused to the open reading frame of
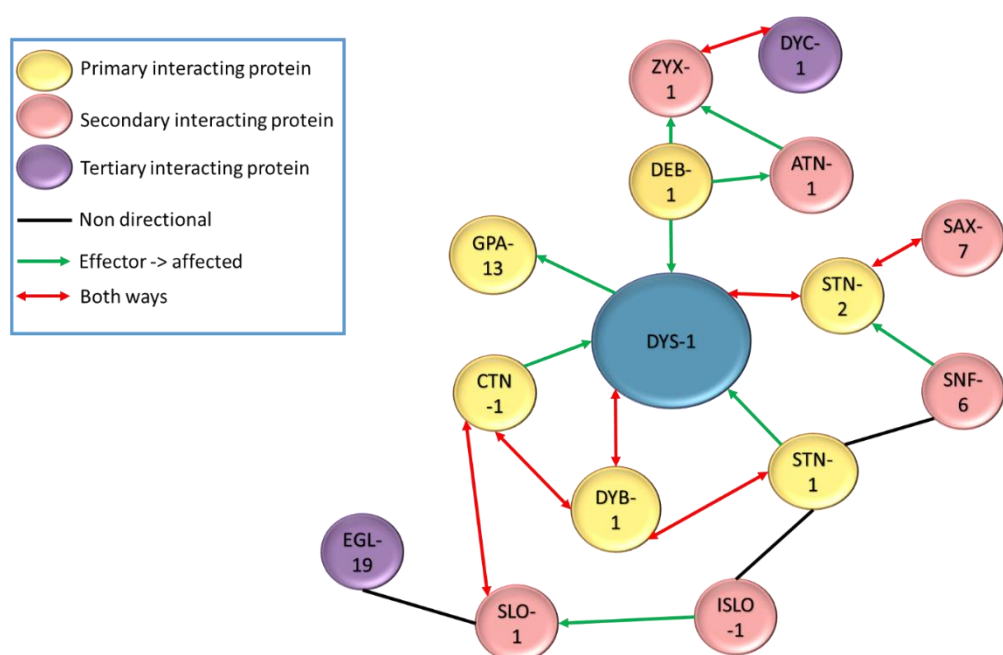
Figure 1.3. Nature of direct and indirect physical interactions with DYS-1.
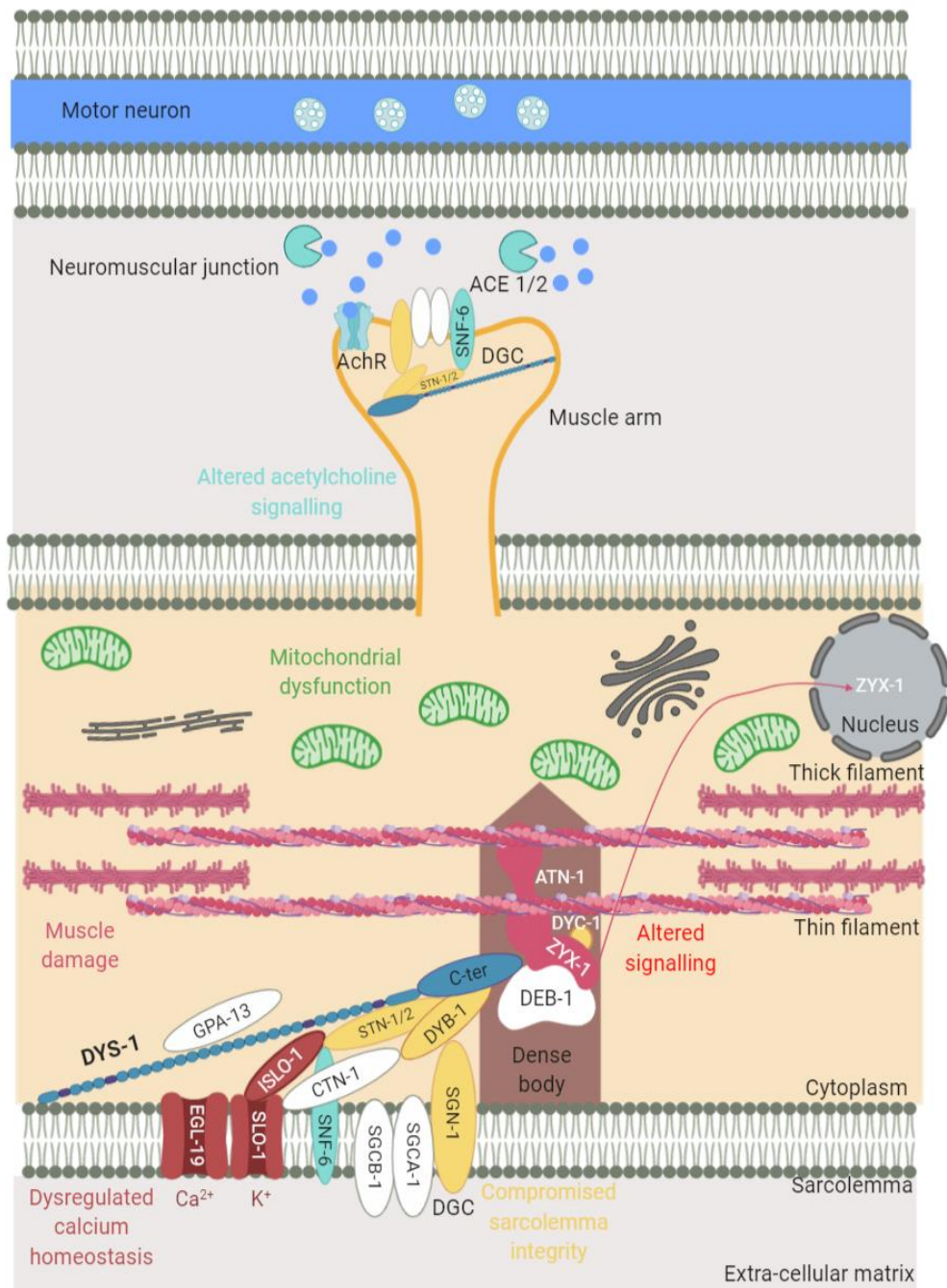
Figure 1.4. The effect of the loss of dystrophin on various processes in the mutants.

Schematic of part of a muscle cell including a dense body anchored to the sarcolemma and actin/myosin filaments. The muscle arm is in close contact with a motor neuron and shows elements of the NMJ (acetylcholine (ACe), acetylcholinesterase (AchE), acetylcholine receptor (AchR)). DYS-1 has many key roles in muscle function as does the DGC that can be seen in the middle. Proteins in yellow represent those that are important for maintaining sarcolemma integrity, those in pink are muscle related, those in red are calcium related and those in blue are acetylcholine signalling related. Processes associated with loss of dystrophin can also be seen. Adapted from Gieseler et al. (2017) [48]. Created with biorender.com.

the human dystrophin gene and this partially rescued the hyperactivity phenotype of the mutant animals [55]. Over the following years, several genes were shown to participate in the same biological function as *dys-1*, had altered activity due to *dys-1* deficiency or could be modified to compensate for the absence of *dys-1* (Table 1.3 and Figure 1.4).

Table 1.3. Genes known to have a genetic interaction with dys-1.

Gene classification	Associated genes
Dystrophin Like	*dyb-1, dyc-1, islo-1, snf-6, slo-1, sgn-1, stn-1/2*
Muscle related	*atn-1, lev-11, pat-10, unc-22, unc-89, unc-96, zyx-1*
Calcium	*clp-1, cmd-1, csq-1, egl-19, islo-1, itr-1, sca-1, slo-1, stn-1, unc-2, unc-36, unc-68*
Acetylcholine signalling	*ace-1, ace-2, snf-6, unc-13, unc-29, unc-38*
Mitochondria	*ced-1, ced-3, cps-6, crn-2, cyc-2.1, cyn-1, drp-1, eat-3, fzo-1, itr-1, psr-1, wah-1*
Other signalling	*daf-2, daf-16, gst-4, let-60*
Other	*cah-4, chn-1, gdi-1, hlh-1*

Colours used in table corresponds with site of action in Figures 1.4 and 1.5.

1.4.5.1 Dystrophin like genes

A handful of genes when mutated in *C. elegans* give phenotypes like *dys-1* mutants, (hyperactivity, head bending, and a tendency to hyper contract), suggesting they may participate in the same biological function as *dys-1*. These genes encode for proteins that are also members of the

DGC or interact with the DGC, highlighting the importance of maintaining the integrity of the DGC. These include *dyb-1* (dystrobrevin) [85], *dyc-1* (capon) [62], *stn-1/2* (syntrophins) [86], *sgn-1* (sarcoglycan) [43], *snf-6* (an Ach transporter) [77], *slo-1* (a potassium channel) [82], and *islo-1* (interactor of *slo-1*) [83] (Figure 1.2 and 1.4).

dyb-1 mutants have a similar phenotype to *dys-1* mutants in that they are hyperactive, have overbent heads, are sensitive to aldicarb, and tend to hyper contract during backwards movements. *dys-1(cx18);dyb-1(cx36)* double mutants are no different from the single ones implying they may be acting through the same pathway. Furthermore, *dyb-1* mutants also have an increased sensitivity to a reduction in acetylcholinesterase levels and have an increased response to Ach. The mutant alone does not show any visible muscle deterioration but it does when in the sensitised background of *hlh-1* [85]. It has also been shown that the absence of dystrophin can partially be compensated by overexpressing *dyb-1* in *dys-1(cx18);hlh-1(cc561)* mutants, it helps to delay the onset of incoordination and muscle cell damage [87]. Furthermore, transmission electron microscopy (TEM) has been used to show that *dyb-1(cx36);hlh-1(cc561)* double mutants have a similar degree of muscle degeneration and fibrosis as *dys-1(cx18);hlh-1(cc561)* mutants, they also both have a shorted lifespan compared to WT [88].

dyc-1 encodes for a protein that is like CAPON proteins found in rodents. These bind to nNOS and are part of the DGC. *dyc-1* mutants have a phenotype resembling *dys-1* suggesting they have a common cellular function. Overexpression of *dyc-1* in the *dys-1(cx18);hlh-*

1(cc561) mutant partially reduced the locomotion and egg laying defects [62].

There are four known sarcoglycans in mammals (α-, β-, γ-, and δ-sarcoglycan), which are integral components of the DGC. In *C. elegans* these are represented by one gene, *sgn-1*. RNAi against *sgn-1* in WT animals gives a similar phenotype to *dys-1(cx18)* animals and RNAi in a sensitised *hlh-1* background led to muscle degeneration similar to *dys-1(cx18);hlh-1(cc561).* This suggests that these genes are acting through a similar mechanism [43].

1.4.5.2 Muscle related genes

C. elegans body wall muscles resemble that of vertebrate skeletal muscle in that they are comprised of sarcomeres. Interestingly, introducing mutations in genes that have a role in muscle contraction in the *dys-1(cx18);hlh-1(cc561),* resulted in suppression of the muscle degeneration usually observed. These included *unc-22* (twitchin), *unc-89* (obscurin), *unc-96* (a M-line protein), *lev-11* (tropomyosin) and *pat-10* (troponin C) [89]. This suggests that reducing sarcomere contraction can slow down muscle degeneration as it reduces the physical tension on the muscle fibres. This is supportive of evidence in mouse models suggesting that denervation and immobilisation of skeletal muscle could be a beneficial treatment in patients [90]–[92]. In addition, triple mutants of *dys-1(cx18);hlh-1(cc561)* with *atn-1* (actin) or *zyx-1* (LIM domain) also show a reduction in muscle degeneration. Surprisingly, overexpression

of *zyx-1* in the double mutant, also reduced muscle degeneration but to a lesser degree [75]. This implies that the ZYX-1 protein could be involved in the muscle degeneration process and targeting zyxin protein could be an effective treatment in DMD.

1.4.5.3 Calcium related genes

One of the pathophysiologic mechanisms in DMD patients is loss of calcium homeostasis resulting in an increase in intracellular calcium levels [5]. It has recently been suggested that calcium increases in the sarcoplasmic reticulum occurs before any other phenotype, which is detrimental to muscle health [81] and there is evidence to show the mis localisation of some calcium channels in the absence of *dys-1* which may be responsible for this rise [82],[83],[93].

Mariol and Seglat were the first to show that this mechanism was conserved in the *dys-1* mutants. *egl-19* is the major voltage-gated calcium channel in *C. elegans* muscle. The *dys-1* phenotype is suppressed by *egl-19(n582),* a partial loss of function mutation. *dys-1(cx18);egl-19(n582)* mutants behave similarly to *egl-19(n582)* in that they are slow and have an egg laying defect. However, *dys-1(cx18);egl-19(ad695)* (which have a gain of function mutation) animals, resemble *dys-1* mutants more closely in that they were short, hypercontracted and uncoordinated. Both *egl-19* mutants, *dys-1*, and *dys-1;egl-19(n582)* show no or limited degenerating cells, while the gain of function double mutants exhibit high levels of muscle degeneration which increased over time. Furthermore, *egl-19* RNAi in *dys-1;egl-19(ad695)* and on *dys-*

1(cx18);hlh-1(cc561) mutants significantly reduces muscle degeneration, suggesting that in these models muscle degeneration is directly correlated with calcium channel activity [94]. *unc-2(e55)*, another voltage-sensitive calcium channel, and *unc-68(RNAi)*, the ryanodine receptor gene, when inactivated also greatly reduces the muscle degeneration seen in *dys-1(cx18);hlh-1(cc561)* [89],[95]. This is likely due to reduced calcium entry into the cell and reduced release of calcium from the sarcoplasmic reticulum to the cytosol.

stn-1 (syntrophin) is also implicated in having a role in the control of calcium signaling. *stn-1* mutants have similar phenotypes to *dys-1* in that they are hyperactive, have an overbent head, hyper contract when moving backwards, have fewer eggs, and are sensitive to aldicarb. Both of these genes are likely to be in the same pathway as *dys-1(cx18);stn-1(ok292)* mutants show no additive affects. *stn-1* can partly suppress and give a slight phenotypic improvement to *egl-19(ad695)* mutants. This provides further evidence that the DGC has a role in the control of maintaining calcium homeostasis [86].

Another gene that has been shown to be important is *slo-1* which encodes for the SLO-1 Bk potassium channel which is mis localised in *dys-1* mutants. *slo-1* mutants have a similar phenotype to *dys-1* in that they are hyperactive, have an overbent head, and in a sensitised background show muscle degeneration. *dys-1(cx18);slo-1(cx29)* were no different to the single mutants suggesting that these two genes do not have an additive effect and are likely to have a common function [82]. As shown earlier SLO-1 is connected to the DGC through ISLO-1 and STN-

29

1. *islo-1* mutants have the same overbent phenotype that *dys-1* mutants' display. Furthermore, *dys-1(eg33);islo-1(eg978)* double mutants did not show a worsened phenotype compared to the single mutants, suggesting that they may have a similar cellular function [83]. *unc-36*, codes for a calcium voltage-gated channel that along with *slo-1* has disrupted localisation in the *dys-1* model [93].

Sarcoplasmic calcium leakage is also a characteristic in DMD and is thought to mediate myofiber death [96]. It is therefore reasonable to propose that altering intracellular calcium movement could be a potential treatment as well. RNAi has been used to inhibit *cmd-1* (calmodulin), *sca-1* (SERCA) and *csq-1* (calsequestrin) in *dys-1(eg33)* animals. Of these, only a reduction in calmodulin was able to improve function in the dystrophic worms by returning calcium levels to those of WT and improving calcium clearance during contraction/relaxation cycles [81]. This result was unexpected as in the mouse model inhibition of calmodulin was found to be detrimental, but calmodulin levels have been found to be elevated in human dystrophic muscle; therefore, targeting calmodulin could be a potential avenue but further work is required to fully understand calmodulin role in DMD [97],[98].

Finally, calpains, which are calcium activated regulated proteases, have been implicated in muscular dystrophy. There are two classes of calpains, typical or atypical, but *C. elegans* only express atypical calpains, and one of these genes is *clp-1*. *dys-1(cx18);hlh-1(cc561ts);clp-1(tm690)* mutants had almost half the number of degenerated muscle cells compared to *dys-1(cx18);hlh-1(cc561ts)*

mutants [99] Reducing calpain activity warrants further investigation as a potential therapeutic target.

1.4.5.4 Excitation-Contraction Coupling Genes

There is some evidence to suggest that improving the excitation–contraction coupling defect seen in DMD could be beneficial but requires further investigation. Excitation–contraction coupling is initiated by the release of Ach from the axon terminal and its binding to receptors on the sarcolemma initiates a muscle action potential. The Ach is then removed from the synaptic cleft by acetylcholinesterase. One of the early phenotypes identified in the dystrophin mutants was a hypersensitivity to Ach and aldicarb (altered cholinergic signalling), and a decline in acetylcholinesterase activity [55],[100]. *dys-1(cx18, cx26, cx35)* were first found to be hypersensitive to Ach and aldicarb, an acetylcholinesterase inhibitor. Acetylcholinesterase is important for breaking down Ach at the NMJ, this sensitivity implies that acetylcholine/cholinergic activity is increased in these mutants [55]. Additionally, it has been shown that there is a decline in acetylcholinesterase activity in *dys-1(cx18, cx26, cx35)*. In *C. elegans,* the genes that exhibit acetylcholinesterase activity are *ace-1* and *ace-2*. *dys-1(cx26);ace-1(p100)* and *dys-1(cx26);ace-2(g72)* double mutants are uncoordinated and hypercontracted, whereas the single mutants move normally. An interaction has been identified between *dys-1* and the *ace* genes as *dys-1* mutants show lower acetylcholinesterase activity, but the nature of this interaction is unknown [100].

Another gene that has been implicated is *snf-6* (which is responsible for clearing Ach from the cholinergic synapse). Kim *et al.* (2004) [77] demonstrated that *snf-6* interacts with the DGC through *stn-1* and has similar phenotypes to *dys-1* mutants. *dys-1(cx18);snf-6(eg28)* mutants do not show a worsened phenotype than the single mutants, and similarly *snf-6(eg28);hlh-1(cc561)* mutants show enhanced paralysis and muscle degeneration to a similar degree as *dys-1(cx18);hlh-1(cc561)* mutants [77]. Therefore, it is proposed that, under normal conditions *snf-6* clears Ach from the cholinergic synapse. When dystrophin is not present, *snf-6* is mis localised resulting in an increase in Ach at the NMJ and insufficient acetylcholinesterase to break it down. Therefore, cholinergic transmission is likely upregulated in the absence of dystrophin [101].

Mariol *et al.* (2007) [89] have investigated the excitation-contraction cascade by using RNAi to knock down genes linked to neurotransmitter release, Ach signalling, and others. Inhibition of *unc-13* (gene required for neurotransmitter release at the NMJ), *unc-38* and *unc-29* (both genes that encode for the Ach receptor), in the *dys-1(cx43);hlh-1(cc561)* model, led to a strong reduction in muscle degeneration [89]. This provides some evidence to suggest that improving the excitation-contraction coupling defect seen in DMD could be beneficial but requires further investigation.

The muscle action potential results in the release of calcium from the sarcoplasmic reticulum, which binds to troponin, displacing tropomyosin and allowing cross bridges to form between actin and myosin. Several genes mentioned in the previous section on calcium also

play a role in this process either through calcium influx or calcium removal. L-type calcium channels such as *egl-19* are triggered by the action potential to release calcium into the cell and this influx can cause further release of calcium from the sarcoplasmic reticulum through ryanodine receptors (*unc-68*). This increase in calcium initiates contraction, and relaxation occurs through the clearance of calcium through channels such as SERCA (*sca-1*). As discussed previously, inhibition of calcium release channels significantly reduced muscle degeneration in this model but inhibition of clearance channels did not [81],[94],[95]. This implies that reducing calcium levels is likely to be important in the treatment of DMD.

1.4.5.5 Mitochondrial genes

Mitochondria dysfunction is one of the underlying mechanisms associated with DMD. mPTP are multiprotein complexes found in the inner mitochondrial membrane under certain pathological conditions [102]. An example is high concentrations of intracellular calcium, as in DMD, which can cause the opening of the mPTP through cyclophilin D and the release of cytochrome c which may trigger loss of functional mitochondria, reduction in ATP production, and apoptosis/cell death. RNAi knock down of *cyn-1* (a cyclophilin D orthologue), and *cyc-2.1* (a cytochrome c orthologue), led to a significant reduction of muscle degeneration and an improvement in locomotion in *dys-1(cx18);hlh-1(cc561)* mutants [103].

It has also recently been found that dystrophin-dependent muscle degeneration is quickly followed by an increase in mitochondria fragmentation and apoptosis. Decreasing mitochondrial fission by inhibiting *drp-1* (mitochondrial fission gene) or *ced-3* (cleaves DRP-1) or increasing mitochondrial fusion by overexpressing *eat-3* or *fzo-1* (inner and outer mitochondrial membrane fusion respectively) in the *dys-1(cx18);hlh-1(cc561)* model, results in a reduction of mitochondrial fragmentation and fewer abnormal muscle cells [64]. In addition to altering mitochondrial dynamics, inhibiting genes involved in apoptosis and DNA degradation could be a potential treatment for DMD. The inhibition of *wah-1* (orthologue of human AIF), *cps-6* (orthologue of human EndoG), *crn-2* (orthologue of human TATDN1), *ced-1* (cell-corpse recognition), and *psr-1* (migration of engulfing cells) in *dys-1(cx18);hlh-1(cc561)*, also caused a decline in the number of abnormal muscle cells, suggesting that they all participate in cell death upon dystrophin-muscle degeneration [64].

1.4.5.6 Other signalling genes

Dystrophin has a variety of signalling influences including calcium, Ach, and mitochondrial. Dystrophin has also been shown to positively modulate the EGF-Ras-MAPK pathway which is important during vulval development in *C. elegans*. Inactivation of *dys-1* strongly suppressed the induction of ectopic vulvae by an activated *let-60* (*Ras* gene), highlighting dystrophins role in regulating EGF signalling during vulva induction [104]. Dystrophin knock down has been shown to lead to a disruption in protein

homeostasis, which consequently leads to an increase in cellular stress levels in the muscle. One gene that has been shown to become overexpressed in *dys-1(eg33)*, is *gst-4*, a transcriptional reporter induced by oxidative stresses. One pathway that is known to enhance stress resistance is insulin growth factor (IGF) signalling. *daf-16*, a FOXO gene, and *daf-2*, the gene encoding for an IGF receptor, can be targeted to reduce IGF signalling. *dys-1(cx18/eg33);daf-2(e1370)* mutants are able to protect the muscle from cell death and increase lifespan. This improvement relies on *daf-16*, as in *daf-2(e1370);daf-16(mu86);dys-1(cx18)* triple mutants, this positive effect was ameliorated [46]. Manipulation of these signalling pathways could also be a target for future studies in DMD.
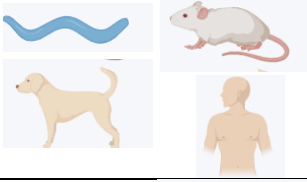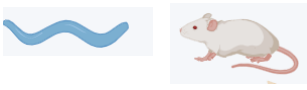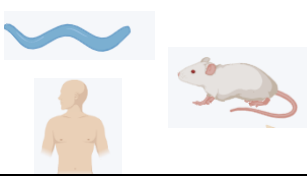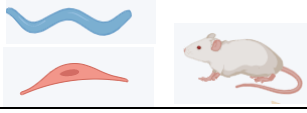
Finally, there are a handful of other genes that have been shown to have a genetic interaction with *dys-1* but not much is known about the nature of these interactions. For example, knock down of *hlh-1* (MyoD ortholog) has been used to give muscle degeneration in the *dys-1* single mutants but mechanisms are unclear [62]. Increased proteasome activity has been implicated in the pathophysiology of DMD. The muscle degeneration seen in the *dys-1(cx18);hlh-1(cc561)* mutants can be reduced by downregulating *chn-1*, the homologue of the human E3/E4 ubiquitylation enzyme CHIP. This potentially could be a new drug target [105]. Another area that could do with further investigation is regarding carbonic anhydrases. Carbonic anhydrase inhibitors have been shown to reduce muscle degeneration in *dys-1(cx18);hlh-1(cc561)* mutants, through the carbonic anhydrase *cah-4*. RNAi knock down of *cah-4*, also

gave a reduction in the muscle degeneration [106]. *gdi-1,* is a rab guanine-nucleotide dissociation inhibitior, in humans this gene is associated with mental retardation and other neurological disorders. In one study, examination for interactors with *gdi-1* revealed *dys-1* and *dyb-1* as key genes. RNAi treatment against *gdi-1* in *dys-1(cx18);hlh-1(cc561)* and *dyb-1(cx36);hlh-1(cc561)*, gave a reduction in muscle degeneration [107].

1.4.6 Pharmacological interventions trialled in *dys-1* mutants

C. elegans has not only proven itself as a useful model for studying human diseases but also as a tool for drug discovery [108]. Several pharmacological interventions have been rationalised and tested in the *dys-1* mutants with varying successes. The translatability of some of these interventions out of the worm model remains unclear. The different treatments that have been trialled can be found in Table 1.4 and their proposed sites of action can be seen in Figure 1.5.

Table 1.4. Pharmacological interventions tested in dys-1 mutants.

Drug class	Tested models	Proposed mechanism of action
Glucocorticoids (Prednisone)		Unknown hypothesised to have a direct effect on striated muscles (likely by repairing dysfunctional mitochondria and the mitochondrial network) [44],[109].
Serotonin		Unknown- as lack of DYS-1 is known to disrupt signalling pathways it could affect serotonin receptors and by replacing the serotonin you can reduce muscle degeneration [44],[110].
Proteasomal inhibitor (MG132)		Inhibition of the proteasome rescues the protein localisation of the members of the DGC [105].
Sulfonamides (methazolamide and dichlorphenamide)		Inhibits *cah-4* [106].
Cyclosporine A		Inhibits *cyn-1* which blocks or delays mPTP opening [103].
IP3R inhibitor aminoethoxydiphenyl borate		Inhibits *itr-1* [103].
Nicotinamide riboside supplementation		Increases NAD+ levels [111].
Melatonin		Reduces oxidative stress [44].
Furin inhibitor I		Inhibits Furin [95].
Actinonin		Inhibits matrix metalloproteinases [95].

Colours used in table corresponds with site of action in Figures 1.4 and 1.5.
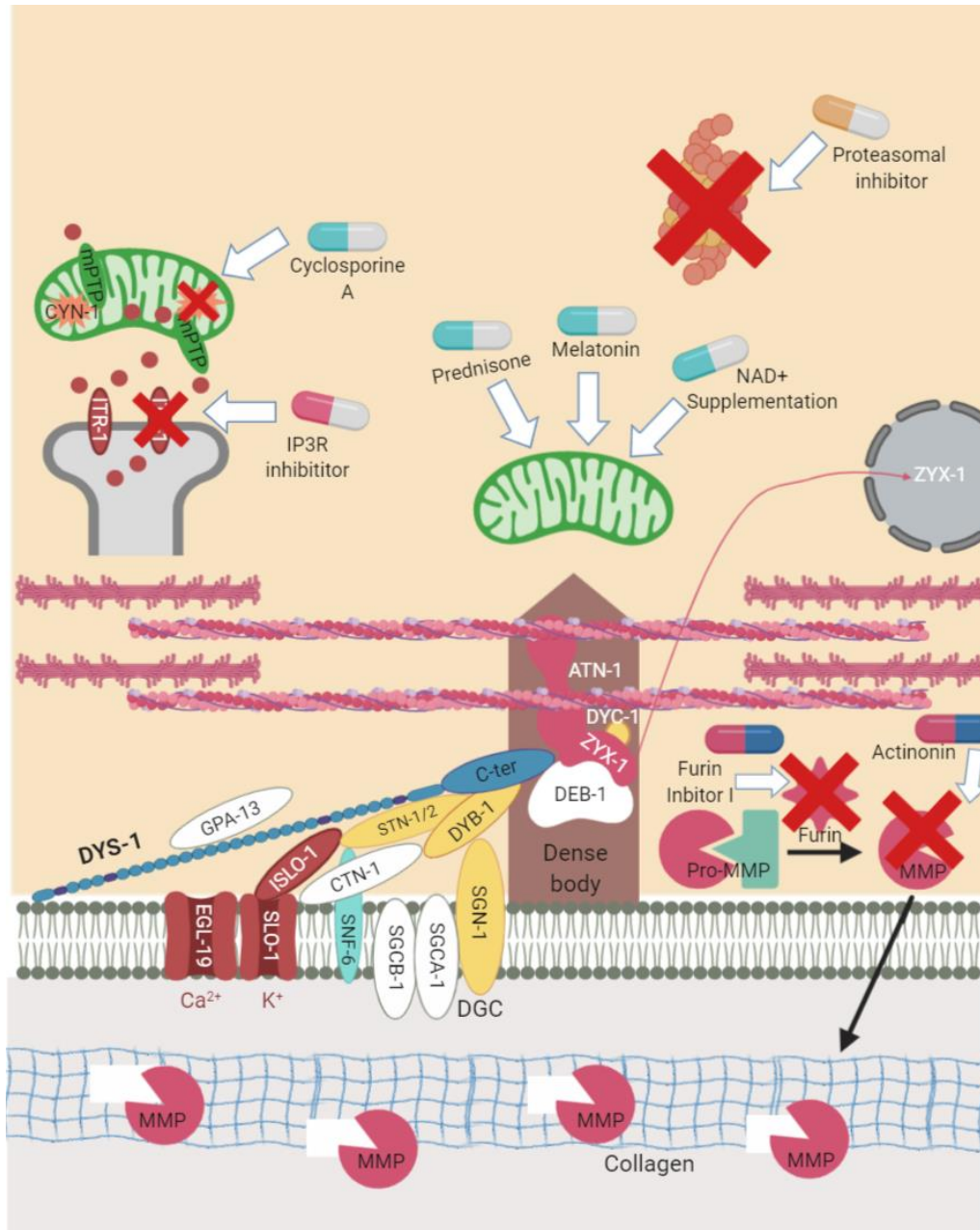
Figure 1.5. Sites of action for pharmacological interventions.

C. elegans has proven itself as a good drug screening platform for DMD. A number of these interventions are represented in the above figure. The pills in light blue and white represent most of the trialled drugs that are acting to improve mitochondrial dysfunction. Those in pink and white are altering calcium signalling. The orange and white pills are proteasomal inhibitors which act to reduce proteasome activity. Those in pink and blue represent extracellular matrix targeting compounds that aim to reduce the breakdown of collagen. Created with biorender.com.

The standard pharmacological treatment given to DMD patients are glucocorticoids, the main one being prednisone. In a blind drug screen of ~100 compounds in the *dys-1* double mutant, prednisone was identified as the most successful in reducing the number of abnormal muscle cells, highlighting the utility of this model in drug screening [109]. There are several hypotheses for how prednisone may be acting but the mechanism is currently unclear. It is proposed that prednisone may decrease inflammation but as *C. elegans* largely lack a conventional inflammatory system, it is likely that it is having other effects as well. In a recent article prednisone was shown to improve movement and strength in the *dys-1(eg33)* model through improvements in the structure of the mitochondrial network and oxygen consumption [44]. Deflazacort is another glucocorticoid which has now received FDA approval for the treatment of DMD; despite exploration of other models [112], studies have yet to commence in *C. elegans*.

1.4.6.2 Hormone related therapies

Hormone related drugs have also been shown to reduce muscle degeneration and improve muscle function in the *dys-1* model [44],[65]. Interventions that modified serotonin levels were shown to be beneficial in *C. elegans* including serotonin itself, drugs that inhibit serotonin reuptake (Fluoxetine (Prozac), Imipramine and Trimipramine) and serotonin agonists (m-chlorophenyl piperazine and N-methyl quipazine) [110]. Serotonin treatment has also been shown to be beneficial in

zebrafish *sapje* model of DMD and in the *mdx* mouse model [113],[114]. Mechanistic insight is lacking; there could be reduced serotonin levels in the absence of dystrophin, so the interventions are simply replacing what is lacking. However, in a small cohort of human patients, serotonin levels in DMD patients were found to be comparable to healthy controls in plasma but lower than controls in platelets [115],[116]. Melatonin is another hormone that has been shown to improve muscle function in *C. elegans*, *mdx* mice, and in patients. This is likely acting by reducing oxidative stress [44],[117]–[120].

1.4.6.3 Proteasomal inhibitors

Proteasome degradation has been shown to decrease dystrophin levels in DMD patients and so providing treatments that focus on stabilising the mutant protein could be beneficial [121]. Reducing proteasome activity by downregulating *chn-1* has been shown to reduce muscle degeneration in the *dys-1* model [105]. As gene knockout is currently not a feasible treatment in humans, MG132 was trialled as well which is a nonspecific proteasome inhibitor. When administered, MG132 at low doses can inactivate *chn-1* and thus, block proteasome degradation in the *dys-1* model [105]. MG132 treatment has also been trialled in the *mdx* mouse model and in freshly isolated skeletal muscle biopsies, in both of which the inhibitor rescued the expression of the DGC (likely due to rescuing the cell membrane localisation) [122]–[124]. However, it seems unlikely that proteasome inhibitors as a stand-alone treatment,

will be able to provide a cure for DMD but they could be used in a 'therapeutic cocktail' [125].

1.4.6.4 Sulfonamides

In a *C. elegans* DMD model screen of 1000 currently approved treatments, carbonic anhydrase inhibitors were identified among the top hits [106]. Previously, carbonic anhydrase levels in plasma were shown to be elevated and carbonic anhydrase inhibitors have had some success in human pilot studies [126]–[128]. In this screen, the two compounds identified were the sulfonamides: methazolamide and dichlorphenamide, which are thought to act by inhibiting *cah-4*. As previously mentioned, RNAi against *cah-4* was also beneficial in the *dys-1 C. elegans* model. These drugs were trialled in both *C. elegans* and in the *mdx* mouse with a decline in muscle degeneration seen in *C. elegans* and an increase in force in the mouse model [106]. It is proposed that these compounds act by modifying the pH which alters the transmembrane potential and excitability.

1.4.6.5 Compounds targeting the mitochondria

Recently, the mitochondria have become an attractive target for drug treatments in DMD. A chemical screening tool was developed for the study of neuromuscular disorders in *C. elegans* [129]. Using these methods, two therapies were identified that targeted the mitochondria. The first was low dose cyclosporine A, thought to act by inhibiting

cyclophilin D, *cyn-1*. It is hypothesised that this drug reduced muscle degeneration through the regulation of mPTP opening [103]. This has also been reported in the *mdx* mouse model, but a clinical trial in patients, did not show significant improvements in muscle function although a high dose not a low dose was used [130],[131]. The second compound identified was the IP3R inhibitor aminoethoxydiphenyl borate. This inhibits the calcium channel ITR-1 which has been shown to have a role in dystrophin-dependent muscle degeneration [103]. It has been shown recently in the *mdx* mouse model, that the IP34 receptor has a role in increasing basal cytoplasmic calcium and blocking this receptor restores muscle function [132]. Another potential mitochondrial drug is NAD+ supplementation; NAD+ depletion has been shown to occur in patients with DMD and so supplementation could be a beneficial treatment. NAD+ is also naturally occurring in the body so the risk of adverse side effects is less. NAD+ supplementation in DMD *C. elegans*, *mdx* mice, and human cells, has been shown to be beneficial [111].

1.4.6.6 ECM targeted drugs

Targeting the ECM could also prove to be beneficial. Collagen has been shown to play a role in protecting muscle cells against dystrophy but gets rapidly degraded by matrix metalloproteinases (which are activated by furin). Using a furin inhibitor (furin inhibitor I) and an inhibitor of matrix metalloproteinases (actinonin), proved beneficial in the double mutant as there was less degradation of collagen [95].

1.4.7 Future work for the *C. elegans* DMD model

C. elegans has proved itself as a very useful model for studying DMD, especially more recently with the use of the *dys-1(eg33)* model and the development of more clinically relevant and translational assays. The mechanism of action of prednisone is largely unknown, improving mechanistic understanding of this drug could potentially identify targets that, at the moment, are not being addressed. One of the main benefits of this model continues to be in its ability to run high-throughput screens of compounds. This could lead to the discovery of novel treatments that could be used instead of prednisone without the side effects. Identifying a drug that could extend lifespan or health span in DMD patients would be a huge breakthrough in this field.

1.5 Hydrogen sulfide and the sulfur containing amino acids

1.5.1 Overview of hydrogen sulfide and the sulfur containing amino acids

Hydrogen sulfide (H_2S) is the third physiologic signalling gas to be identified, the other two being carbon monoxide (CO) and nitric oxide (NO). H_2S was originally known as a toxic gas but it has been shown that physiologically relevant concentrations could have beneficial effects. Endogenous H_2S has been shown to have cytoprotective and antiapoptotic effects, that may help to regulate various functions within the human body [133]. H_2S has been found to be decreased in several conditions (e.g., ageing, ischemia, and diabetes mellitus) and are increased in other states (e.g., cancer, critical illness, and inflammation).

H_2S enzymatic generation and signalling is conserved between organisms including mammals, invertebrates, and bacteria [134]. Enzymatic H_2S production predominantly occurs through the action of three enzymes: cystathionine-γ-lyase (CSE), cystathionine-β-synthase (CBS) and 3-mercaptopyruvate transferase (3-MST) [135]. These three enzymes have been found to be expressed in both mammals and in *C. elegans* [136]. CSE and CBS are mainly cytosolic enzymes but may translocate to the mitochondria in stress conditions. 3-MST is found in both the cytosol and in the mitochondria [137]. CBS and CSE work independently to metabolise the sulfur amino acid cysteine to produce H_2S. Whereas 3-MST works in combination with cysteine aminotransferase (CAT) to produce H_2S [138]. H_2S is also produced as a biproduct from the metabolism of other sulfur amino acids but the main production is from cysteine (Figure 1.6).

The sulfur amino acid pathway plays a key role in sulfur metabolism and redox regulation. The aim of this pathway is to encourage methionine metabolism away from proteinogenesis and towards the production and catabolism of cysteine. This is the only way that cysteine can be produced endogenously within the organism [139]. Methionine is first converted to homocysteine through the enzymatic activity of S- Adenosyl Methionine (SAMS) and S- Adenosyl Homocysteine (SAH), this process is called transmethylation (TMP). Homocysteine can be recycled back to methionine through a process called remethylation (RMP). CBS along with the addition of serine, then converts homocysteine to cystathionine [140]. Under high homocysteine levels (hyperhomocysteinemia), CSE converts homocysteine to homolanthionine and H_2S. With the addition of water, homocysteine may also be converted to homoserine and H_2S [141]. CSE then acts upon cystathionine to generate cysteine, ammonia, and α-ketobutyrate. Cysteine can then be metabolised further by either of the three enzymes, this is the TMP. For example, CBS can metabolise cysteine to serine and H_2S, and CSE can produce H_2S, pyruvate, and ammonia from cysteine. 3-MST breaks down cysteine in a 2-step manner to produce H_2S and pyruvate. First CAT breaks down cysteine and α-ketoglutarate (αKG) to 3-mercaptopyruvate and glutamate. Then 3-MST converts 3-mercaptopyruvate to pyruvate and H_2S [142]. Importantly, cysteine is also broken down into two other sulfur containing amino acids (SAA): glutathione and taurine (Figure 1.6).

1.5.2 H₂S and the sulfur containing amino acids in DMD

There is very little literature exploring H_2S and DMD. There is one paper showing that total thiol, native thiol, and disulphide levels were lower in DMD patients compared to control [143]. This hints that potentially there could be a decline in H_2S in DMD as well, but this has not been examined to our knowledge. Duchenne cardiomyopathy was shown to be preserved through the H_2S donor drug SG1002, in a humanised dystrophic mouse model. SG1002 preserved cardiac function, attenuated fibrosis, and mitochondrial function [144]. To our knowledge there have been no human studies. As our search yielded few results, the following section will discuss the known impact of H_2S in ageing, as DMD shares some similarities with ageing.

There has been some examination into the SAA in DMD but still not a great deal has been explored. A literature search looking at homocysteine levels in DMD models and/or supplementation yielded no results. A deficiency in methionine has been found in the muscles of *mdx* mice [145],[146]. Cysteine levels were found to be perturbed in the *mdx* mouse model compared to control. 18 day old mice were found to have a deficiency in cysteine in the liver, plasma, and muscle [147]. Supplementation of cysteine through N-acetyl cysteine (NAC), which is commonly used as an intervention in respiratory disorders, has been shown in the *mdx* mouse model to improve the diaphragm of the animals [148]. Of all the SAA, taurine is the most well researched in DMD.
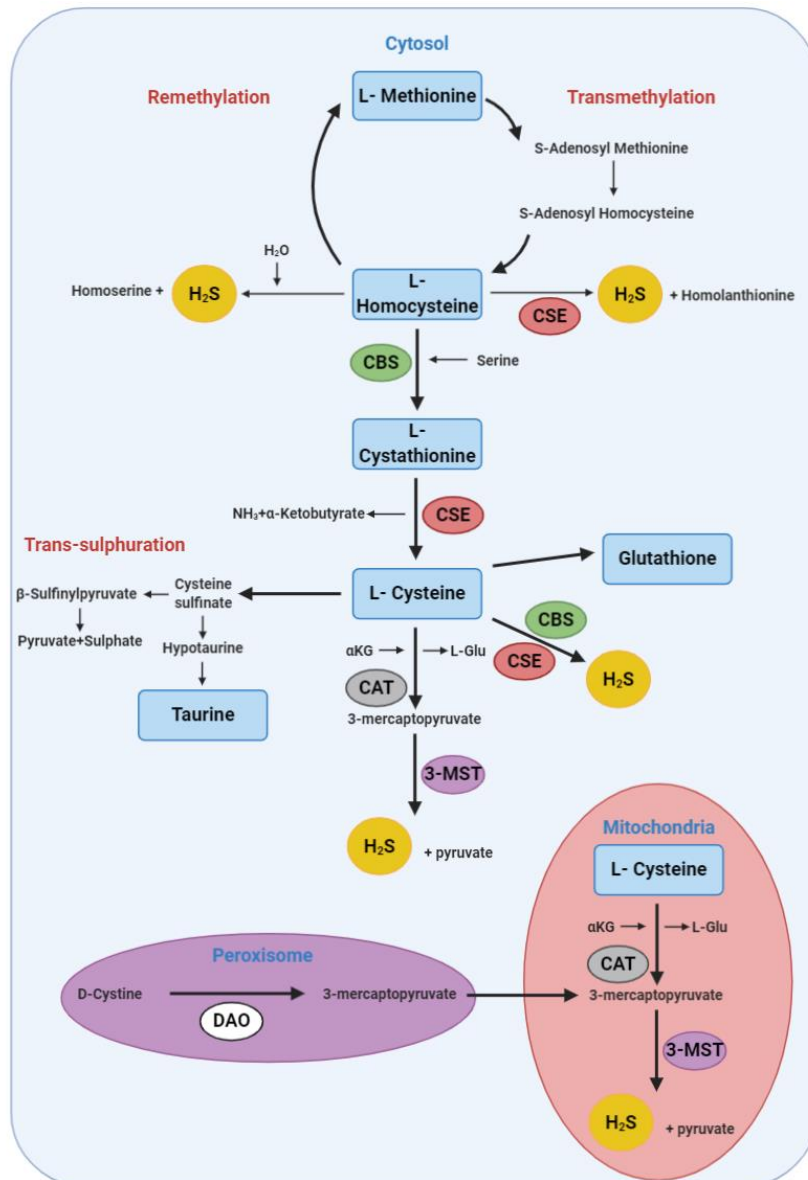
Figure 1.6. Pathways of H₂S generation.

Cystathionine-γ-lyase (CSE), cystathionine-β-synthase (CBS) and 3-mercaptopyruavate transferase (3-MST), are the three primary enzymes responsible for the endogenous production of H_2S. CBS and CES for part of the sulfur amino acid pathway, whose role is to convert methionine to cysteine and H_2S is often produced as a biproduct. The third enzyme, 3-MST, works in combination with cysteine aminotransferase (CAT) to metabolise cysteine and again producing H_2S. This process can occur in the cytosol and in the mitochondria. 3-mercaptopyruvate can also be metabolised from D-cysteine in the peroxisome via D-amino acid oxidase (DAO), thus providing additional substrate for H_2S production. Figure adapted from Wu *et al*, 2018.

Taurine exerts many physiological functions including, cytoprotective effects, antioxidant, and anti-inflammatory actions as well as modulation of intracellular calcium concentration. Taurine levels have been shown to be declined in the *mdx* mouse model compared to control during pre-dystropathology (18 days old). In addition, taurine metabolism is perturbed in the muscle, liver, and kidney [146],[147]. Taurine supplementation has been shown to improve muscle strength, reduce inflammation, and protect against muscle wasting in the *mdx* mouse model [149]. The final SAA to be discussed is glutathione. Again, research here is lacking but in cultured patient skin fibroblasts from DMD patients showed no difference in glutathione levels to healthy controls [150].

To date there have been two gene expression studies in DMD *C. elegans* models, one was a microarray study and the other used RNA sequencing [66],[67]. This has provided some insight into changes in the expression of enzymes that have a role in sulfur metabolism. Both studies shown an increase in expression of S-adenosylmethionine synthetase (*sams-1*/*sams-3*/*sams-4*) which converts methionine to SAM [66],[67]. The microarray study also showed an increase in expression of methyl transferase, which converts SAM to SAH [67]. Hrach *et al.*, (2020), also showed an increase in expression of S-adenosylhomocysteine hydrolase (*ahcy-1*) which is responsible for the conversion of SAH to homocysteine. Furthermore, they showed a reduction in expression of cystathionine beta-lyase (*cbs-1*) and cystathionine gamma-lyase (*cth-1*). The former is partially responsible for the addition of serine necessary for the conversion of homocysteine to cystathionine and the latter for the

production of αKG from cystathionine [66]. Both studies showed a reduction in expression of methionine synthase (*metr-1*) which is responsible for the conversion of homocysteine back to methionine and glutathione S-transferase (*gst-1*) which breaks down glutathione [66],[67]. Taken together this could suggest that there is an increase drive to taurine synthesis. The increased expression in the enzymes responsible for converting methionine to cysteine indicates there is a larger need for cysteine. However, as there is a reduction in glutathione break down, it suggests that the need is for taurine. Further research is required before these assumptions can be confirmed.

1.5.3 The connection between ageing research and DMD

The symptoms of DMD share similarities with those of accelerated ageing, predominantly a loss of muscle strength, a loss of mobility and frequent falls. DMD is associated with progressive muscle degeneration whereas ageing is associated with sarcopenia. Both cases result in progressive muscle decline but occurs more quickly in DMD. Primarily both are associated with the loss of skeletal muscle mass. Interestingly, a study looking at gene expression in DMD, ageing, and healthy skeletal muscle, identified 528 differentially expressed genes between the groups, of those 328 were co-expressed in DMD and ageing muscle. 50% of these genes had the same gene expression profile and were mainly focused in the immune response and mitochondrial metabolism categories [151]. This provides further evidence that there are similarities between the two. This is also the case in *C. elegans* where progressive

muscle decline can be seen in both DMD [76] and with age [152]. In both cases, loss of mitochondrial structure is an early feature. Alterations in mitochondrial gene expression are known to occur prior to onset of symptoms in DMD *C. elegans* [66] and this impairment of mitochondrial function causes sarcomere disorganisation [95]. Furthermore, steroids which are the most common class of drugs prescribed for DMD are often also prescribed for age related conditions such as arthritis.

Despite the little research into H_2S and DMD, there has been significantly more looking at H_2S and ageing. This research initially started in *C. elegans* where exogenous H_2S was shown to prolong lifespan [136],[153]. In human subjects 50 to 80 years old, a decline in H_2S in plasma was shown, providing further evidence of the utility of H_2S [154]. Supplementation of H_2S research to date, has been in ageing models predominantly nematodes, cells, and rodents. In this case the focus will be on the nematode model. Initial research focused on exposing nematodes to different atmospheres containing different concentrations of H_2S. Expectedly, high concentrations were toxic but low concentrations increased thermotolerance and lifespan [153]. Next to be explored was the slow releasing H_2S donor GYY4137, which also improved lifespan and healthspan [136],[155]. This improvement was likely due to the antioxidative properties of H_2S.

The SAA have also been somewhat explored in ageing models. Methionine restriction (through restriction of dietary methionine) has been shown to extend the lifespan of rats, mice, fruit flies, and nematodes (reviewed in [156]). Interestingly, methionine supplementation

has also been shown to improve lifespan in *C. elegans* as well [157]. Hyperhomocysteinemia (increased levels of homocysteine) is a characteristic feature of ageing, suggesting homocysteine suppression could be beneficial in ageing [158]. However, homocysteine supplementation has been shown to increase lifespan in *C. elegans* [157]. Supplementation of cysteine has been shown to have positive effects in early clinical trials in ageing. Cysteine supplementation has improved skeletal muscle function, decreased plasma levels of inflammatory cytokines, and improved immune functions (reviewed in [159]). Supplementation has also improved lifespan in *C. elegans* [157]. Taurine supplementation has also been shown to be beneficial in ageing, particularly in the treatment of sarcopenia and improving skeletal muscle function (as is the case in DMD) [160]. Finally, glutathione levels decline with age in both animal models and humans. Supplementation of glutathione or its precursor cysteine are both viable options in the treatment of ageing [161].

1.6 Scientific basis for this PhD and aims

As has been demonstrated throughout this introductory chapter, *C. elegans* is a good early model for DMD and displays several phenotypes that are directly comparable with human patients. In addition, *C. elegans* has proven itself as a good model for doing high-throughput drug screening and in relation to the DMD model, the gold-standard treatment prednisone has been identified through one of these screens. Given the similarities between DMD and ageing muscle, it seems reasonable to assess potential treatments used for ageing in DMD. The scientific basis for this PhD is therefore as there are declines in H_2S levels with age and H_2S supplementation has been shown to improve lifespan and healthspan, could this be then used in DMD. The aims are therefore to i) determine whether H_2S supplementation could be a potential treatment for DMD and if so, ii) what are the mechanisms of action behind the treatment and iii) why this deficiency occurs in the first place. A secondary aim is to strengthen the DMD *C. elegans* model by establishing methods that are more clinically relevant.

Chapter 2: General methods

2.1 Maintenance of *C. elegans*

2.1.1 Culturing OP50 *Escherichia coli (E. coli)*

In the laboratory *C. elegans* are usually grown monoxenically using OP50 *E. coli* as a food source [162]. A starter culture of *E. coli* was initially obtained from the Caenorhabditis Genetics Center (CGC). Using aseptic technique, the starter culture was streaked onto LB agar plates [30 g LB agar (Duchefa biochemie), 7 g high gel strength agar (Melford), ddH$_2$O to 1 litre and autoclaved] and grown overnight at 37°C. A single colony was selected from the streaked plate and used to inoculate 50 ml LB broth [20 g LB broth (Melford) ddH$_2$O to 1 litre and autoclaved]. This was then grown in a shaking incubator (140 rpm) overnight at 37°C. Both the plates and broth can be stored at 4°C and useable for several months [163].

2.1.2 Culturing *C. elegans*

C. elegans were maintained on Nematode Growth Medium (NGM) agar, which was aseptically poured into petri plates, the size of which depended on the type of experiments that were being carried out [162]. To make the NGM agar the following was required: 3 g NaCl (Sigma), 17 g high gel strength agar, 2.5 g bacto-peptone (Sigma), ddH$_2$O to 975 ml, and autoclaved. Once it had cooled to 55°C, 1 ml 5 mg/ml cholesterol (Sigma), 1 ml 1 M CaCl$_2$ (Sigma), 1 ml 1 M MgSO$_4$ (Sigma) and 25 ml 1 M KPO$_4$ buffer [108.3 g KH$_2$PO$_4$ (Sigma), 35.6 g K$_2$HPO$_4$ (Sigma), ddH$_2$O

to 1 litre and autoclaved] was added. The agar was dispensed into petri plates and left for 2-3 days before use. *E. coli* OP50 was then added to the surface of the plate (the volume depended on the size of the plate) and spread to create a lawn. The plates were left to dry overnight at room temperature before worms were added. *C. elegans* stocks were maintained at 20°C in this case but can be maintained at 15°C or 25°C. Worm stocks were maintained by transferring them to fresh plates once per week using the "chunking" method.

2.1.3 Cleaning contaminated *C. elegans* stocks

On occasion stocks would become contaminated, although the contaminants are not usually harmful to the worms it is best to have clean stocks. A bleach egg prep was used on these occasions. Plates were washed with 4 ml sterile ddH$_2$O to loosen worms and eggs stuck in the bacteria and collected in a falcon tube. 500 µl 5 N NaOH (Sigma) and 1 ml household bleach (Sainsburys) was added to the tube. The tube was shaken for 10 seconds, every 2 minutes for a total of 10 minutes. The tube was then centrifuged for 1 minute at 1300 xg to pellet the released eggs. The supernatant was removed, leaving around 500 µl which was added to a fresh clean plate.

2.1.4 Freezing and thawing of *C. elegans* stocks

C. elegans can be stored indefinitely in liquid nitrogen or long term at -80°C. Freshly starved L1-L2 animals survive the freezing process the best (35-45% are usually recoverable). Plates were washed with 2-3 ml

of S buffer [129 ml 0.05 M K_2HPO_4, 871 ml 0.05 M KH_2PO_4, 5.85 g NaCl] and 500 µl was added to a 1.8 ml cryovial. Then 700 µl S buffer and 300 µl 30% glycerol (Sigma) was also added to the cryovial. The cryovial was placed into a Mr. Frosty[TM] freezing container and put immediately into a -80°C freezer. After a couple of days, it can be removed from the Mr. Frosty[TM] and placed into the liquid nitrogen. To thaw stocks, remove them from the freezer or liquid nitrogen and allow them to melt at room temperature. Then pour the contents onto a seeded agar plate and transfer worms to another seeded plate after 2-3 days.

2.2 Synchronisation of animals

2.2.1 Growth synchronisation of L1 animals

For most experiments synchronised populations are required. To obtain a synchronised population of L1 animals, a week-old plate was washed with 3 ml of M9 buffer [3 g KH_2PO_4 , 6 g Na_2HPO_4 (Sigma), 5 g NaCl, 1 ml 1 M $MgSO_4$, ddH_2O to 1 litre and autoclaved] and added to a flacon tube. It was then left for 2.5 minutes and 20 µl of worms are taken from the top of the surface to a fresh seeded plate. Animal were then left to grow at 20°C until the desired time point, when assays were then conducted.

2.3 Pharmacological interventions

2.3.1 Prednisone

Prednisone drug plates were prepared by making an initial stock of prednisone (Sigma) in 100% ethanol which was then added directly to cooled NGM (as described in *2.1.2*) and dispensed to 60 mm plates (VWR). The final concentration of drug required was 370 µM (as determined previously [44],[109]). After 2-3 days once the plates had set, they were ready to be seeded and used in assays.

2.3.2 Sodium GYY4137

Sodium GYY4137 (NaGYY) was synthesised and kindly gifted by Whiteman lab at the University of Exeter, as previously published [164]. Commercially sourced GYY4137 is a morpholine salt (itself biologically active) complexed to undisclosed quantities of highly toxic, carcinogenic solvent [dichloromethane; xCHCl2; at least 1 dichloromethane:2 GYY4137 molecules [164]], which is metabolised by cells and in vivo to carbon monoxide [165],[166]. We therefore used a pharmaceutically more acceptable sodium salt devoid of these two confounding factors (NaGYY), in addition to using its established and characterized hydrolysis product [164], to ensure that our observations were due to slowly released H_2S, and not the parent molecule or hydrolysis product. Samples can be stored at room temperature or in a desiccator. H_2S is released upon the addition of water and stocks can only be kept for 2 weeks. The final concentration of drug used was 100 µM unless otherwise stated and was dispensed onto the top of a seeded 30 mm NGM plate (alpha laboratories), 24 hours prior to use. Plates were sealed

with parafilm. A control compound was also synthesised which was devoid of H_2S but had the same parent compound and hydrolysis product, this was used to confirm the effect was due to the H_2S [164].

2.3.3 AP39

AP39 is a mitochondrial-targeted H_2S donor which was also synthesised and kindly gifted by Whiteman lab at the University of Exeter, following previously published protocol [167]. AP39 stocks were prepared in dimethyl sulfoxide (DMSO) (Sigma) before being diluted down further in ddH$_2$O, as *C. elegans* can only tolerate concentrations of up to 2% vol/vol of DMSO. AP39 was aliquoted onto the top of a seeded 30 mm NGM plates, to a final concentration of 100 pM 24 hours prior to use. Plates were sealed with parafilm.

2.3.4 Sulfur containing amino acid compounds

The sulfur containing amino acids used were as follows: L-methionine (Sigma, M9625), L-homocysteine (Sigma, 69453), L-cysteine (Sigma, 168149), L-glutathione (Sigma, PHR1359) and L-taurine (Sigma, T0625). All compounds were diluted in ddH$_2$O. For all the sulfur containing amino acid compounds, stock solutions were aliquoted onto the surface of seeded 30 mm NGM plates at the following concentration L-methionine (10 mM), L-homocysteine (10 μM), L-cysteine (10 μM), L-glutathione (100 μM) and L-taurine (10 μM).

2.4 Using RNAi to knockdown gene function

2.4.1 Identification and growth of bacteria containing RNAi clones

The RNAi feeding method was utilised in the experiments in this thesis, where worms were fed bacteria expressing dsRNA [168]. Clones were identified by searching the Vidal and Ahringer libraries with the gene sequence. The desired strain was then streaked onto a LB plate containing ampicillin and tetracycline [30 g LB agar, 7 g high gel strength agar, ddH$_2$O to 1 litre and autoclaved. 1 ml of 100 mg/ml ampicillin (Sigma) and 1 ml of 10 mg/ml tetracycline (Sigma) was added once cooled to 55˚C] and grown overnight at 37˚C. A single colony was then selected, and cultures grown in LB medium containing ampicillin [20 g LB broth, ddH$_2$O to 1 litre and autoclaved. Once cooled to 55˚C, 1 ml of 100 mg/ml ampicillin was added]. This was then grown in a shaking incubator (140 rpm) overnight at 37°C.

2.4.2 Experimentation using RNAi against target genes

RNAi plates were prepared in advance [NGM agar plates as prepared in *2.1.2* but with 1 ml of 100 mg/ml ampicillin and 1 ml of 1 M IPTG (Sigma)] and seeded with bacteria containing the RNAi clone from *2.4.1*. Worms were synced as in *2.2.1* onto the plates to knockdown the desired gene.

2.5 Assessment of *C. elegans* muscle

2.5.1 Microscopy

The NemaFlex strength assay was performed on a Zeiss Axio Observer 7 microscope with a 5x objective and a Hamamatsu OCRA-Flash 4.0 digital camera. The CeleST swim test was performed on a LEICA MDG41 microscope at 10 x magnification with a Leica DFC3000G camera. Mitochondrial and cell death imaging was performed at 400 × magnification and 100 x magnification respectively using a Nikon Eclipse 50i microscope. The Nikon Eclipse 50i microscope was also used at 100 x magnification for the calcium sensor strain imaging.

2.5.2 Movement assay

Movement assay also referred to as thrashing assay, are carried out to assess how well the animals moved which is a direct correlation of muscle function. These were carried out by picking a single adult animal into 20 µl of M9 buffer on a microscope slide. The number of bends in 10 seconds was counted and repeated five times for each worm for three independent biological replicates. These thrash counts were then multiplied by six to give the movement rate per minute. One body bend was recorded as one rightward body bend and leftward body bend. [169].

2.5.3 CeleST swim assay

CeleST (C. elegans Swim Test) is a specialised computer programme that tracks the swimming behaviour of multiple animals in liquid [170]. It provides a readout of morphological, and activity related

parameters associated with swim behaviour, that would not necessarily be noted just by eye. 4-5 animals were picked into the swimming zone (50 μl M9 buffer into a 10 mm ring pre-printed on a microscope slide) and 30 second movies were taken with ~15 images per second on a LEICA MDG41 microscope at 10 x magnification with a Leica DFC3000G camera. The analysis utilised a swim analysis programme in MATLAB. The four activity parameters include wave initiation rate, travel speed, brush stroke and activity index. The wave initiation rate is the number of head or tail bends over a set time, most like the movement assay in *2.5.2*. Travel speed measures the longitudinal distance that an animal travels during a set period. Brush stroke measures the extent of movement and bending per stroke. Activity index provides a sense of how forcefully the animal bends whilst swimming. The four morphological parameters are body wave number, asymmetry, curling, and stretch. Body wave number measures the number of waves travelling along the body at a given time. Asymmetry reports if the animal bends more to one side than the other. Curling measures how much time the animal spends bent around to the point that it overlaps itself. Stretch describes how deep or flat body bends are by finding the maximum difference ("stretch") between the two most extreme curvatures at any part of the body at a given stroke.

2.5.4 Nemaflex strength assay

The 'Nemaflex' is a microfluidics-based system that allows strength measures to be taken from *C. elegans* [171]. First a mould was designed using soft lithography that contained an arena containing a

pillar matrix. This mould was specifically designed to allow for assessment of worms at Day 2 of adulthood. A two-layer mould was made using SU-8 2050 negative photoresist (Microchem) on a 3" silicon wafer as substrate (University Wafer). The first layer forms the boundary of the arena, and the second layer has cylindrical holes which forms the micropillars. The distance from centre to centre of one pillar to another was 115 µm, the pillar diameter was 44 µm on average, therefore there was ~71 µm of space that the worm could occupy between pillars. The pillar height was ~87µm. Devices were then casted from this mould using polydimethylsiloxane (PDMS) (Sylgard 184 Part A (base)) and Part B (curing agent) 10:1 by weight; Dow Corning) over the SU-8 mould by curing for ~2 hours at 75°C. The PDMS replica was then treated in an air-plasma cleaner (Harrick Plasma, Ithaca, NY) for 1 minute and bonded to a 1×3" glass slide. To prepare the device for worm loading, 5 wt% Pluronic F127 (Sigma) solution was first loaded into the device and left to incubate at room temperature for 30 minutes and then washed with M9 buffer. Prior to the start of the assay, plates were flooded with 3-4 ml of M9 solution and single animals were loaded into the devices using a syringe connected to tubing. Once the animals were loaded, one-minute videos were taken at a rate of ~5 images per second on a Zeiss Axio Observer 7 microscope with a 5 x objective and a Hamamatsu OCRA-Flash4.0 digital camera. Movies were then processed using an in-house-built image processing software (MATLAB, R2015b), where pillar deflections were converted to a force value.

2.6 Assessment of lifespan

2.6.1 Nemalife

Lifespan assays were conducted by using the microfluidics-based Infinity Screening System (NemaLife Inc.). Worms were grown as described to Day 0 of adulthood. Day 0 animals were then washed from plates with 2 mL of M9 and collected in conical tubes. Animals were washed three times with 14 mL of M9, allowing young adults to settle at the bottom, and the supernatant was removed to clear bacterial debris. Worms were then collected in a 2.5-mL sterile syringe, where ~70 animals were loaded into each microfluidic chip (Infinity chip, NemaLife Inc.) for whole-life culture [172]. Survival analysis began from Day 1 of adulthood and was repeated daily until cessation of life. Each day, the microfluidic culture chips were washed to remove progeny and imaged for 90 seconds, followed by feeding of 20 mg/mL *E. coli* OP50 in liquid NGM. Chips were then placed in Petri dishes with damp tissue wrapped in parafilm and stored at 20 °C until subsequent use. The acquired videos were scored for live/dead animals by using the Infinity Code software (NemaLife Inc.).

2.7 Assessment of mitochondrial structure and function

2.7.1 Imaging of muscle mitochondria and nuclei

The development of green fluorescent protein (GFP) has enabled the visualisation of specific proteins in the general structure of organelles in *C. elegans*. The strains used for imaging of muscle mitochondria and cell nuclei were CB5600 [*ccIs4251* (*Pmyo-3::Ngfp-lacZ; Pmyo-3::Mtgfp*) I; *him-8(e1489)* IV] and CC91 [*dys-1(eg33)* I; *ccIs4251* I; *him-8(e1489)* IV] which have GFP expressed specifically within body wall muscle mitochondria and nuclei. Animals were picked into M9 buffer on a microscope slide with a cover slip applied. When exposed to blue light the GFP expresses green fluorescence allowing images to be captured. In this case images were taken at 400 × magnification using a Nikon Eclipse 50i microscope. These animals were also used for the determination of cell death. Images were taken on Day 4 and Day 8 of adulthood at 100 x magnification and cell death was determined by counting the number of missing nuclei in each animal [46].

2.7.2 Assessment of mitochondrial membrane potential

JC-10 (Enzo Life Sciences, 52305) is a mitochondrial dye that is used to assess membrane potential. JC-10 concentrates in the mitochondrial matrix when membrane potential is intact or diffuses out when it is compromised. 83 µM JC-10 was prepared in freeze-dried OP50 solution (LabTIE). Animals were picked into the JC-10 solution and left for 4 hours prior to imaging. Representative images were taken at 400 × magnification using a Nikon Eclipse 50i microscope.

2.7.3 Isolating functional mitochondria from *C. elegans*

Mitochondrial isolation is a useful method for assessing the functionality of mitochondria. To isolate mitochondria from *C. elegans*, first 2/3 plates of Day 1 adults were washed with M9 buffer. The supernatant was collected in a falcon tube and left to gravity sink for 5-10 minutes. All the supernatant was removed and then 1 ml of M9 buffer was added and transferred to a 1.5 ml Eppendorf. This was then centrifuged at 0.4 RCF for 75 seconds in a microcentrifuge at room temperature. The supernatant was then removed and another 1 ml of M9 was added, this was repeated 5 times. Following the washes in M9 buffer, this was then repeated 3 times in 300 µl MAPR homogenisation buffer (without ATP) [100 mM KCL (Sigma), 50 mM KH_2PO_4, 50 mM Tris (Sigma), 5 mM $MgCl_2$ (Sigma), 1 mM EDTA (Sigma) at pH 7.2]. Following the final wash, the supernatant was removed and 300 µl homogenisation buffer with ATP and saponin [100 mM KCL, 50 mM KH_2PO_4, 50 mM Tris, 5 mM $MgCl_2$, 1 mM EDTA, 1.8 mM ATP, 817 µM saponin at pH 7.2] was added. This was then transferred to a pre-cooled Wheaton 2 ml Tissue Grinder, Potter-ELV mortar ((Wheaton, 358029) and homogenised with Wheaton 2 ml Tissue Grinder, Potter-ELV plastic pestle ((Wheaton, 358029) for 3 minutes at 150 rpm on ice. The crude homogenate was transferred using a plastic pastette to a clean pre-cooled Eppendorf. This was then washed with 200 µl of homogenisation buffer (without ATP) and transferred to the same Eppendorf. The homogenate was centrifuged for 3 minutes at 650 RCF at 4°C. The supernatant was transferred to another clean pre-cooled Eppendorf and the pellet was discarded. The supernatant was centrifuged for 3 minutes at 15,000 RCF at 4°C. The

supernatant was removed and discarded until there was no supernatant remaining. 100 µl of resuspension buffer [0.5 mg/ml human serum albumin (HSA) (Sigma), 240 mM sucrose (Sigma), 15 mM KH_2PO_4, 2 mM $(CH_3COO)_2MG.4H_2O$ (Sigma) and 0.5 mM EDTA at pH 7.2] was added and the pellet was gently resuspended. The isolated mitochondria needed to be stored on ice and used within 4 hours.

2.7.4 Measurement of mitochondria ATP production rate (MAPR)

First, mitochondria were isolated from *C. elegans* as in *2.6.1*. ATP reagent buffer [187 mM sucrose, 19 mM K_2HO_4 (Sigma), 2.5 mM $Mg(CH_3COO)_2$ (Sigma), 0.6 mM EDTA and 1.8 mM ATP (Sigma) at pH 7.2] was prepared in advance and 40 ml was added to ATP monitoring reagent (Biothema), this was then wrapped in foil and stored in the fridge, it can only be kept for up to 2 weeks. The following substrates were also prepared in advance: 16.4 mM glutamate (Sigma) with 15 mM succinate (Sigma), 5 µM palmitoyl-L-carnitine (Sigma) with 1.5 mM malate (Sigma) and 0.14 mg/ml human serum albumin (Sigma), 50 mM pyruvate with 22 mM malate, 2.5 mM succinate and 32.75 mM glutamate with 22 mM malate. To each well of a white 96 well plate the following was added: 200 µl ATP monitoring reagent, 35 µl of one of the substrates or water, 12.5 µl 12 mM ADP (Sigma) and 5 µl diluted mitochondrial suspension. Mitochondrial ATP production was determined luminometrically using the FLUOstar OPTIMA (BMG LABTECH). Luminescence was measured continuously for 10 minutes with an injection of 150 pM ATP occurring at 4.6 minutes. ATP production was determined by change in comparison

compared to a known standard. All data was normalised to mitochondrial protein content as determined using the Bradford method in *2.7.8*.

2.7.5 Citrate synthase assay

Citrate synthase is an enzyme responsible for catalysing the first reaction of the citric acid cycle and is a validated measure for mitochondrial content. To measure citrate synthase activity in *C. elegans*, first 20 worms were picked into 20 µl of M9 buffer. 180 µl of homogenisation buffer [50 mM KH_2PO_4, 1 mM EDTA at pH 7.1] plus 1% triton X-100 was then added to the suspension. This was then transferred to a pre-cooled Duall Tissue Grinder Glass- Size 20 1ml (Anachem (95016866)) and homogenised on ice for 3 minutes at 250 rpm. The homogenate was then transferred to a pre-cooled Eppendorf using a disposable pastette Pasteur. This was centrifuged for 3 minutes at 22,000 g at 4°C and the supernatant transferred to another pre-cooled Eppendorf. 300 µl of citrate synthase master mix [2 ml 395 mM tris buffer, 75 µl DNTB (Sigma), 550 µl 1.5 mM acetyl CoA (Sigma), 50 µl oxaloacetate (Sigma), 4.825 ml H_2O], was added to a see-through 96 well plate (GBO, 655801) and incubated for 5 minutes at 25°C. The sample was then read for 2 minutes at 412 nm in a spectrophotometer to make a blank. 20 µl of the sample was then added to the well and mixed then read for 3 minutes at 412 nm in the spectrophotometer. Citrate synthase activity was then calculated.

2.7.6 Rotenone

Rotenone (Sigma) was dissolved in 100% DMSO and diluted in M9 buffer to contain 2 µM of rotenone. Rotenone is an inhibitor of complex I. 1 ml was added to a seeded NGM 3 cm Petri dish. Around 30 animals were picked into the buffer and left for 24 hours at 20°C. Thrash assays were then performed by picking animals out of the buffer into M9 on a microscope slide as in *2.5.2*.

2.7.7 Antimycin A

Antimycin A (Enzo Life Sciences) was dissolved in 100% ethanol and diluted in M9 buffer to contain 2 µM of antimycin A. Antimycin A is an inhibitor of complex III. 1 ml was added to a seeded NGM 3 cm Petri dish. Around 30 animals were picked into the buffer and left for 24 hours at 20°C. Thrash assays were then performed by picking animals out of the buffer into M9 on a microscope slide as in *2.5.2*.

2.7.8 Bradford protein assay

The Bradford assay is a colorimetric assay for determining total protein concentration. A 1 mg/ml BSA (Sigma) protein standard was used in the runs for this thesis. The protein standard was serially diluted giving a linear range of 0-10 µg/µl. 400 µl of each dilution was prepared in Eppendorfs, along with the samples. 100 µl Bradford dye (Bio-rad) was added to each standard and sample and vortexed. The colour was left to develop for 5 minutes. 200 µl of each standard and sample was added

in duplicate to the wells of a UV-star 96 well plate (GBO) and read at 595 nm in a spectrophotometer [173].

2.7.9 Western blot

Protein expression was measured by western blot analysis. 15 worms were picked into 10 µl 3x Laemmli SDS sample buffer. Samples were then boiled at 95°C for 5 minutes and the entire sample was loaded into the wells of a 12% Criterion™ TGX™ Precast Midi protein gel (Bio-Rad) and separated by sodium dodecyl sulfate–polyacrylamide gel (SDS-PAGE) electrophoresis at a constant voltage (1 hour at 200 V) using the XT MOPS running buffer (Bio-Rad). The gels were then rinsed with ddH$_2$O and placed face down in transfer buffer for 5-10 minutes. In the meantime, pre chilled transfer buffer was added to the Bio-Rad transfer tank and freezer blocks were inserted to keep the buffer chilled. The gel sandwich (consisting of fibre pads, blotting paper, gel, and polyvinylidene difluoride (PVDF) membrane) was then assembled for the transfer to the PVDF membranes. Once assembled this was placed into the transfer tank and run for 45 minutes at 100 V. After transfer the membranes were washed several times in 1x tris-buffered saline (TBST) and incubated in 2.5 % Milk in 1x TBST, with gentle agitation on a rocker for 1 hour. Membranes were then cut if needed for probing with multiple antibodies. The membranes were then incubated overnight at 4°C with gentle agitation in the relevant primary antibody (these were prepared in advance in 2.5 % BSA in 1x TBST). The next day, membranes were washed 3 times for 5 minutes in 1x TBST with gentle agitation. The

membranes were then again incubated for 1 hour at room temperature with gentle agitation in 2.5 % Milk in 1x TBST containing the relevant secondary antibody. The membranes were then again washed 3 times for 5 minutes in 1x TBST with gentle agitation. The membrane was then incubated in HRP reagent (Millipore) for 5 minutes at room temperature, ensuring the whole membrane was covered and did not dry out. The membrane was then placed between two overhead transparencies and put in the Chemidoc (Bio-rad) for analyses. Band intensity was determined using the Image Lab Software (Bio-Rad).

2.7.10 ATP content

ATP content was determined using the CellTiter-Glo 2.0 assay (Promega) with ATP standard curve (Sigma). The CellTiter-Glo determines the number of viable cells by measuring the ATP present, but we have adapted this method to use in *C. elegans.* 90 animals were picked into 40 µl of M9 and snap-frozen in liquid nitrogen (they can either be used immediately or stored at -80°C until required). When the assay was carried out, 3 freeze-thaw snap cycles were completed, and samples stored on ice. They were then centrifuged at 13,000 rpm for 10 minutes at 4°C in a microcentrifuge. The supernatant was then collected, and some removed and stored at -20°C for protein quantification as in *2.7.8.* The ATP standards were then prepared (0.0001µM – 100 µM) using a 1 mM stock and diluting in M9. 50 µl of standards were loaded into a black 96 well plate in duplicate along with a blank sample of 50 µl M9 buffer. 50 µl of samples (2 µl worm lysate plus 48 µl M9 buffer) were loaded in

triplicate into the plate as well. Following this, 50 µl of CellTiter-Glo reagent was added to each well and the plate was covered with foil. It was then placed on a horizonal mixer for 2 minutes and then left in the dark for 10 minutes at room temperature. Luminescence was then measured on the BMG fluorostar to determine ATP concentrations which were normalised to protein content.

2.8 Assessment of calcium signalling

2.8.1 GCaMP

HBR4 {*goeIs3* [*myo-3p::GCamP3.35::unc54 3' utr + unc-119*(+)]} and HBR4 crossed with BZ33 (*dys-1(eg33)*) was used to assess calcium concentration in the body wall muscles of *C. elegans.* Crosses were carried out in this lab by generating males in the HBR4 strain using heat shock and mating these with the BZ33 strain. Animals were selected based on having GCaMP and a thrash rate less than 60 in 1 minute. Images were taken on a Nikon Eclipse 50i microscope at 100 x magnification and GFP intensity was measured using ImageJ (National Institutes of Health, Bethesda, MD, USA) software.

2.8.2 Levamisole sensitivity assay

Levamisole is a potent cholinergic agonist which allows for analysis of Ach signalling. Animals were picked into 2.5 ml 100 μM levamisole hydrochloride (Sigma) and the percentage of animals paralysed was recorded every 10 minutes.

2.8.3 NemaMetrix ScreenChipTM electropharyngeogram recordings

All animals were synchronised to the L4 stage before being collected from the plates with M9 buffer. Worms were then washed twice with M9 by centrifugation (2500 rpm, 90 seconds). After washing, worms were resuspended in M9 containing 10 mM serotonin (5-hydroxytryptamine) and incubated for 10 minutes to stimulate pumping. Electropharyngeogram (EPG) recordings were taken using the

NemaMetrix ScreenChipTM system using an SC30 chip. Each EPG recording was two minutes in duration and analysed using the NemAquire software. Representative images of the pumps were extracted from the NemAnalysis 0.2 software.

2.9 Quantification of H_2S and sulfur metabolising enzymes

2.9.1 Quantifying H_2S levels using AzMC

H_2S levels were quantified in *C. elegans* using the H_2S detector fluorogenic probe 7-azido-4-methylcoumarin (AzMC). Previously whole worms were incubated in AzMC and imaged under a fluorescent microscope [174]. However, we found this technique unreliable when we tried to reproduce it as we found the animals did not take up a lot of the dye which made our quantification difficult. We therefore established a different method with this dye that we have found to be more robust. First 90 animals were picked into 40 µl of M9 buffer and snap frozen. 3 freeze-thaw cycles were performed, and samples were centrifuged at 13,000 rpm for 10 minutes in a microcentrifuge. The supernatant was then collected and some stored at -20°C for protein quantification as in *2.7.8.* A 10 mM stock of AzMC was then prepared in DMSO and diluted down to a working stock of 62.5 µM. 10 µl of the supernatant was diluted with 30 µl of M9 buffer (so that samples could be run in triplicate). 10 µl of this was then added to an Eppendorf with 40 µl of 62.5 µM AzMC to give a final concentration of 50 µM. Samples were incubated for 2 hours in the dark at 20°C and fluorescence was read on a BMG fluorostar at 340/445 nm. Relative fluorescence was then normalised to protein content.

2.9.2 RT-qPCR

First RNA was extracted from Day 1 animals using the TRIzol method [175]. Approximately 150-200 worms were washed off plates with M9 buffer and left to gravity syncronise for 10 minutes. The animals were

then washed 3 times in M9 buffer with centrifugation to remove any bacteria that may have been carried over. 500 µl TRIzol reagent (Sigma) was then added on ice and incubated at 4°C for 10 minutes, this was the homogenisation process in this extraction. 100 µl of chloroform (Sigma) was then added and incubated at 4°C for 10 minutes. Samples were then centrifuged at 12,000 rpm at 4°C for 15 minutes, this was to isolate the RNA from DNA and proteins via phase separation. The upper aqueous phase was then removed and added to a fresh Eppendorf, avoiding the middle layer. An equal volume of isopropanol (Sigma) was then added and left for 10 minutes at room temperature to precipitate the RNA. This was then centrifuged at 7,000 rpm at 4°C for 10 minutes to pellet the RNA. All supernatant was then removed, and the pellet washed with 500 µl of 80% ethanol to remove any unwanted salts whilst leaving the RNA intact as RNA is insoluble in ethanol. This was repeated for a second time and all ethanol removed. The pellet was then left for 10-15 minutes to dry and finally resuspended in 20 µl of RNA free water. The concentration of the sample and 260/280 ratio (to assess RNA purity) was then measured on the NanoDrop 1000 (Thermo Scientific) and stored at -80°C.

The quality of the RNA was then assessed via gel electrophoresis looking for two bands at 18S and 28S. A 1% agarose gel (Thermo Fisher) was cast in 1x TBE (Tris-borate-EDTA) buffer (Thermo Fisher) with 1 µl of SYBR safe (Thermo Fisher). 5 µl of sample plus 2 µl of BlueJuice RNA loading dye (Thermo Fisher) was loaded into the wells plus RNA ladder

(Thermo Fisher) was loaded. The gel was run for 30 minutes at 90 V and the gel was read on the Chemidoc (Bio-rad).

cDNA synthesis took place using the PrimeScript™ RT reagent Kit (Perfect Real Time) (Takara) as per manufacturers instructions. In this case 500 ng of RNA was reverse transcribed per 10 µl reaction using oligo dT Primer and random 6 mers. The reverse transcription cycle consisted of a 37°C for 15 minutes incubation, followed by 85°C for 5 seconds to inactivate the reverse transcriptase with heat treatment. Samples were then store at -20°C. Each sample also had a control sample without the reverse transcriptase.

RT-qPCR was performed using TB Green Premix Ex Taq™ II (Takara) on a CFX Connect™ Real-Time PCR Detection System (Bio-Rad) as per manufacturers instructions. Final primer concentration used was 0.4 µM with 50 ng of cDNA template used per reaction (determined via standard curve). Samples were run in duplicate with one negative reverse transcriptase sample and one negative control. The PCR protocol used was as follows: initial denaturation at 95°C for 30 seconds and then 40 cycles of 95°C for 5 seconds and 60°C for 30 seconds. Relative fold change was determined by $2^{-\Delta\Delta CT}$ method and normalised to a housekeeping gene.

Chapter 3: Exogenous hydrogen sulfide treatment improves muscle health in *C. elegans* DMD model.

3.1 Introduction

The details of DMD are discussed in depth in Chapter 1 but will be summarised briefly here. DMD is an X-linked neuromuscular disorder characterised by progressive muscle degeneration and weakness [176]. It is caused by mutations in the gene which encodes for dystrophin, resulting in a lack of functional dystrophin protein in muscle cells and neurones. Dystrophin links the intracellular cytoskeletal network to the transmembrane components of the DGC, which provides stability to the muscle membrane. Destabilisation of this complex from the reduction of dystrophin results in progressive fibre damage and membrane leakage [1]. Additionally, reduction of dystrophin causes increased sarcoplasmic calcium levels which may cause a cascade of detrimental effects including mitochondrial damage [5],[177]. DMD is a lethal disorder affecting over 1 in 3,500 live male births, to which there is currently no cure. It has a poor prognosis and treatment is largely targeted at controlling the onset of symptoms to maximise the quality of life. The standard approved treatment for DMD is the corticosteroid prednisone. Although it extends ambulatory period by a couple of years, it is associated with several undesirable side effects, such as weight gain, behavioural difficulties, and may lead to osteoporosis [13]. Thus, there is an unmet clinical need in seeking new and/or alternative treatments for DMD that can be used independently or in conjunction with other emerging therapies.

The invertebrate model *C. elegans* has been used alongside mouse and canine models in the study of DMD as they are cost-effective, have a short lifespan, and are low maintenance. In addition, they have a fully sequenced genome and conserved biological pathways, which increases its chance of translatability to more complex organisms [50]. *C. elegans* has proven itself as a useful model for studying muscle disorders such as muscular dystrophy and sarcopenia, due to its largely conserved musculature and NMJ [48]. These DMD worm models have also been employed for studying the use of pharmacological treatments and in large-scale drug screens [109]. Several *C. elegans* models have been established for studying DMD by causing mutations in *dys-1* (the dystrophin orthologue), which results in a loss of fully functional dystrophin. This is discussed in further detail in Chapter 1. Here we utilised *C. elegans* with a nonsense mutation at position 3287 of the DYS-1 dystrophin orthologue. Unlike previous models, it does not require a sensitised background to show muscle degeneration [46]. Furthermore, it has impaired locomotion, reduced strength, a severely fragmented mitochondrial network, and elevated basal OCR [44],[59]. Prednisone treated animals were shown to have an improvement in all of the afore mentioned phenotypes, providing evidence for its utility as a drug screening platform [44].

DMD and ageing share some similarities, primarily the progressive loss of skeletal muscle mass [151]. DMD is characterised by rapidly progressive muscle degeneration, and ageing is usually associated with sarcopenia. It has recently been shown that H_2S,

improved both survival and health of ageing *C. elegans* by attenuating intracellular ROS generation and protecting against various stressors [136],[155].

H$_2$S is a signalling gasotransmitter which is produced endogenously in mammals and in *C. elegans.* It is generated through a combination of the enzymes CSE, CBS, and 3-MST. Endogenous H$_2$S has been shown to have cytoprotective and antiapoptotic effects, that may help to regulate various functions within the human body [133],[136],[155]. In recent years, the use of exogenous H$_2$S has been gaining attention due to its potential use in ageing and age associated diseases. H$_2$S supplementation has been shown to slow the ageing process by inhibiting oxidative stress and free-radical reactions (reviewed in [133]). We therefore hypothesised that H$_2$S supplementation, using a slow release H$_2$S donor (sodium GYY4137(NaGYY)), would also give some beneficial effects in the *C. elegans dys-1(eg33)* model.

Here we report that NaGYY improved DMD worm movement, strength, gait, and muscle mitochondrial structure. Like prednisone treatment, NaGYY treatment did not improve mitochondrial membrane potential. NaGYY also delayed muscle cell death but did not significantly alter overall lifespan. The health improvements of either treatment required the action of the kinase JNK-1, the transcription factor SKN-1, and the NAD-dependent deacetylase SIR-2.1. The transcription factor DAF-16 was required for the health benefits of NaGYY treatment but not prednisone treatment. Despite at least partially non-overlapping mechanisms of action, combined treatment of DMD worms with both

NaGYY and prednisone did not improve health more than the use of either single compound. Our results demonstrate the positive effects of H_2S supplementation on DMD nematode health and opens new avenues of both therapeutic and mechanistic inquiry.

3.2 Materials and Methods

3.2.1 Strains and culture conditions

C. elegans strains were cultured at 20°C on Petri dishes containing NGM agar and a lawn of *E.coli* OP50 unless stated otherwise (*2.1.2*). Animals for the study were age synchronised by gravity synchronisation from L1 stage and allowed to grow to the desired day of adulthood (*2.2.1*). The *C. elegans* strains used in this study were Bristol strain N2 (WT, wildtype), *dys-1(eg33)* (strain BZ33) which has a nonsense mutation in the *dys-1* gene, provided by CGC. Mitochondrial network integrity was assessed using CB5600 [*ccIs4251 (Pmyo-3::Ngfp-lacZ; Pmyo-3::Mtgfp*) I; *him-8 (e1489)* IV] and CC91 [*dys-1(eg33)* I; *ccIs4251* I; *him-8(e1489)* IV] (developed previously in this lab). Calcium flux was measured in real time using the HBR4 {*goeIs3* [*myo-3p::GCamP3.35::unc54 3' utr + unc-119*(+)]} and HBR4xBZ33 (generated in this lab) strains.

3.2.2 Pharmacological compounds

Prednisone was dissolved in 100% ethanol and added directly to NGM after it had been autoclaved and cooled to 55°C. The final concentration used was 370 µM unless otherwise stated. This concentration was selected as it falls within the range previously reported to reduce the number of degenerating cells in the *dys-1(cx18);hlh-1(cc561)* model and *dys-1(eg33)* model [44],[109] (*2.3.1*). NaGYY and its inert hydrolysis product were synthesised as previously described by us [164] (*2.3.2).* Compounds were dissolved in ddH$_2$O before being added to

the surface of a seeded NGM 3 cm Petri dish ~24 hours before use. A thrash assay was used to determine the optimal dose of 100 µM for NaGYY, and this dose was used for all studies unless otherwise stated.

3.2.3 Movement assay

Movement assays were carried out as described in *2.5.2*. Briefly, the number of thrashes a worm moved within a liquid medium was counted. For each treatment, movement rates for ten worms were measured with three biologically independent repeats [169].

3.2.4 NemaFlex strength assay

The NemaFlex is a microfluidic device containing an arena of pillars. The methods used to conduct the NemaFlex strength assay were as described previously [44],[171] and a full description can be found at *2.5.4*. Briefly, the devices were loaded with one animal per chamber and one-minute videos were taken. Movies were then processed using an in-house-built image processing software (MATLAB, R2015b), where pillar deflections were converted to a force value. Approximately 30 worms were imaged per strain/treatment group.

3.2.5 CeleST swim test

CeleST (a specialised computer programme that tracks the swimming behaviour of multiple animals in liquid [170]) was used to explore swimming gait in WT, *dys-1(eg33),* and drug-treated worms.

Methods used were as described [178] (*2.5.3*). Briefly, 4-5 animals were picked into the swimming zone and 30 second videos were taken. The analysis utilised a swim analysis programme in MATLAB that read out on several parameters associated with ageing. Approximately 60 worms were imaged per strain/treatment group.

3.2.6 Lifespan assay

Whole-life studies with *C. elegans* were carried out on an automated microfluidics lifespan machine (NemaLife Inc., TX). Approximately 70 Day 0 animals were loaded into microfluidics chips (Infinity chip, NemaLife Inc., TX) and survival analysis (daily videos) commenced on Day 1 of adulthood until the cessation of life. The acquired videos were scored for live/dead animals using the Infinity Code software (NemaLife Inc., TX) [172] (*2.6.1*).

3.2.7 Mitochondrial and cell death imaging

Mitochondrial imaging was used in Day 1 adults, with or without treatment, to examine the mitochondrial network. The CB5600 [*ccIs4251 (Pmyo-3::Ngfp-lacZ; Pmyo-3::Mtgfp*) I; *him-8(e1489)* IV] strain and CC91 [*dys-1(eg33)* I; *ccIs4251* I; *him-8(e1489*) IV] were used for WT imaging and dystrophy imaging respectively. Worms were cultured on NaGYY as described previously (*2.2.1*). Approximately 20 Day 1 adults or aged animals were picked into M9 buffer on a microscope slide with a cover slip applied. Worms were imaged at 400 × magnification (*2.7.1*). CB5600 and CC91 animals were also used for the cell death images. The protocol

used was as described previously [46] (*2.7.1*). Briefly animals were assessed at Day 4 and Day 8 of adulthood, where the number of dead muscle cells was determined by quantifying the number of muscle cells that had lost their distinct circular nuclear GFP signal. Approximately 30 animals were picked into M9 buffer on a microscope slide with a cover slip applied. Worms were imaged at 100 x magnification.

3.2.8 Assessment of mitochondrial membrane potential

JC-10 was used to assess mitochondrial membrane potential. Worms used for assessing mitochondrial membrane potential were WT and *dys-1(eg33)*. ~40 Day 1 adults were picked into 83 μM JC-10 in freeze-dried OP50 solution for 4 hours before imaging. Representative images were taken at 400 × magnification (*2.7.2*).

3.2.9 Measurement of calcium flux

A calcium sensor strain was used to measure calcium flux in real time. The strains used were HBR4 {*goeIs3* [*myo-3p::GCamP3.35::unc54 3′ utr + unc-119*(+)]} and HBR4 crossed with BZ33 (*dys-1(eg33)*) generated in this lab (*2.8.1*). Approximately 20 worms were imaged per condition/treatment.

3.2.10 EPG recordings

Synchronised worms were grown to L4 stage as described previously, with or without treatment (*2.2.1*). EPG recordings were taken using the NemaMetrix ScreenChipTM system after pumping of the pharyngeal muscle has been stimulated with serotonin. Each EPG recording was 2 minutes in duration and analysed using the NemAquire software. Worms for each condition were analysed in two independent experiments and the data combined, consisting of approximately 30 animals per strain/treatment. Representative images of the pumps were extracted from the NemAnalysis 0.2 software (2.8.4).

3.2.11 Levamisole assay

To assess the differences in levamisole sensitivity between WT, *dys-1(eg33),* and NaGYY treatment, each group was exposed to levamisole hydrochloride at 100 µM in M9 buffer. The percentage of paralysed animals is reported at 10 minutes (*2.8.2*). Approximately 30 worms were assayed for each experiment with three biological replicates.

3.2.12 Development of animals on RNAi

The RNAi feeding method was adopted in this case, where worms were fed bacteria expressing dsRNA [168] (*2.4*). Starved L1s were synchronised onto standard RNAi plates with bacterial lawns expressing dsRNA for the relevant genes and allowed to reach Day 1 of adulthood before assessment by movement assay. Clones were obtained from the Open Biosystems Vidal Library. Clones used were as follows: *jnk-1*:

B0478.1, *skn-1*: T19E7.2 and *daf-16*: R13H8.1. *sir-2.1*: R11A8.4 clone was obtained from the Ahringer library. For each treatment, movement rates for ten worms were measured with three biologically independent repeats.

3.2.13 Statistical analysis

All data are presented as violin plots from at least three replicates unless otherwise stated. Normality was first assessed using the D'Agostino and Pearson tests, and then the statistical test was selected based on normality. Statistical differences were assessed using either one-way ANOVA, two-way ANOVA, or Kruskal-Wallis test. Survival was analysed using Kaplan-Meier curves, with Bonferroni-corrected multiple comparisons. Significance was determined as $P < 0.05$, and all statistical analyses were completed using GraphPad Prism (USA).

3.3 Results

3.3.1 Sodium GYY4137 treatment improved functional defects in movement, strength, and gait.

As is the case with DMD patients, worms with a mutation in dystrophin exhibit decreased movement [44]. Locomotion defects can be detected in *C. elegans* by measuring the worms thrash rate in a liquid medium [169]. This is an indirect method of measuring muscle function. In line with previous literature, here we show that *dys-1(eg33)* has a decline in movement compared to WT (Figure 3.1b). As shown in Figure 3.1a, the decreased movement of *dys-1(eg33)* worms was attenuated by treatment with NaGYY. This improved movement was observed in a dose-dependent manner from 10 µM to 1 mM; 100 µM was subsequently used throughout the study unless otherwise stated (Figure 3.1a). Control experiments performed using a hydrolysed compound [164] incapable of generating H_2S confirmed the effects observed were due to H_2S and not either the parent compound or hydrolysis product (Figure 3.1a). In this movement assay, NaGYY gave a larger increase in movement compared to *dys-1(eg33)* without treatment and to prednisone treatment (Figure 3.1b). Interestingly, NaGYY gave a decline in movement for WT animals. However, it is likely that as these animals are only at Day 1 of adulthood, a beneficial effect would not be detected until they're aged (Figure 3.1b).
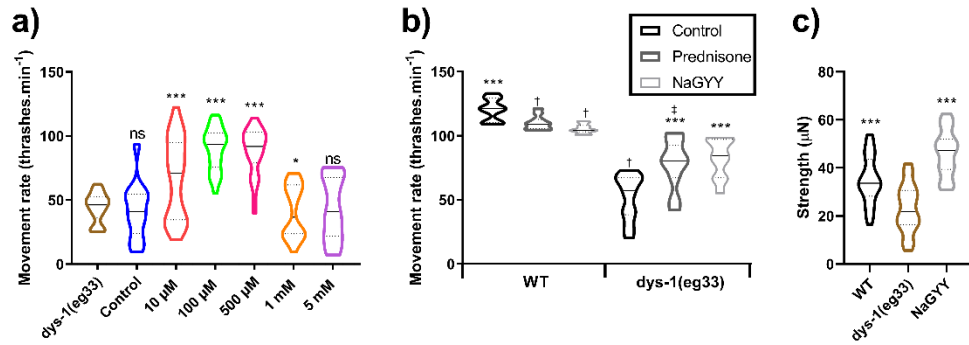
Figure 3.1. Effect of NaGYY on movement and strength in dys-1(eg33).

a) NaGYY treatment significantly improved the thrash rate of *dys-1(eg33)* in a dose-dependent manner (10 µM-1 mM). The NaGYY hydrolysis compound (100 µM) which was unable to generate H_2S was also assessed and showed no difference in thrash rate compared to *dys-1(eg33)* demonstrating that it is H_2S from NaGYY and not the parent molecule or hydrolysis product formed after H_2S generation that was providing the beneficial effect. b) *dys-1(eg33)* has a lower thrash rate than WT. *dys-1(eg33)* is improved under NaGYY (100 µM) and prednisone treatment (370 µM) but WT is not. For all strains and treatment *N*=10 with five replicates with three biological repeats for a total of 150 data points per violin plot. Results were analysed with a two-way ANOVA. All significance points were compared to *dys-1(eg33)* ***$P<0.0001$, *$P<0.05$, ns$P>0.05$. Compared to WT represented by †$P<0.0001$. Compared to NaGYY represented by ‡$P<0.0001$. c) The *dys-1* mutant had reduced strength compared to WT animals. NaGYY improves the strength of *dys-1(eg33)* animals beyond WT levels. For all strains and treatment groups *N*=21-33. Significance was analysed using one-way ANOVA. ***$P<0.0001$.

One of the phenotypes displayed in muscular dystrophy patients is muscular weakness. This has also been previously shown in the *dys-1(eg33)* mutant through use of the NemaFlex assay, a more direct measure of muscle function [44],[171]. On Day 3 of adulthood *dys-1(eg33)* is significantly weaker than the WT control [44] and has also been used to demonstrate muscle weakness in a worm limb girdle muscular dystrophy model previously [179]. Here, we have used a modified NemaFlex device that has pillars with a smaller diameter and tighter spacing, so that we could assess the worms at an earlier stage of adulthood. We were able to recapitulate the results previously shown, in that *dys-1(eg33)* worms

are significantly weaker than the WT control. NaGYY treatment attenuated the strength decline of *dys-1(eg33)* (Figure 3.1c)*.

Both DMD patients and *dys-1(eg33)* worms are known to display an altered gait, with patients displaying a waddling gait and worms displaying alterations in head and body bending [55],[180],[181]. Recently, CeleST- <u>*C. elegans*</u> <u>S</u>wim <u>T</u>est- has been developed as an objective method for assessing worm gait [170]. CeleST reports on eight different parameters, four of which are morphological and the other four are activity related. Activity-related parameters in *dys-1(eg33)* are shown in Figure 3.2a; these include wave initiation rate, travel speed, brush stroke, and activity index (Figure 3.2a). These activity-related parameters have previously been found to decline with age, [170] and *dys-1(eg33)* also showed a decline in all these parameters compared to WT (Figure 3.2a). Aside from travel speed, all parameters are modestly improved with NaGYY (Figure 3.2a). Body wave number, asymmetry, curling, and stretch are all morphological parameters that have all been shown to increase with age [170]. These four measures, apart from curling, are also increased in *dys-1(eg33)* compared to WT (Figure 3.2b). NaGYY drastically reduced the number of body waves and modestly improved stretch but did not impact curling or asymmetry (Figure 3.2b). These results suggested that DMD worms displayed gait abnormalities as in older worms and that NaGYY treatment improved most activity parameters but largely did not improve the morphological features of the DMD worms' altered gait.
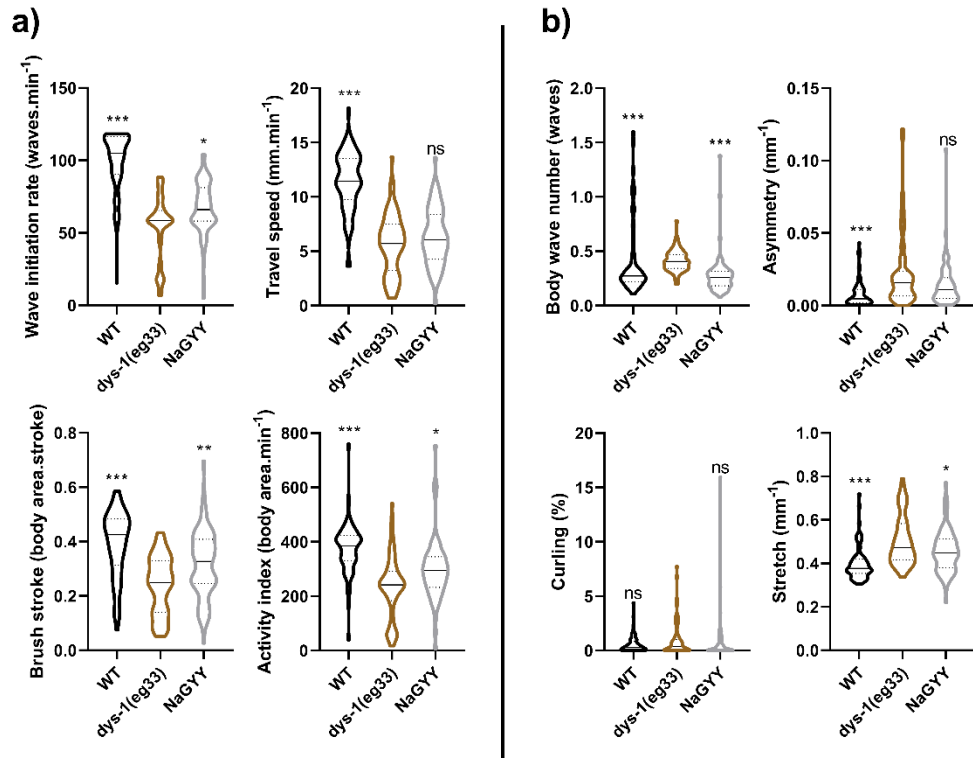
Figure 3.2. Effect of NaGYY on gait in dys-1(eg33).

a) Activity parameters that decline with age also declined in the DMD worm model. NaGYY (100 µM) improved wave initiation rate, brush stroke, and activity index but not travel speed. b) Morphological parameters which increase with age were also increased in the DMD model, with the exception of curling (no significant difference with respect to WT animals). NaGYY (100 µM) improved body wave number and stretch but did not improve asymmetry or curling. For all strains and treatments, *N*=74-79. Results were analysed using a Kruskal-Wallis test. All significance points compared to *dys-1(eg33)* ***P<0.0001, **P<0.01, *P<0.05, ns *P*>0.05.

3.3.2 Sodium GYY4137 does not improve lifespan but delays the onset of cell death in *dys-1(eg33)* animals.

In a previous study GYY4137 was shown to extend lifespan in ageing animals [155]. We therefore decided to assess whether NaGYY could extend lifespan in the *dys-1(eg33)* animals as well. Using an automated lifespan machine, we found that *dys-1(eg33)* (median 9 days, mean 9.5 days, and maximum 22 days) had a significantly reduced lifespan compared to WT (median 11 days, mean 11.5, and maximum 24 days). However, NaGYY did not significantly improve the lifespan of

the *dys-1(eg33)* animals (median 10 days, mean 9.8 days, maximum 21 days) (Figure 3.3a).

We also assessed muscle cell death in these mutants with NaGYY treatment as age dependent muscle cell death has previously been shown to be accelerated in *dys-1* mutants [46] and this acceleration was
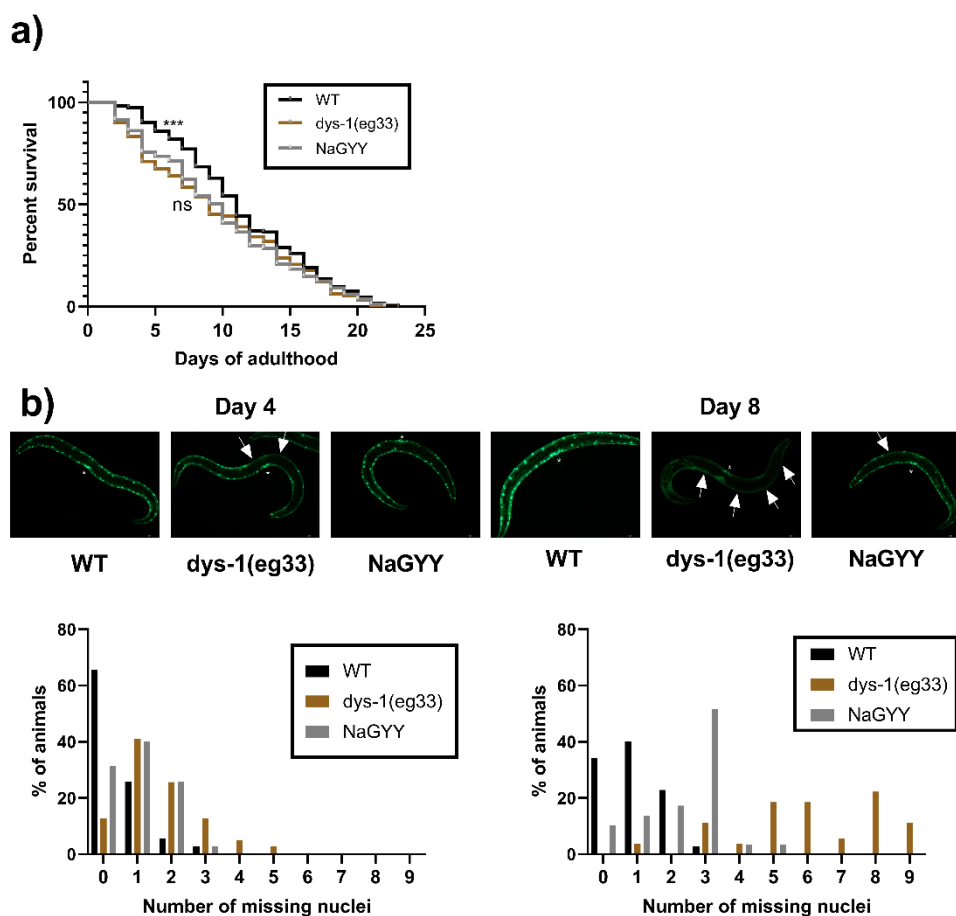
Figure 3.3. NaGYY did not improve lifespan of dys-1(eg33) animals but did delay the onset of cell death.

a) Lifespan curves were obtained using the NemaLife. *dys-1(eg33)* has a shorter median lifespan (9 days) than WT (11 days) but NaGYY (100 µM) did not appear to extend lifespan in *dys-1(eg33)* animals (10 days). For all strains and treatments *N*=274-315, from two biologically independent repeats. Results were analysed using Kaplan-Meier curves, with Bonferroni-corrected multiple comparisons. ***$P<0.01$, ns $P>0.05$. b) Representative images of muscle cell death in CB5600, CC91 and CC91 treated with NaGYY (100 µM). Muscle cell death (as identified by the absence of muscle nuclei) increased with age in all animals but is more severe in the *dys-1(eg33)* animals. NaGYY (100 µM) treatment appeared to slow the onset in cell death in *dys-1* animals. Vulva is identified by the * and arrows show the missing nuclei. For all strains and treatments *N*=30. Scale bar: 30 µm.

reduced with prednisone treatment [109]. We assessed cell death on Day 4 and Day 8 of adulthood as Day 4 was previously shown to be the earliest time point at which cell death could be detected in the *dys-1(eg33)* animals [46]. We found that NaGYY was able delay muscle cell death, suggesting an improvement in healthspan but not lifespan (Figure 3.3b).

3.3.3 Sodium GYY4137 improved mitochondrial structure in *dys-1(eg33)* worms.

Previously, improvements in thrash rate and strength in *dys-1(eg33)* with prednisone treatment was linked to the correction of the mitochondrial network [44]. To test if the mechanisms were similar between prednisone and NaGYY we therefore tested whether the beneficial effects induced by NaGYY shown in Figure 3.1 and 3.2, were due to improved mitochondrial structure. To assess the mitochondrial integrity of the muscle, we used the strain CC91 (*dys-1(eg33)* with GFP tagged mitochondria), which showed that *dys-1(eg33)* animals have a severely fragmented mitochondrial network, compared to WT animals of the same age (Figure 3.4a). H_2S has been shown to help in the maintenance of mitochondrial integrity with age [182], and unsurprisingly, NaGYY is also able to improve the mitochondrial structure of the *dys-1* mutants, confirming that it is able to improve muscle health (Figure 3.4a).

We therefore next examined the effects of both compounds on $\Delta\Psi m$ using the potentiometric fluorophore JC-10, which accumulates inside the mitochondrial membrane and exits the mitochondria based on

mitochondrial membrane potential [169]. Previously, prednisone had been shown to be not significantly improve $\Delta\Psi m$ [44]. This is also the case here, where NaGYY failed to improve $\Delta\Psi m$ suggesting that H_2S-mediated improvement of DMD worm health proceeds through similar mechanisms (i.e. mitochondrial structural improvement) as the clinically used drug prednisone (Figure 3.4b).
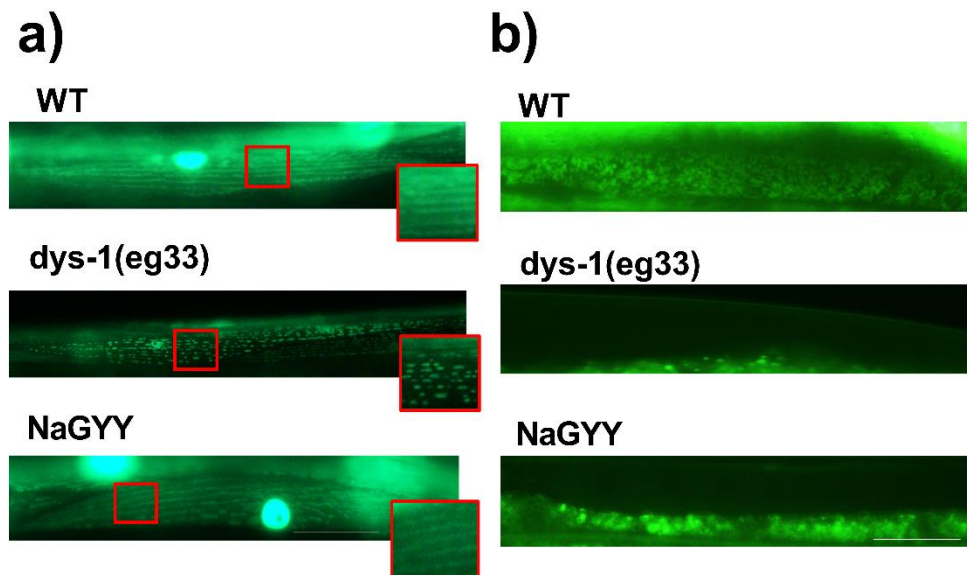
Figure 3.4. H_2S ameliorated fragmentation of the mitochondrial network does not improve defects in mitochondrial membrane potential

a) Representative images of CB5600 (WT with GFP tagged mitochondria) which displayed a tubular mitochondrial network. CC91 (*dys-1(eg33)* with GFP tagged mitochondria) which showed severe fragmentation of the mitochondrial network. NaGYY (100 µM) treated CC91 animals displayed a normal mitochondrial network similar to that of WT. For all strains and treatments *N*=20. b) JC-10 stained mitochondria in WT animals and *dys-1(eg33)* showed a severely depolarised mitochondrial membrane, which is not improved by NaGYY (100 µM) treatment. For all strains and treatments *N*=20. Scale bar: 30 µm.

3.3.4 Sodium GYY4137 partially improves calcium homeostasis but does not fully restore it.

Dysregulated calcium homeostasis is one of the pathophysiological events that underlies DMD, resulting in elevated cytosolic calcium levels [5],[183]. As calcium is thought to play an important role in regulating mitochondrial function, we were interested to see whether it was calcium handling that was being restored and consequently improving the mitochondria because of this, or whether it was due to direct improvement of the mitochondria themselves. To assess global calcium handling we used the HBR4 strain (which has the calcium sensor GCaMP3.35 in striated body-wall muscles) and HBR4 crossed with *dys-1(eg33)*. As expected, the *dys-1(eg33)* animals displayed elevated levels of calcium across all body wall muscles regardless of if the muscle was contracted or relaxed. NaGYY treatment of *dys-1(eg33)* animals was not able to restore overall global calcium changes (Figure 3.5a-5b).

To confirm this, we looked at levamisole sensitivity which is a potent cholinergic agonist of the major subtype of ligand-gated Ach receptors present on the postsynaptic side of the NMJ. Previously, *dys-1(eg33)* has been shown to be resistant to levamisole, indicating defects in postsynaptic excitation-contraction coupling [44]. NaGYY was not able to improve the resistance to levamisole either (Figure 3.5c).

Finally, although there were not global changes in calcium handling, we wanted to see if we could detect some subtler changes. We therefore took EPG recordings of stimulated pumping where each

contraction is associated with an action potential [184]. The traces for the *dys-1(eg33)* animals were significantly different from WT. They had a reduced frequency in pumping, an increase in pump duration, and an increased inter-pump interval (Figure 3.5d). NaGYY treatment significantly improved these measures but, like movement, not to WT levels. This is likely why we could not detect changes in global calcium handling.
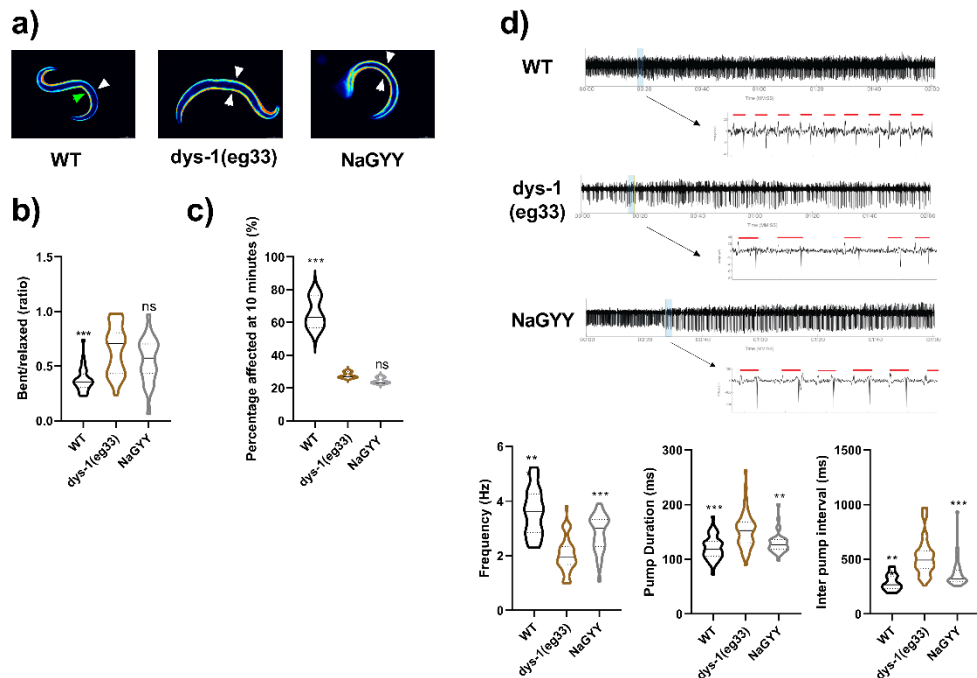
Figure 3.5. NaGYY partially restores calcium handling.

a) Representative images of calcium reporter strain in HBR4 (WT), HBR4xBZ33 (*dys-1(eg33)*), and HBR4xBZ33 treated with NaGYY. In WT animals, high levels of calcium can be detected on the contracted side (green arrow) of the body wall muscles with no calcium being detected on the relaxed side (white arrow). In *dys-1(eg33)* animals, high levels of calcium can be detected on both the relaxed and contracted sides. Treatment with NaGYY did not restore calcium handling b) Quantification of the relative ratio of calcium intensity for bent (contracted) side vs relaxed side. The ratio is higher than WT in *dys-1(eg33)* and is not restored by treatment with NaGYY. For all strains and treatments N=20. Scale bar: 30 µm c) *dys-1(eg33)* animals are resistant to levamisole compared to WT which become affected quickly after 10 minutes exposure. NaGYY (100 µM) does not improve this resistance. For all strains and conditions N=30 with three independent biological repeats, equating to 90 data points per bar. Results were analysed by one-way ANOVA. All significance points are compared to *dys-1(eg33)* ***$P<0.001$, ns $P>0.05$. d) EPG traces show a decline in pump frequency, an increase in pump duration, and an increase in the inter pump interval in *dys-1(eg33)* animals. NaGYY (100 µM) treated animals showed a partial improvement in these parameters. For all strains and conditions *N*=15 with two independent biological repeats, equating to 30 data points per violin. Results were analysed by one-way ANOVA. All significance points are compared to *dys-1(eg33)* ***$P<0.001$, **$P<0.01$.

3.3.5 Sodium GYY4137 improved movement response required the same genes in both older worms and DMD worms.

The mechanisms by which NaGYY treatment extended lifespan and improved healthspan had been assessed previously by examining changes in gene expression in response to treatment [136],[155]. Therefore, to determine if the mechanisms by which H_2S improved health in DMD worms were largely the same as those in ageing worms, we assessed the same genes in DMD worms. Additionally, the molecular mechanism(s) responsible for prednisone's clinical efficacy in DMD are still under investigation but at least part of the mechanism is likely due to its anti-inflammatory effects. Although *C. elegans* lack an inflammatory system and satellite cells [48], prednisone is still able to improve DMD worm health. We therefore wanted to determine whether the mechanism(s) by which NaGYY treatment improved DMD health were like prednisone.

RNAi was used to knock down the specific gene in the *dys-1(eg33)* animals and then they were treated with either NaGYY or prednisone to see whether there was an improvement in movement even in the absence of the gene. In ageing, *jnk-1(gk7)* and *skn-1(zu67)* mutants, treated with NaGYY, show no difference in lifespan [155]. In the absence of *jnk-1* and *skn-1* in *dys-1(eg33)* animals, neither NaGYY nor prednisone can give an improvement in movement. In fact, there is a further decline compared to *dys-1(eg33)* without RNAi or compound treatment (Figure 3.6a-6b). The *daf-16(mgDf50)* mutant treated with NaGYY, also does not show any difference in lifespan [155]. Knock down of *daf-16* in the *dys-1(eg33)* animals with NaGYY treatment show a slight

but insignificant increase in movement compared to *dys-1(eg33)*, demonstrating that *daf-16* is required for the full beneficial effect of treatment. Interestingly, prednisone is still able to give a significant improvement in the *dys-1(eg33)* animals even in the absence of *daf-16*. In the absence of *daf-16*, prednisone still resulted in a 30% increase in movement, compared to a 40% increase with *daf-16* present, this difference is not statistically significant (Figure 3.6c). Finally, mutant *sir-2.1(ok434)* animals treated with NaGYY show a shortening in lifespan compared to *sir-2.1* mutants without treatment [155]. Surprisingly, NaGYY can give a modest but significant improvement in the absence of *sir-2.1* in the *dys-1(eg33)* animals but prednisone seems to require its presence as there is no significant improvement in movement (Figure 3.6d). These results suggested that the mechanisms by which NaGYY treatment improved health with age, are likely the same mechanisms which improved health in DMD worms. They also imply that the mechanisms by which NaGYY and prednisone treatment improved health in DMD worms are broadly similar, but that insulin signalling did not appear to be a major component of the mechanisms by which prednisone improved health in DMD worms.
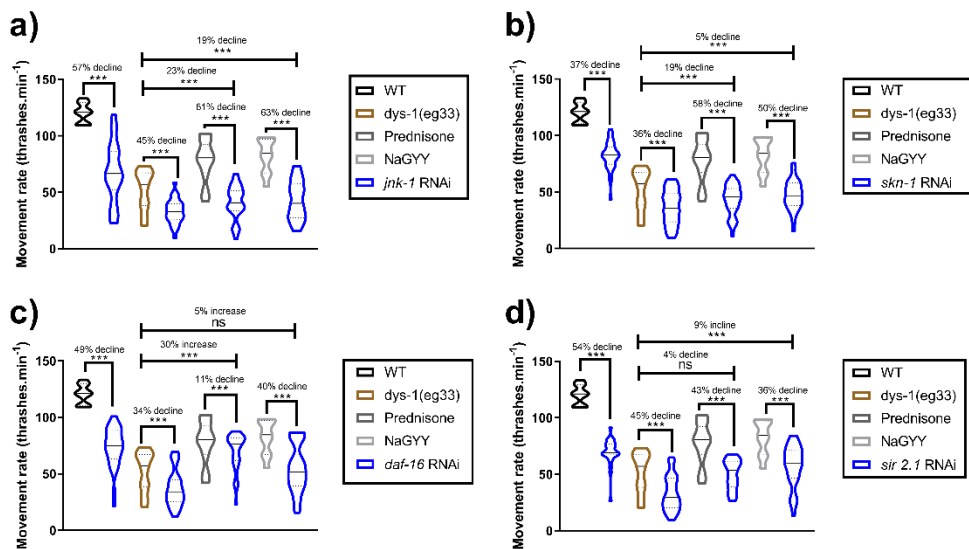
Figure 3.6. The effect of RNAi treatment on ageing and stress related genes, in relation to the mechanism of action of prednisone and NaGYY.

a) *jnk-1* is required for prednisone and NaGYY to have their beneficial effects. b) *skn-1* is required for prednisone and NaGYY to give an improvement in movement. c) Prednisone does not require the presence of *daf-16* for its beneficial effect but NaGYY does. d) NaGYY is not reliant on the presence of *sir-2.1* to give an improvement in movement but prednisone is. All strains and conditions *N*=10 with five replication and three biological independent repeats, equating to 150 points per violin plot. Results were analysed with a two-way ANOVA. ***P<0.0001, ns P>0.05.

3.3.6 Combined sodium GYY4137 and prednisone treatment does not provide additional health improvement in DMD worms

Prednisone's mechanism of action is still under investigation, and it does not improve all parameters to maximal capacity, implying that it is only correcting some of the underlying defects in patients and in the *dys-1(eg33)* model. There is increased evidence to suggest that future treatments in DMD will include combined therapies in order to optimise treatment efficacy [185]. As NaGYY and prednisone appeared to have similar beneficial effects acting via at least partially distinct mechanisms, we next investigated whether utilising a combined treatment of prednisone and NaGYY would provide a greater improvement in DMD

worm movement than the treatments being given independently. As shown in Figure 3.7, when 370 µM prednisone and 100 µM NaGYY were given in combination DMD worms experienced a decrement in movement. In fact, combination of prednisone and NaGYY made the worms movement worse than the *dys-1(eg33)* animals without any treatment, the beneficial effect of the drugs given independently was diminished. This result suggested an interaction between prednisone and NaGYY, perhaps due to overlapping mechanism(s) of action. To confirm that the interaction was reflective of the doses used in each treatment, we examined the dose dependence of the interaction. As shown in Figure 3.7, when either prednisone or NaGYY was used to treat DMD worms at the optimal dose (370 µM and 100 µM respectively) and the other treatment was given in combination at lower doses, DMD worm movement improved, though not to the level when either compound was given independently. These results suggested the interaction between the treatments was dose dependent (Figure 3.7).
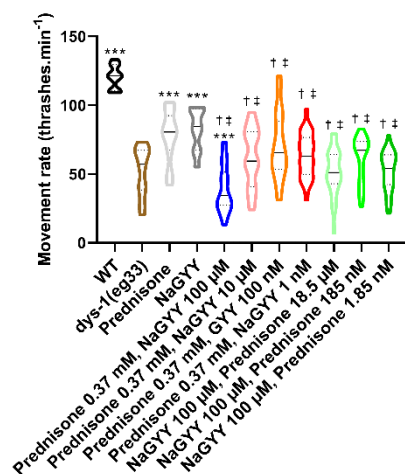
Figure 3.7. Independent compound treatment is better than combination therapy.

Combination therapy of prednisone and NaGYY did not provide increased beneficial effect. For all strains and conditions N=10 with five replicates and three biological independent repeats, equating to 150 points per violin. Results were analysed with a two-way ANOVA. Statistical significance compared to *dys-1(eg33)* ***P<0.0001. Statistical significance compared to prednisone † P<0.0001. Statistical significance compared to NaGYY ‡ P<0.0001.

3.3.7 Sodium GYY4137 given post developmentally rapidly improved health

Clinically, DMD patients are usually diagnosed before age five, where diagnosis is defined by the onset of associated symptoms [186]. Therefore, any potential treatment needs to be able to have a beneficial effect during childhood and ideally during adulthood as well. Previously, chronic treatment with H_2S has been shown to modulate the effects of age-related declines in muscle function and structure, yet insulin-like signalling has been shown to act in adulthood to regulate *C. elegans* lifespan [187]. Thus, we investigated whether NaGYY supplementation in adulthood was able to delay the movement decline in aged *dys-1(eg33)* animals. As shown in Figure 3.8a, DMD worms displayed a progressive decline in movement, as reported previously in ageing WT worms [152]. DMD worms were then grown to adulthood on non-compound plates. On Day 1 of adulthood, worms were transferred to NaGYY plates to see if acute treatment would be useful. Acute treatment with NaGYY on Day 1 of adulthood improved movement for at least the next two days (Figure 3.8b). Acutely treating DMD worms with NaGYY can yield improved movement in animals as old as Day 5 adults, as these animals exhibited higher movement 24 and 48 hours after treatment (Figure 3.8c-8f). These results confirm that improved DMD worm health from NaGYY treatment can be achieved into the post-reproductive stage for worms. As acute NaGYY treatment in adults gave an improved movement, we were curious how quickly movement could be improved in response to NaGYY treatment. As shown in Figure 3.8g, movement improved within 1 hour of

treatment with NaGYY for Day 1 adults (Figure 3.8g), indicating the ability

of NaGYY to rapidly improve animal movement.
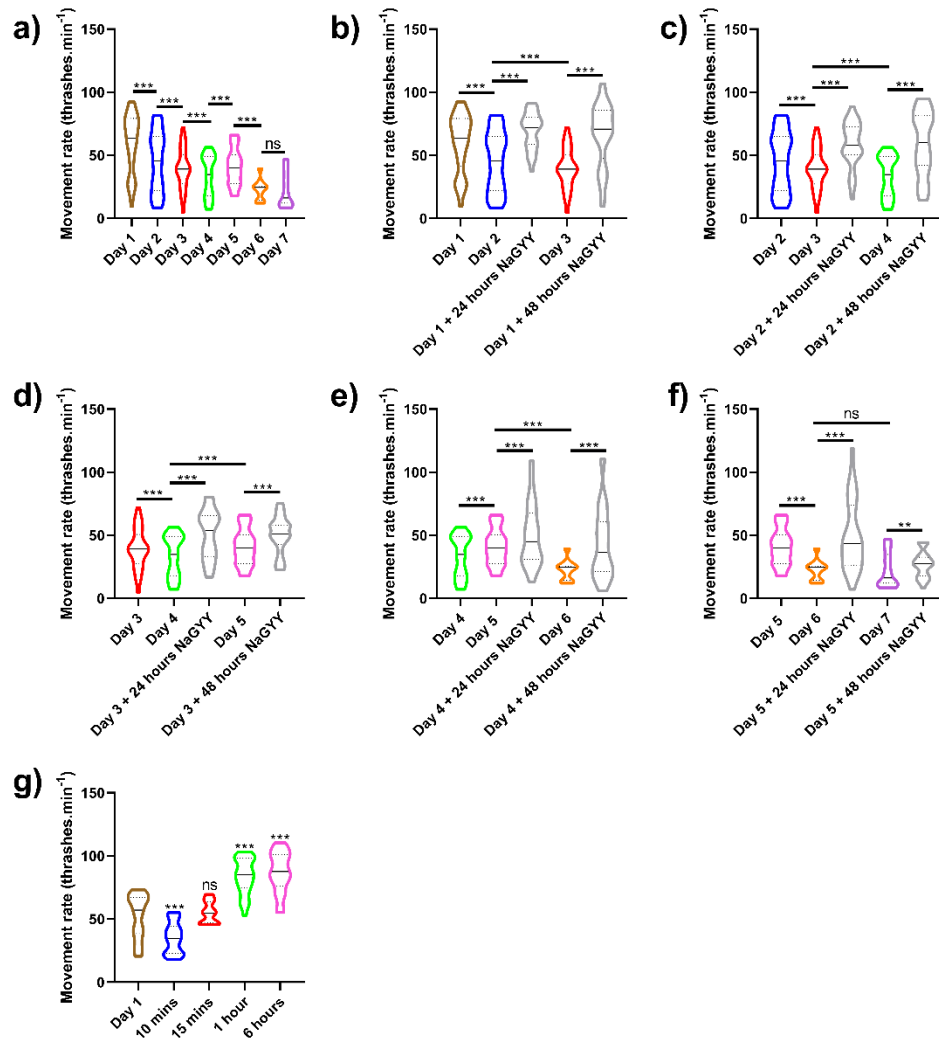
Figure 3.8. Acute treatment with NaGYY initially increased the movement capacity of dys-1(eg33) animals and delays the age-related movement decline.

a) *dys-1(eg33)* animals show a movement decline with age. b) NaGYY (100 µM) increased movement capacity of Day 1 adults and delayed the decline in movement through the 48 hour exposure. c) NaGYY (100 µM) increased movement capacity of Day 2 adults and delayed the decline in movement compared to untreated Day 2 adults. d) There is an increase in movement at Day 5 of adulthood at the end of the reproductive period, despite this, NaGYY (100 µM) was able to improve the movement capacity of the animals and delayed the movement decline. e) Having seen an increase in movement at the end of the reproductive period at Day 5 of adulthood, the movement decline can be seen again at Day 6 of adulthood. NaGYY (100 µM) is still able to give an improvement in movement and delay the movement decline seen with age. f) At Day 7 we are not seeing as severe decline in movement as we have been previously, NaGYY (100 µM) still gives an increase in movement. g) Short term treatments of Day 1 treated animals. 1 hour exposure time is required for NaGYY (100 µM) to start showing an improvement in movement. For all strains and conditions N=10 with five replicates and three biological independent repeats, equating to 150 points per violin. Results were analysed with a two-way ANOVA. ****P*<0.0001, ***P*<0.01, ns *P*>0.05.

3.4 Discussion

3.4.1 Chronic NaGYY treatment improved muscle health in *C. elegans* DMD model.

In the current study, NaGYY, an exogenous H_2S slow-releasing donor, has been demonstrated as a potential treatment of *C. elegans dys-1(eg33)* model. *C. elegans* DMD models have been used in the past to screen for compounds. In one of these screens, the gold standard treatment in patients, prednisone, was identified providing a proof-of-principle for the use of DMD models in the screening of compounds [109].

H_2S was previously considered a highly toxic gas to mammals but recent evidence demonstrated that it is endogenously produced in animals, which suggests that it may exhibit anti-apoptotic, anti-inflammatory, and have cytoprotective effects [188]. NaGYY has previously been demonstrated to modulate the effects of age-related declines in muscle function and structure in *C. elegans* and to modulate lifespan and heathspan [136],[155]. Due to similarities in loss of muscle function with age and in DMD worms, we tested if NaGYY could improve DMD health.

DMD patients usually present with difficulty walking and standing, with the majority needing a wheelchair by their 12th year [10]. Therefore, movement decline as assessed by a thrash assay in *C. elegans*, is a good indicator of problems with muscle physiology and neuromuscular function [169]. Previously, this assay has been used to detect movement decline in *dys-1(eg33)* and improvements were detected with prednisone treatment [44]. Having proved its utility, we opted to use this measure initially to determine if NaGYY was able to reverse the movement decline

and if so, what the optimal dose was. The optimal dose was selected based on the lowest dose that gave the largest improvement in movement rate, 100 µM (Figure 3.1a). This is also the same dose that has been used in ageing studies [136],[155]. NaGYY does improve movement of the *dys-1* model but it cannot restore movement to WT levels (Figure 3.1b). This could be because the treatments may only be improving some aspects of the underlying pathophysiology of the disease. A control compound has been used in this study which provides further evidence to demonstrate that it is likely the H_2S that has been supplemented, that is having the therapeutic effect. A limitation of this study is that we did not know what the drug concentration was inside of the animal, only the dose that we administered. However, the dose we used was the same as what has been reported previously with commercial GYY4137 [136],[155].

The ability to measure muscle strength in *C. elegans* is a relatively new concept but one that holds significant clinical relevance, in particular for DMD, where muscle weakness is one of the main symptoms in patients. Strength can be directly measured in *C. elegans* using a microfluidic NemaFlex device, without the need for a stimulus [171]. It has been demonstrated previously that *dys-1(eg33)* animals show a strength decline and prednisone gave a positive increase in strength [44]. Thrashing rate and muscle strength do not necessarily correlate and may not be reporting on the same aspects of muscle physiology. Having seen an improvement in thrash rate with NaGYY treatment, we wanted to validate this using the strength assay as a more direct measure of muscle

function. Not only do we see an improvement in strength with NaGYY treatment, the *dys-1(eg33)* treated animals are stronger than WT (Figure 3.1c).

We also assessed changes in gait in the *dys-1(eg33)* animals treated with NaGYY. Patients are often described as having an "unusual gait" and this also is the case in *dys-1(eg33)* animals. CeleST was used to assess gait and it provides readouts of four activity-related and four morphological parameters. Like in ageing worms, *dys-1(eg33)* shows a decline in the activity-related parameters (Figure 3.2a) and an increase in the morphological parameters (Figure 3.2b). NaGYY was able to improve three of the activity related parameters (wave initiation rate, brush stroke, and activity index) and two of the morphological parameters (body wave number and stretch) but in most cases not to WT levels. This further suggests that like prednisone treatment, NaGYY is only improving some of the underlying defects not all.

3.4.2 Mechanisms underlying prednisone and sodium GYY4137 treatment in improved DMD worm health.

The primary cause of DMD is the loss of or misfolding of dystrophin protein which results in a loss of membrane stability. In *C. elegans*, DYS-1 is required for the proper localisation of several calcium channels [82]–[84],[93]. The mis localisation of these channels disrupts calcium homeostasis resulting in elevated cytosolic calcium [81], a condition known to impair mitochondrial membrane potential [189]. We therefore wanted to determine whether the improvement in the nematode

physiology was due to an improvement in the dysregulated calcium homeostasis or the mitochondrial dysfunction (as has been shown previously with prednisone treatment [44]).

First, we wanted to explore if NaGYY was potentially acting through improving mitochondria dysfunction. *dys-1(eg33)* does not display major defects in its sarcomere structure but it does have severe fragmentation of the mitochondrial network [44]. NaGYY treatment was able to restore the mitochondrial network to one that resembled WT (Figure 3.4a). It is therefore sensible to assume that NaGYY treatment is improving thrash and strength assays by correcting some of the mitochondrial deficits. However, when we looked at mitochondrial function, using the mitochondrial dye JC-10, we did not see an improvement in the highly depolarised mitochondrial membrane which the *dys-1(eg33)* animals have, with NaGYY supplementation (Figure 3.4b). Thus, the underlying loss of calcium homeostasis in DMD worms [81],[95] does not appear to be corrected by either prednisone or NaGYY treatment since mitochondrial membrane potential is not restored by either treatment in DMD worms. This was confirmed by NaGYY's failure to restore global calcium homeostasis as determined using a strain with GCaMP in body wall muscles (Figure 3.5a-5b) and by NaGYY not improving the resistance to levamisole (Figure 3.5c). EPG traces confirmed altered electrophysiologic function in DMD worms, and NaGYY treatment did not fully restore normal electrophysiologic function in DMD worms (Figure 3.5d). Taken together, these results suggest that

calcium homeostasis is improved but not to an extent that allows for sustained improvements in mitochondrial membrane potential.

However, the improved structure of muscle mitochondria suggests that prednisone and NaGYY target mitochondria via an alternate mechanism. This raises the interesting question of whether prednisone and/or H_2S supplementation are acting in a manner similar to NAD supplementation, which has also been shown to be beneficial in worm and rodent DMD muscle, [111] or if they are acting in other ways to improve mitochondrial function to compensate for impaired membrane potential. The mitochondrial site of action likely explains the decreased cell death in response to NaGYY treatment (Figure 3.3b). Importantly, it has recently been shown that while NAD supplementation does improve rodent DMD muscle, it does not fix all elements of the pathology [190]. As H_2S acts on mitochondria we similarly do not anticipate that H_2S supplementation will fix all elements of the pathology, a suggestion supported by the lack of lifespan improvement despite cell death improvement (Figure 3.3a).

In addition to potentially having direct effects upon the respiratory chain, [136],[191]–[193] prednisone and H_2S could be improving health via activation of stress and/or adaptation pathways. Previously, *jnk-1*, *skn-1*, *daf-16*, and *sir-2.1* were shown to be required for the beneficial effects of H_2S treatment on *C. elegans* lifespan extension [155]. *jnk-1* is an orthologue of human MAPK, a stress activated protein kinase. *jnk-1* has previously been demonstrated as a positive regulator of lifespan, overexpression of *jnk-1* increased lifespan by ~40% [194]. In WT worms

106

treated with NaGYY there were no changes in *jnk-1* gene expression but there were some changes in downstream genes of the associated pathway. Additionally, when a *jnk-1* mutant was treated with NaGYY, there were no changes in lifespan, implying NaGYY requires MAPK signalling pathway to give lifespan extension [155]. Thus, as *jnk-1* was required for the full beneficial effects of both prednisone and NaGYY treatment in this model, it appears that one mechanism of action of both treatments is via improved stress tolerance (Figure 3.6a).

skn-1, orthologue of human NFE2 (regulator of oxidative stress and proteostasis, [195]), is a transcription factor that has been demonstrated to extend lifespan [195]. Similarly to *jnk-1*, WT worms treated with NaGYY did not show any changes in gene expression of *skn-1*. However, some genes that are under transcriptional control of *skn-1*, did have changes in their gene expression, suggesting *skn-1* might be changing the expression of these genes [155]. In the current study, both NaGYY and prednisone rely on the presence of *skn-1* to have its beneficial effect in *dys-1(eg33)* animals (Figure 3.6b). Thus, as *skn-1* was required for the full beneficial effects of both treatments, they appear to induce nuclear encoded gene expression, which may have accounted for the improved mitochondrial structure observed in response to both treatments.

daf-16, orthologue of FOXO family of transcription factors, is responsible for activating genes involved in longevity and stress responses. *daf-16* induces longevity by affecting several pathways, predominantly by reducing insulin signalling, although there are other

pathways that are also affected such as TOR, AMPK, and JNK signalling (reviewed in [196]). There are no changes in gene expression of *daf-16* in WT animals with NaGYY treatment and *daf-16* mutants with NaGYY show no difference in their lifespan [155]. Similarly, in the *dys-1(eg33)* model with *daf-16* RNAi and NaGYY treatment, there is no significant difference in movement compared to *dys-1(eg33)* alone. However, prednisone is still able to improve movement even in the absence of *daf-16* (Figure 3.6c). As *daf-16* was required for the positive effects of NaGYY but not prednisone treatment, altered expression of metabolic genes may underlie part of the mechanisms of action of NaGYY but not prednisone treatment. This observation is interesting given that prednisone can induce steroid diabetes with prolonged use [197],[198].

sir-2.1, orthologue of human sirtuin 1 (NAD-dependent deacetylase), is involved in many cellular processes including stress, cellular senescence, and ageing. Overexpression of *sir-2.1* causes an extension in lifespan and deletion of the gene shortens lifespan [199]. *sir-2.1* mutants with NaGYY treatment have a shorter lifespan compared to *sir-2.1* without NaGYY [155]. Both NaGYY and prednisone require *sir-2.1* for their full beneficial effect in the *dys-1(eg33)* model (Figure 3.6d). Thus, there is a common theme: genes required for the full therapeutic effects of prednisone and NaGYY are involved in the regulation of the stress response and mitochondrial gene expression. These observations seem consistent with the improved mitochondrial structure and overall animal health and suggest that DMD worms may be hypersensitive to

any external stressors such as the recently reported hypersensitivity to exercise [81].

Combination drug therapy has proven successful in several disorders, where usually two different drugs are given that work by different mechanisms. Combination therapy is being investigated in DMD, but no combined therapies are being used routinely currently. The main aim is to combine a therapy that corrects the genetic defect with a second that will improve the recipient muscles [185]. Here we combined prednisone and NaGYY treatment to see if this would give a synergist effect. This was not the case and had a detrimental effect on *dys-1(eg33)* health (Figure 3.7). This suggests that prednisone and NaGYY are likely acting through a similar mechanism, providing further evidence that NaGYY could be a safe alternative to prednisone. However, further examination of combination therapy involving prednisone and decreased insulin signalling might still be examined.

3.4.3 Acute NaGYY treatment improves muscle health in DMD *C. elegans.*

To date there is no routine new born screening diagnostic system for DMD. There have been several screening studies, but most have been discontinued, despite there being some evidence to suggest that starting therapies before the onset of symptoms could be more effective. Currently, diagnosis usually occurs in early childhood when the child begins to develop suggestive symptoms of DMD including weakness, difficulty with stair climbing and, toe walking. Therefore, any treatment

given needs to provide a beneficial effect in older individuals and in those with varying degrees of functional decline. Current guidelines for glucocorticoids initiation are it should occur before substantial physical decline and should be reduced/stopped if the side effects are unmanageable [11]. We wanted to assess whether NaGYY would be able to provide a beneficial effect in aged *dys-1(eg33)* animals. Reassuringly we found that NaGYY could provide a beneficial effect in early adulthood, during the reproductive period, and post reproduction. Not only did it slow the movement decline, but it also improved the movement initially as well. We also show that the beneficial effect from NaGYY treatment can be detected after only 1 hour (Figure 3.8).

3.4.4 The potential use of H_2S as a therapeutic treatment for DMD.

There has been increasing interest in the potential therapeutic value of gasotransmitters in a variety of disorders. Three main gasotransmitters have been identified to date: NO, CO and H_2S. The safety and tolerability of using gasotransmitters as therapeutic treatments is currently being explored. Some early examples include SG1002, a H_2S prodrug, which was shown to be safe and well tolerated in healthy and heart failure patients [200] and ATB-346, a H_2S-releasing anti-inflammatory and analgesic drug, which was shown to be a safer option in terms of gastrointestinal outcomes compared to naproxen which is used to treat pain and inflammation associated disorders [201]. This provides evidence that H_2S treatment could be a viable option for DMD patients. Here we show that both NaGYY and prednisone can improve

movement and strength in the *dys-1(eg33)* model. In both cases this is likely due in part to an improvement in mitochondrial network integrity. However, the mechanism of action is likely to be slightly different between the two treatment options as shown through our RNAi experiments. Although currently we do not know the full mechanism of how NaGYY is providing its beneficial effect, we would like to highlight that prednisone, the most prescribed treatment for DMD, its mechanism is also largely unknown. Prednisone is also used in the treatment of asthma and recent animal studies have suggested H_2S supplementation could be an alternative treatment [202]. Taken together, it is reasonable to suggest that H_2S compounds could be a good alternative to steroids without the undesirable side effects, but further study is required in this area.

The finding that NaGYY treatment recapitulated the beneficial effects of prednisone for DMD phenotypes in worms suggests that not only could H_2S be examined as a new potential treatment for DMD but also for greater understanding of why H_2S has therapeutic value. For example, enzymes involved in the synthesis of H_2S are known to translocate to the mitochondria in response to stress. In particular, CBS and CSE translocate to the mitochondria in response to hypoxia to sustain ATP production [203]. 3-MST is found in both the cytosol and the mitochondria, but predominantly in the mitochondria. If this is the result of mitochondrial H_2S depletion then it is likely that the supplementation is acting to restore some mitochondrial function, much like NAD+ supplementation has been shown to do [111]. Similarly, if increased H_2S

is improving mitochondrial function without altering membrane potential, the question arises of whether there are other treatments/mechanisms that could be similarly explored. Lastly, if it is mitochondrial H_2S that is producing the effect, exploring targeted delivery of H_2S may be worthwhile, as this could allow lower doses with fewer off target effects to be achieved.

3.4.5 Improving the clinical relevance of the DMD nematode model.

This study has utilised a handful of techniques that have not been used in the study of DMD nematodes before. These can be used to provide a greater clinical relevance to data obtained from this model. Movement decline is a well-known clinically relevant phenotype of this model and more recently this has been strengthened by showing they display muscle weakness as well [44].

In this study we used CeleST, a software used to assess multiple parameters associated with swim locomotion, to provide more descriptive measures than looking at thrash data alone [170],[178]. As DMD patients are often described as having an "unusual" or "waddling" gait, we were interested to see if the *dys-1(eg33)* animals had any changes in their gait as well. There are four morphological parameters (shown to increase with age) and four activity parameters (shown to decrease with age) that we have assessed using CeleST. The wave initiation rate is the number of head or tail bends over a set time period. This measure is intended to be akin to the manually recorded thrash assay, with similar values recorded. However, although we see similar patterns to our

manual thrash assay (a decline in *dys-1(eg33)* compared to WT and an improvement with NaGYY treatment), the raw values are lower in CeleST (Figure 3.2a). This could potentially be because the wave initiation rate looks at head or tail bends as opposed to body bends which are recorded in the manual thrash assay. Travel speed measures the longitudinal distance that an animal travels during a set period, and there is likely variability in the amount of movement across animals. There is a decline in *dys-1(eg33)* animals compared to WT (Figure 3.2a). This suggests that although the treated animals may be thrashing more, they're not moving as much around the swimming arena. Brush stroke measures the extent of movement and bending per stroke. This is also declined in *dys-1(eg33)* compared to WT (Figure 3.2a). Activity index provides a sense of how forcefully the animal bends whilst swimming. This is also declined in *dys-1(eg33)* compared to WT (Figure 3.2a). All the morphological parameters were increased in the *dys-1(eg33)* model, bar curling (Figure 3.2b). Body wave number measures the number of waves travelling along the body at a given time. Asymmetry reports if the animal bends more to one side than the other, there is increased asymmetry in the *dys-1(eg33)* animals compared to WT (Figure 3.2b). Due to its variability, we did not observe any significant differences in curling (Figure 3.2b). Curling measures how much time the animal spends bent around to the point that it overlaps itself. Stretch describes how deep or flat body bends are by finding the maximum difference ("stretch") between the two most extreme curvatures at any part of the body at a given stroke (Fig 3.2b). The four activity parameters thar decline with age also decline in DMD and the

113

four morphological parameters that increase with age also increase in DMD (Figure 3.2a-2.b).

Although lifespan decline has been shown previously in the *dys-1(eg33)* model compared to WT, in this study we used a microfluidic automated lifespan machine to carry out lifespan analysis. This machine (called the NemaLife [172]) removes a number of the issues associated with doing standard longevity assays on agar plates such as picking and transferring animals. This provides the opportunity in the future to carry out large-scale studies in the dystrophin model. It should also be noted that the WT lifespan is shorter than what we see in standard plate-based lifespan assays indicating that perhaps the animals are stressed in the automated machine.

Finally, we have shown that there are distinct changes in EPG traces in the worm DMD model. The pharynx is a muscular pump that contracts rhythmically during feeding and can potentially be used as a model for the vertebrate heart [184]. In ~40% of cases in DMD the cause of death is cardiac failure, so the ability to study cardiac dysfunction in model organisms is invaluable [10]. Our results raise the possibility of using the worm DMD model to gain greater mechanistic insight into DMD cardiac pathology as well as screening for compounds to ameliorate it.

3.5 Conclusion

This work demonstrates the beneficial effect of NaGYY on *dys-1(eg33)* health. Using clinically relevant phenotypes, we demonstrated the potential of H_2S releasing compounds in the treatment of DMD. NaGYY alleviated the loss of muscle strength and ambulation in the *C. elegans* model, which is likely due at least in part to improvements in the mitochondrial integrity. Control experiments performed using hydrolysed compound (incapable of generating H_2S) confirmed that the effects shown were due to H_2S and not either the parent compound or hydrolysis product. The mechanism of action of NaGYY requires further investigation, but we have shown that its mechanism overlaps with that of prednisone, which is also largely unknown. Given that prednisone and NaGYY do not provide any enhanced effect when used in combination, identifying a different class of drugs with a different mechanism could also be beneficial. Further study should also investigate H_2S compounds that are targeted and have a different delivery mechanism, given our results, a mitochondrially targeted H_2S compound could be highly beneficial. Overall, we provide evidence for the use of H_2S compounds in the treatment of DMD.

Chapter 4: Mitochondrial hydrogen sulfide supplementation improves muscle health in *C. elegans* DMD model.

4.1 Introduction

DMD and its underlying pathophysiology have been discussed extensively in Chapter 1 and further explored in Chapter 3. In brief, DMD is an X-linked recessive disorder that affects 1 in 3500 new-born males, making it one of the most common fatal genetic diseases diagnosed in children [9]. DMD causes progressive muscle weakness and atrophy of both skeletal and heart muscles [176]. DMD is caused by mutations in the dystrophin gene which is the largest known human gene encoding for the protein dystrophin [176]. Dystrophin forms part of the DGC which is important for muscle contraction and cell membrane stability. Lack of dystrophin results in the destabilisation of the DGC resulting in progressive fibre damage and membrane leakage [1]. There is little to no consensus regarding the pathophysiology of the disease but loss of calcium homeostasis and mitochondrial dysfunction have both been previously shown to underly the disease [5],[177]. There is currently no cure and the standard approved treatment, corticosteroids, have their own associated side effects meaning they can only be prescribed for a short period of time. Taken together, this highlights the need for steroid alternatives.

There are several animal models that are currently available to use in the study of DMD including rodents and canines. However, these systems have low throughput, are costly, and require ethical approval [29]. The nematode *C. elegans* is a good alternate model organism which has

contributed greatly to our understanding of human diseases including DMD [204]. The *C. elegans* genome encodes a dystrophin ortholog, *dys-1*, and mutations in *dys-1* have been shown to worsen muscle health [55],[100]. The majority of studies have used the *dys-1;hlh-1* model, which requires the *MyoD* mutation to cause muscle degeneration [62]. A more recent model, *dys-1(eg33)*, shows muscle degeneration without the need for a sensitised background and is arguably a better model of DMD in *C. elegans* [44],[46]. In Chapter 3 we highlighted the clinically relevant phenotypes of this model including movement and strength decline, gait changes, and demonstrated that *dys-1(eg33)* could also be used to study DMD cardiac dysfunction.

In Chapter 3, we identified the slow-releasing H_2S compound NaGYY as a potential treatment for DMD in *C. elegans*. Like mammals, *C. elegans* can synthesis H_2S endogenously through a combination of the following enzymes: CSE, CBS, and 3-MST. Therefore, as H_2S is naturally produced, its presence in treatments should not cause adverse effects at low doses [136]. We demonstrated that NaGYY improved muscle health in this DMD model and this is likely due in part to improvements in mitochondrial health.

To further understand the mechanism of action of H_2S in the treatment of DMD, we utilise the mitochondrial targeted H_2S donor, AP39. AP39 has a H_2S-donating moiety (dithiolethione) coupled to a mitochondrial targeting motif, triphenylphosphonium (TPP), by an aliphatic linker [205]. As AP39 acts directly on the mitochondria it can be used at a significantly lower dose than NaGYY, meaning toxicity is less

likely. AP39 has been demonstrated to have antioxidant and cytoprotective effects under oxidative stress conditions and as oxidative stress is involved in the pathogenesis of DMD it could be a good potential treatment [205],[206].

Here we demonstrate that AP39 (100 pM) improves muscle health in the *dys-1(eg33) C. elegans* model. Similarly, to NaGYY (100 µM), we can see a beneficial effect in muscle weakness and in both chronic and acute treatment on movement. This provides evidence that the beneficial effect we see with NaGYY (100 µM) treatment is indeed in part due to improvements in mitochondrial health. We then wanted to determine in what way was AP39 improving the mitochondria. Like NaGYY, we show improvement in mitochondrial structure and provide evidence that this is likely due to the donation of electrons to complex III of the ETC. Unlike NaGYY, AP39 did not alter calcium homeostasis showing that NaGYY is likely having unexplored off target effects and acting via alternative mechanisms.

4.2 Materials and Methods

4.2.1 Strains and culture conditions

The following strains were obtained from the CGC: Bristol strain N2 (WT, wildtype) and *dys-1(eg33)* (strain BZ33) which has a nonsense mutation in the *dys-1* gene. Mitochondrial network integrity was assessed using CB5600 [*ccIs4251* (*Pmyo-3::Ngfp-lacZ; Pmyo-3::Mtgfp*) I; *him-8 (e1489)* IV] and CC91 [*dys-1(eg33)* I; *ccIs4251* I; *him-8(e1489)* IV] (developed previously in this lab). HBR4 {*goeIs3* [*myo-3p::GCamP3.35::unc54 3' utr + unc-119*(+)]} and HBR4xBZ33 (generated in this lab), were used for calcium imaging. All strains were cultured on NGM seeded with a lawn of *E.coli* OP50 at 20°C (*2.1.2*). Animals for the study were age synchronised by washing plates with M9 buffer, and worms at the L1 stage were cultured on plates until adulthood (*2.2.1*).

4.2.2 Pharmacological compounds

AP39 was synthesised as previously described by us [167]. The compound was dissolved in DMSO and diluted in ddH$_2$O, before being added to the surface of a seeded NGM 3 cm Petri dish ~24 hours before use (*2.3.3*). A thrash assay was used to determine the optimal dose of 100 pM (dose response curve 1 pM- 100 μM was performed and 100 pM was the lowest dose to give a beneficial effect, Figure 4.1a) and this dose was used for all studies.

4.2.3 Movement assay

Animals were picked into a single drop of M9 buffer, and the number of rightward/leftward body bends were counted in 10 seconds (*2.5.2*). For each treatment, movement rates for ten worms were measured with three biologically independent repeats [169].

4.2.4 NemaFlex strength assay

Strength was measured using the NemaFlex microfluidic device as described previously [171] (*2.5.4*). One animal was loaded per chamber and one-minute videos were taken with a 5 x objective. Videos were then processed using an in-house-built image processing software (MATLAB, R2015b), where pillar deflections were transformed to a strength value. Approximately 30 worms were imaged per strain/treatment group.

4.2.5 Lifespan assay

Lifespan studies were carried out using the NemaLife system which is an automated microfluids lifespan machine (NemaLife Inc., TX). Around 70 Day 0 animals were loaded into microfluidics chips (Infinity chip, NemaLife Inc., TX) and survival analysis (daily videos) commenced on Day 1 of adulthood until the cessation of life. The acquired videos were scored for live/dead animals using the Infinity Code software (NemaLife Inc., TX) [172] (*2.6.1*).

4.2.6 Mitochondrial imaging

Animals were grown to Day 1 of adulthood and imaged to analyse the mitochondrial network. Animals used were CB5600 [*ccIs4251 (Pmyo-3::Ngfp-lacZ; Pmyo-3::Mtgfp*) I; *him-8(e1489*) IV] strain and CC91 [*dys-1(eg33*) I; *ccIs4251* I; *him-8(e1489*) IV]. CC91 animals, were also cultured on AP39 plates as described previously, prior to assessment of their mitochondrial network. Magnification used was 400 x (*2.7.1*). Approximately 20 animals were imaged per strain/condition.

4.2.7 Assessment of mitochondrial membrane potential

To assess mitochondrial membrane potential, JC-10 was used. Worms used were WT and *dys-1(eg33)* with and without AP39 treatment. These were incubated in 83 µM JC-10 for 4 hours prior to imaging. Representative images were taken at 400 × magnification with approximately 20 animals being imaged per strain/condition.

4.2.8 Determination of mitochondrial ATP production rate (MAPR)

MAPR was assessed on isolated mitochondria and determined luminometrically at 25°C as described previously [207] (*2.7.3/2.7.4*). Briefly, Day 1 age synchronised animals were homogenised using a Teflon pestle with saponin. The mitochondria were then isolated via centrifugation and resuspended in resuspension buffer. Mitochondria were then added to wells in a 96 well plate containing ATP monitoring reagent, ADP, and one of the following substrate combinations in duplicate: glutamate and succinate (GS); glutamate and malate (GM);

pyruvate and malate (PyM); palmitoyl-l-cartinate and malate (PalM); succinate (S); and ddH$_2$O. MAPR was calculated from the change in luminescence delivered by an injection with an ATP standard (*2.7.4*). Mitochondria was extracted from 250-300 worms with five biologically independent repeats.

4.2.9 Determination of maximal citrate synthase activity

Maximal citrate synthase activity was used to assess mitochondrial content as described previously [152] (*2.7.5*). Worms used were WT and *dys-1(eg33)*. Approximately 20 worms per strain/ treatment group were homogenised using a glass pestle and mitochondria was separated by centrifugation. The supernatant was measured spectrophotometrically at 412 nm to determine CS activity using a CS master mix. Five independent biological repeats were run.

4.2.10 Rotenone

Worms were grown to Day 1 of adulthood either with or without treatment as described previously (*2.2.1*). Approximately 30 animals were picked into 2 µM of rotenone and left for 24 hours at 20°C (*2.7.6*). Individual animals were picked out of the buffer and a thrash assay was carried out as described previously (*2.5.2*). For each treatment, movement rates for ten worms were measured with three biologically independent repeats.

4.2.11 Western blot

Western blots were performed to detect proteins that are part of the complexes from the ETC. Methods are described as in *2.7.9*. Briefly, 15 worms were picked into Laemmli buffer and boiled to denature the proteins. The whole sample was then loaded into the wells of a precast gel and separated by SDS-PAGE at 200 V for 1 hour. A wet transfer was then used for the transfer of proteins to the PVDF membranes. The membranes were then incubated overnight in one of the following primary antibodies prepared in TBST and 2.5% BSA: complex III (UQCRC2; ab14745; 1:3000), complex IV (MTCO1; ab14705; 1:3000), and cytochrome C (Cytochrome C; ab110325; 1:2000). The membranes were then incubated in the secondary antibody HRP-linked anti-mouse (Cell Signalling, 7076). Following IgG binding, the membranes were read on the Chemidoc and band intensity quantified.

4.2.12 Antimycin A

Worms were grown to Day 1 of adulthood either with or without treatment as described previously (*2.2.1*). Approximately 30 animals were picked into 2 µM of antimycin A and left for 24 hours at 20°C. Individual animals were picked out of the buffer and a thrash assay was carried out as described previously (*2.5.2*). For each treatment, movement rates for ten worms were measured with three biologically independent repeats.

4.2.13 ATP content

ATP content was determined as in *2.7.10*. Approximately 90 animals were picked into M9 buffer and snap-frozen. After three freeze-thaw cycles the supernatant was incubated in CellTiter-Glo reagent and luminescence read on a plate reader. Samples were normalised to protein concentration.

4.2.14 Measurement of calcium flux

A calcium sensor strain was used to measure calcium flux in real time. The strains used were HBR4 {*goeIs3* [*myo-3p::GCamP3.35::unc54 3′ utr + unc-119*(+)]} and HBR4 crossed with BZ33 (*dys-1(eg33)*) generated in this lab (*2.8.1*). Approximately 20 worms were imaged per condition/treatment.

4.2.15 Levamisole sensitivity assay

WT and *dys-1(eg33)* animals were exposed to levamisole hydrochloride at 100 μM in ddH_2O to assess differences in levamisole sensitivity. ~30 Day 1 animals were picked into levamisole and the number of paralysed animals were scored after 10 minutes. Each strain/treatment group had three independent biological replicates.

4.2.16 EPG recordings

All animals were synchronised to the L4 stage before being collected from the plates with M9 buffer (*2.2.1*). EPG recordings were taken using the NemaMetrix ScreenChipTM system using an SC30 chip. Each EPG recording was two minutes in duration and was analysed using the NemAquire software. Worms for each condition were analysed in two independent experiments with approximately 30 worms used per strain/treatment.

4.2.17 Statistical analysis

First normality was assessed using the D'Agostino and Pearson tests, and next the appropriate statistical test was selected based on normality. Statistical differences were assessed using either one-way ANOVA, two-way ANOVA, or Kruskal-Wallis test. Significance was determined as $P < 0.05$, and all statistical analyses were completed using GraphPad Prism (USA). Graphs are presented as violin plots.

4.3 Results

4.3.1 Mitochondrial targeted H_2S improves muscle health both chronically and acutely.

Previously, we have shown that the slow-releasing H_2S donor, NaGYY (100 µM), which is untargeted, improves functional defects in *dys-1(eg33)*. We wanted to determine whether the mitochondrially targeted H_2S donor, AP39, had the same beneficial effect and if so, what the optimal dose was. *C. elegans* locomotive behaviour is a good indicator of muscle function, in *dys-1(eg33)* animals we can detect defects in thrash rate [44],[169],[208]. We used a simple thrash assay to show that indeed AP39 can improve movement in the *dys-1(eg33)* animals and AP39's effect was observed from 1 pM-10 µM (Figure 4.1a). Optimal dose was selected based on the lowest dose that gave the most significant improvement in thrash rate which was 100 pM. We recapitulated the decline in movement in *dys-1(eg33)* animals and demonstrate that like NaGYY, AP39 (100 pM) gives a decline in movement on Day 1 of adulthood in WT animals but gives an improvement in dystrophic animals (Figure 4.1b).

Muscle weakness is one of the main symptoms seen in DMD patients and can also be detected in *C. elegans*. Strength measures can be obtained in *C. elegans* using the microfluids-based system called NemaFlex. Animals crawl through a forest of pillars and strength is determined based on pillar deflections [171]. Improvements in strength have been detected previously with various pharmacological interventions in the *dys-1(eg33)* model, including with prednisone[44] and

with NaGYY in Chapter 3. AP39 (100 pM) also gave a significant improvement in strength, further demonstrating an enhancement in muscle function with AP39 treatment (Figure 4.1c).

Another consequence of DMD is a shortened lifespan in DMD patients. Using an automated lifespan machine in Chapter 3 we were able to demonstrate that *dys-1(eg33)* animals have a shortened lifespan, but this was not increased by treatment with NaGYY. Here we show that
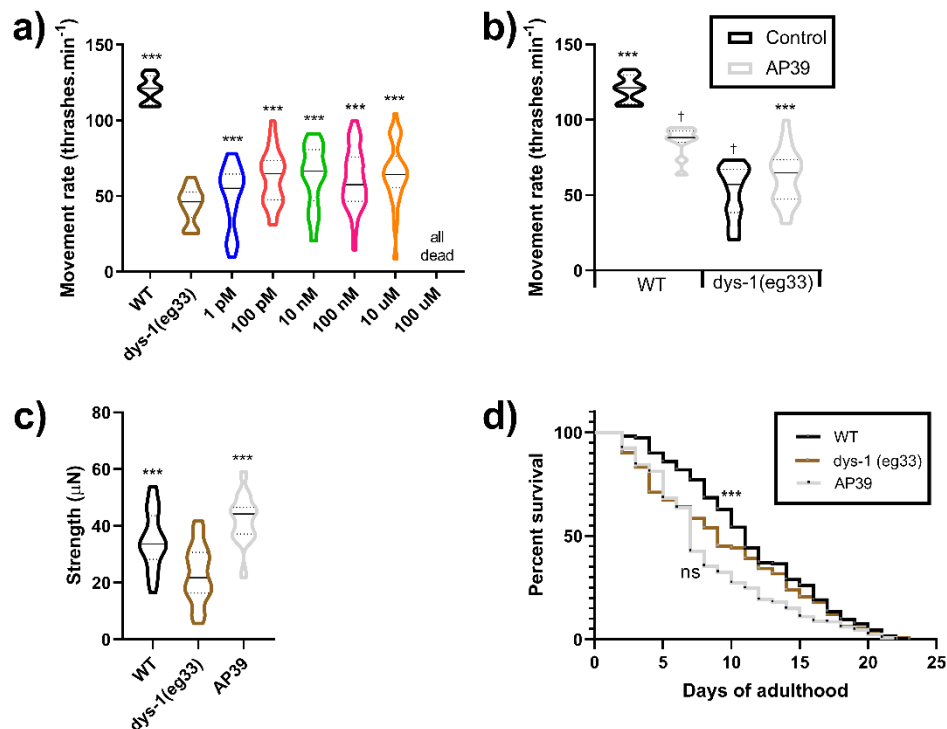
Figure 4.1. Effect of AP39 on movement, strength, and lifespan.

a) Dose-response curve of the thrash rate of *dys-1(eg33)* at different AP39 concentrations. AP39 treatment at 1 pM-10 µM significantly improved the trash rate of *dys-1(eg33)* ***$P < 0.001$. b) *dys-1(eg33)* has a lower thrash rate than WT. *dys-1(eg33)* is improved with AP39 (100 pM) but WT is not. For all strains and treatment N=10 with five replicates with three biological repeats for a total of 150 data points per violin. Results were analysed with a two-way ANOVA. All results compared to *dys-1(eg33)* ***$P<0.001$. c) The *dys-1* mutant has a decline in strength compared to WT animals. AP39 (100 pM) improved strength beyond WT. For all strains and treatment groups N=21-33. Results were analysed with a one-way ANOVA. All results compared to *dys-1(eg33)* ***$P<0.001$. d) Lifespan curves were obtained using the NemaLife. *dys-1(eg33)* has a shorter median lifespan (9 days) than WT (11 days) but AP39 (100 pM) did not appear to extend lifespan in *dys-1(eg33)* animals (8 days). For all strains and treatments N=274-315, from two biologically independent repeats. Results were analysed using Kaplan-Meier curves, with Bonferroni-corrected multiple comparisons. ***$P<0.01$, ns $P>0.05$.

AP39 treatment also does not increase lifespan in these animals (Figure 4.1d).

We also previously demonstrated that NaGYY can be given post developmentally, and this beneficial effect can be detected after only one hour from the treatment being given. Here we show that AP39 can also be given acutely but its maximal beneficial effect is detected after the animals have been exposed for a longer period. Animals were grown on
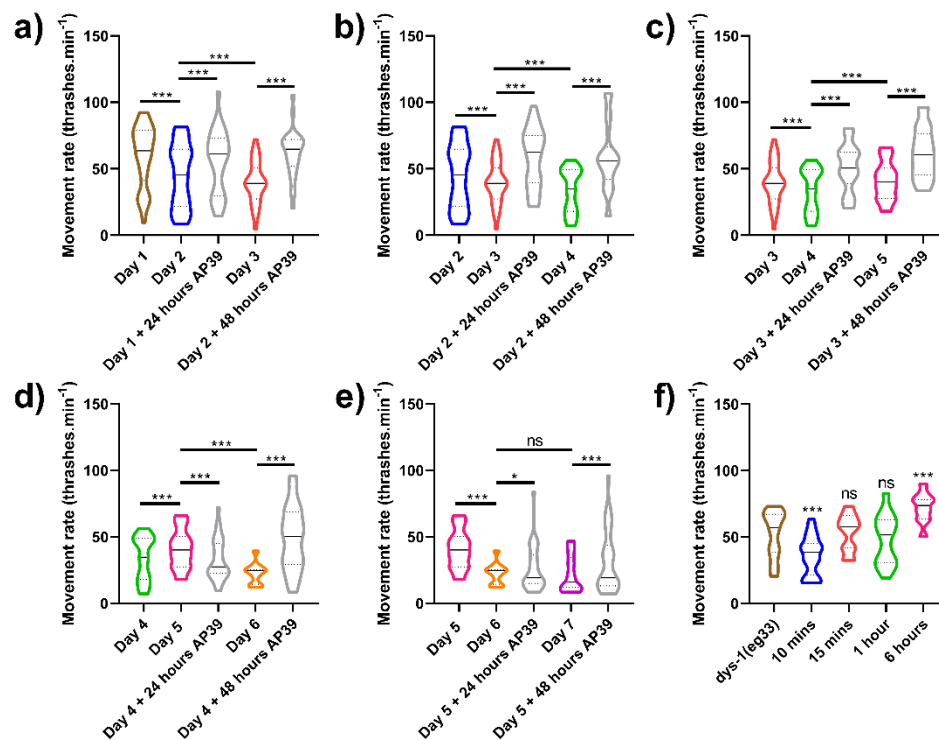
Figure 4.2. Acute AP39 treatment improves movement in aged dys-1(eg33) animals

a) *dys-1(eg33)* animals show a movement decline with age. AP39 (100 pM) treatment improves movement at both 24 and 48 hours. b) AP39 increased movement capacity of Day 2 adults and delayed the decline in movement compared to untreated Day 2 adults. c) There is an increase at Day 5 of adulthood at the end of the reproductive period, despite this, AP39 was able to improve the movement capacity of the animals and delayed the movement decline. d) Having seen an increase in movement at the end of the reproductive period at Day 5 of adulthood, the movement decline can be seen again at Day 6 of adults. However, AP39 was not able to improve movement at 24 hours but delayed the decline at 48 hours. e) At Day 7 we are not seeing as severe decline in movement as we have been previously. AP39 still gives an improvement in movement at this late time point. f) Short term treatments of Day 1 treated animals. 6 hours are required for AP39 exposed animals to display a beneficial effect. For all strains and conditions *N*=10 with five replicates and three biological independent repeats, equating to 150 points per violin. Results were analysed with a two-way ANOVA. ****$P<0.0001$, *$P<0.05$, ns $P>0.05$.

normal NGM plates before being transferred to drug plates and their movement was assessed after 24 hours and 48 hours. There is a decline in movement with age in the *dys-1(eg33)* animals apart from Day 5 where there is an increased movement, this is likely due to this time point being the end of the reproductive period, as movement drops of again at Day 6 (Figure 4.2a-2e). AP39 (100 pM) gave increased movement across all days apart from Day 5. This effect can be seen after 24 hours but is even greater after 48 hours, this is observed across all days (Figure 4.2a-2e). We next wanted to determine, how quickly AP39's effect could be detected in Day 1 adults, which was after 6 hours exposure (Figure 4.2f).

4.3.2 Mitochondrial H_2S improves some markers of mitochondrial health.

Mitochondrial dysfunction is a pathological feature of DMD in patients and in *C. elegans* dystrophic model. Previously, we demonstrated that part of NaGYY's mechanism of action was through improvements in mitochondrial structure but not mitochondrial membrane potential. We are now using a mitochondrial targeted H_2S compound, AP39, to further probe the mechanism of action of H_2S. We assessed mitochondria network integrity using our *dys-1* strain crossed with the CB5600 strain, which expresses GFP in the mitochondria and nuclei of body wall muscles. This strain (which we called CC91), shows severe fragmentation of the mitochondria network in *dys-1* animals. We have shown previously in Chapter 3 that NaGYY (100 µM) improved muscle health through correcting the fragmentation of the mitochondria network and this has been shown to correlate with improvements in

movement and strength [44]. Similarly, AP39 (100 pM) is also able to improve the mitochondrial structure of the *dys-1* mutants (Figure 4.3a).

We then evaluated the effects of AP39 on mitochondrial $\Delta\Psi$m using JC-10, a dye that accumulates and exits the mitochondria based on $\Delta\Psi$m. *dys-1(eg33)* has a severely depolarised mitochondrial membrane compared to WT. AP39 (100 pM) does not fully restore $\Delta\Psi$m but some stain seems to be retained indicating it is having a better effect that NaGYY potentially (Figure 4.3b).
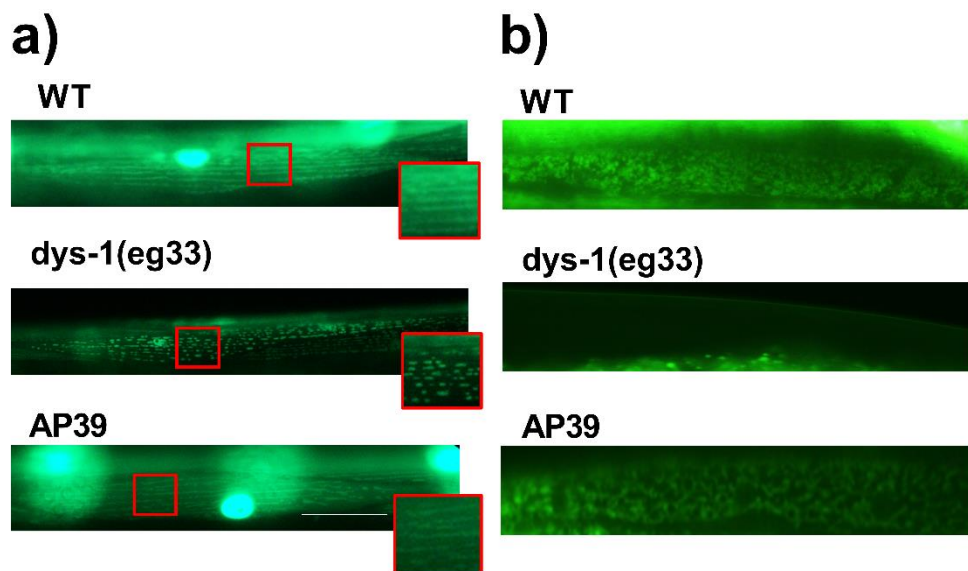
Figure 4.3. AP39 restores mitochondrial network integrity but does not correct mitochondrial membrane potential defect

a) Representative images of CB5600, (WT with GFP tagged mitochondria) which displayed a tubular mitochondrial network. CC91, (*dys-1(eg33)* with GFP tagged mitochondria) displayed severe fragmentation of the mitochondrial network. AP39 (100 pM) treated worms display a normal mitochondrial network like that of WT. b) Mitochondrial membrane potential was assessed using JC-10 dye. *dys-1(eg33)* have a severely depolarised mitochondrial network which is not fully corrected by AP39 (100 pM) treatment. Scale bar: 30 µM.

An inability to maintain mitochondrial membrane potential should lead to an inability to maintain ATP production due to a decreased proton gradient to drive hydrogen ions through ATP synthase. To explore this, mitochondria was extracted from age-synchronised populations and maximal mitochondrial function was measured *ex vivo* using the reaction of ATP with firefly luciferase [152]. Maximal rates of MAPR were determined luminometrically in response to a 150 pM ATP standard injection and the addition of respiratory substrates. A decline can be seen in all substrate combinations in the *dys-1* mutants, bar palmitoyl-L-carnitine plus malate and succinate. Unsurprisingly, AP39 (100 pM) was not able to significantly improve substrate utilisation other than succinate, but there is an upward trend in all substrates (Figure 4.4a).
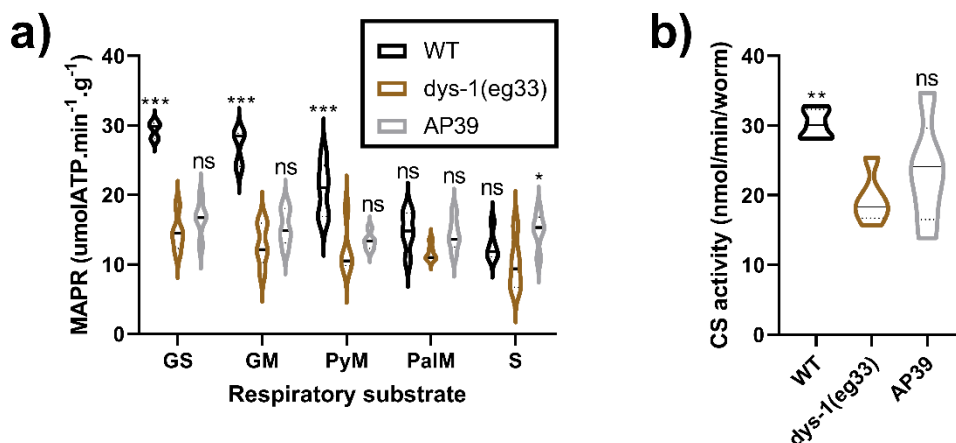
Figure 4.4. AP39 is not able to improve respiratory substrate utilisation in isolated mitochondria or increase mitochondrial content in the dys-1(eg33) animals.

a) Measurement of maximal rates of mitochondrial ATP production. Displayed are data for mitochondria isolated from Day 1 animals. Substrate combinations were (GS) glutamate and succinate; (GM) glutamate and malate; (PyM) pyruvate and malate; (Palm) palmitoyl-L-carnitine and malate and (S) succinate. There is a decline in GS, GM and PyM in *dys-1(eg33)* animals compared to WT, this is not remedied by AP39. Data are normalied to protein content. For all strains and treatments, on average N=250-300 worms with five biological repeats. Significance was analysed using two-way ANOVA. All significance compared to *dys-1(eg33)* ***P<0.0001, *P<0.05, ns P>0.05. b) Measurement of citrate synthase activity (CS); the standard marker of mitochondrial content. There is a decline in CS in *dys-1(eg33)* but this is not corrected by AP39 treatment. For all strains and treatments, N=50 with five biological repeats. Significance was analysed using two-way ANOVA. Significance compared to *dys-1(eg33)* **P<0.01, ns P>0.05.

Next, we assessed mitochondrial content by measuring citrate synthase (CS) activity, which has previously been shown to be a good biomarker for mitochondrial content. CS activity was determined from worm homogenate, and the *dys-1(eg33)* animals showed a decline in mitochondrial content compared to WT. AP39 (100 pM) was not able to rectify the decline seen in the *dys-1* mutant (Figure 4.4b). Thus, it seems that the mechanism(s) to improve muscle health are not associated with large overall improvements in ATP substrate utilisation or mitochondrial content.

4.3.3 Improvements in electron transport across the electron transport chain could underly improvements in muscle health.

A reduction in the maximal rate of respiration is well documented in both DMD patients and mice which has also been demonstrated here for the first time in the *C. elegans dys-1* model (Figure 4.4a). This deficit can be accounted for by reduced activity of the ETC, and previously H_2S has been shown to be an electron donor to the ETC [193]. There are two electron transport pathways in the ETC: Complex I/III/V which uses NADH as a substrate and complex II/III/IV, which uses succinic acid as its substrate. As shown in our MAPR response there is a significant reduction in complex I activity (GS) in *dys-1(eg33)* which is not improved with AP39 treatment (Figure 4.4a). To confirm this, we used rotenone which is an inhibitor of complex I and saw that there was a further decline
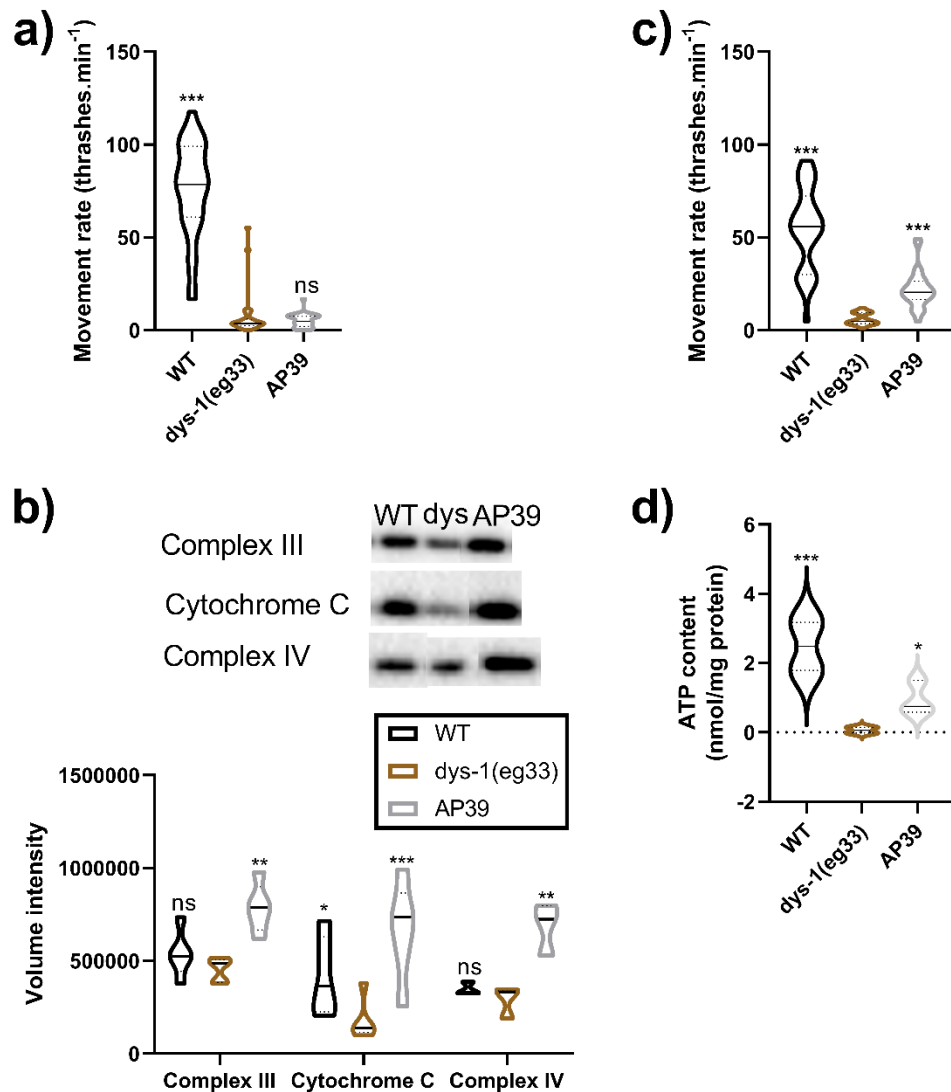
Figure 4.5. AP39 is potentially improving health via complex III/ cytochrome c/complex IV.

a) Rotenone was used to inhibit complex I of the ETC. There is a decline in movement in *dys-1(eg33)* compared to WT, which is not improved by AP39 treatment implying AP39 is not compensating for this decline. For all strains and treatment *N*=10 with five replicates with three biological repeats for a total of 150 data points per violin. Results were analysed with a one-way ANOVA. Significance compared to *dys-1(eg33)* ***P<0.001, ns *P*>0.05. b) Western blot of complex III, cytochrome C, and complex IV. There is a downward trend in *dys-1(eg33)* in each part tested but only cytochrome C was significant compared to WT. AP39 increased expression of each of the complexes tested. For all strains and treatment *N*=15 with five replicates. Results were analysed with a one-way ANOVA. Significance compared to *dys-1(eg33)* ***P<0.001, **P<0.01, *P<0.05, ns *P*>0.05. c) Antimycin A reduces movement in all strains but there is a significant improvement in movement with AP39 treatment. For all strains and treatment *N*=10 with five replicates with three biological repeats for a total of 150 data points per violin. Results were analysed with a two-way ANOVA. ***P<0.001. d) There is a decline in ATP content in the *dys-1(eg33)* animals compared to WT. This is increased with AP39 treatment but not to WT levels. For all strains and treatment *N*=90 with three biological repeats. Results were analysed with a one-way ANOVA. Significance compared to *dys-1(eg33)* ***P<0.001 and *P<0.05.

133

in *dys-1(eg33)* movement compared to WT. This was not improved with AP39 (100 pM) treatment (Figure 4.5a). As NADH/NAD+ has been shown to be depleted in the dystrophin mutants [111] and because we saw an increase in ATP production with succinate as a substrate in AP39 treated *dys-1(eg33)* (Fig 4.4a) we decided to focus on the alternative pathway.

We decided to assess the abundance of specific ETC proteins through western blot. We looked at complex III, cytochrome C, and complex IV. We did not see a difference in expression of complex III or IV in *dys-1(eg33)* compared to WT, but we do in cytochrome C. However, in *dys-1(eg33)* animals treated with AP39 we saw an increased abundance across all of these (Figure 4.5b). H_2S has been shown to feed electrons into the ETC to coenzyme Q which feeds into complex III and increases the transport of electrons through complex III [193]. *dys-1(eg33)* worms appear to have less complex III protein compared to WT, but this is not significant and likely due to the high variability in the *dys-1(eg33)* animals.

To confirm if complex III activity is compromised *in dys-1(eg33)* animals and if AP39 improves this, we used antimycin A which is an inhibitor of complex III. Previously, this treatment in WT animals has resulted in muscle damage through ECM degradation, and these animals resemble dystrophic animals [95]. We assessed movement rate of WT and *dys-1(eg33)* animals treated with antimycin A and there was a significant decline in both. AP39 (100 pM) treated animals with antimycin A move better than *dys-1(eg33)* animals with antimycin A treatment, implying that

AP39 may be working by compensating through this alternate pathway (Figure 4.5c).

Improving electron transport down the ETC should improve or maintain an electrochemical gradient which would result in an increase in ATP. To explore if this is the case, we measured ATP levels luminometrically after treatment with AP39. Unsurprisingly, we found that *dys-1(eg33)* animals have a decline in ATP compared to WT and with AP39 treatment, ATP content is increased (Figure 4.5d). It therefore seems reasonable to assume that part of AP39's mechanism is by donating electrons through complex III, creating an electrochemical gradient that then results in increased ATP levels.

4.3.4 Mitochondrial H_2S does not influence calcium homeostasis.

Along with mitochondrial dysfunction, dysregulated calcium homeostasis is a characteristic of DMD in both patients and in *C. elegans* [44],[81],[177]. It has recently been suggested that calcium increase occurs before any other phenotype, resulting in mitochondrial fragmentation and muscle degeneration [81]. H_2S has been shown previously to reduce intracellular calcium concentrations and regulate calcium channels [209],[210]. We therefore decided to explore the effect of AP39 on various aspects of calcium handling and excitation-contraction coupling.

To assess overall calcium flux in the *dys-1* animals we used a strain that contained a calcium sensor (GCaMP) in the body wall muscle. This allows us to measure changes in calcium levels during muscle

contraction. In WT animals there are high levels of calcium in the contracted muscle and none/little in the relaxed muscle. However, the *dys-1* animals contained elevated levels of calcium in both contracted and relaxed muscles demonstrating the known disrupted calcium homeostasis and elevated calcium levels. This was not altered by treatment with AP39 (100 pm) (Figure 4.6a-6b).

d*ys-1* mutants have been shown to have an altered response to neuromuscular agents, they're hypersensitive to aldicarb and have resistance to levamisole [44],[55]. In this case, we were interested to see whether AP39 was able to improve the defects seen in postsynaptic excitation-contraction coupling, using the levamisole assay. Similarly, we see that *dys-1(eg33)* has resistance to levamisole compared to WT. Treatment with AP39 (100 pM) was not able to induce paralysis in response to levamisole (Figure 4.6c).

Having not seen improvements in calcium homeostasis or an increased sensitivity to levamisole with the compounds, we decided to take a more in depth look at the electrophysiological readouts of neuromuscular function. EPG recordings were taken using the NemaMetrix ScreenChip™. This technique has multiple applications and effects have been observed both with ageing and in compound testing. With age there is a decline in pumping frequency and irregularities can be seen in traces [211]. Expectedly, here we show that the *dys-1* mutants also have a decrease in pump frequency and displays irregularities in

their pumping. However, AP39 (100 pM) treated animals did not show any improvements in their EPG traces (Figure 4.6d).
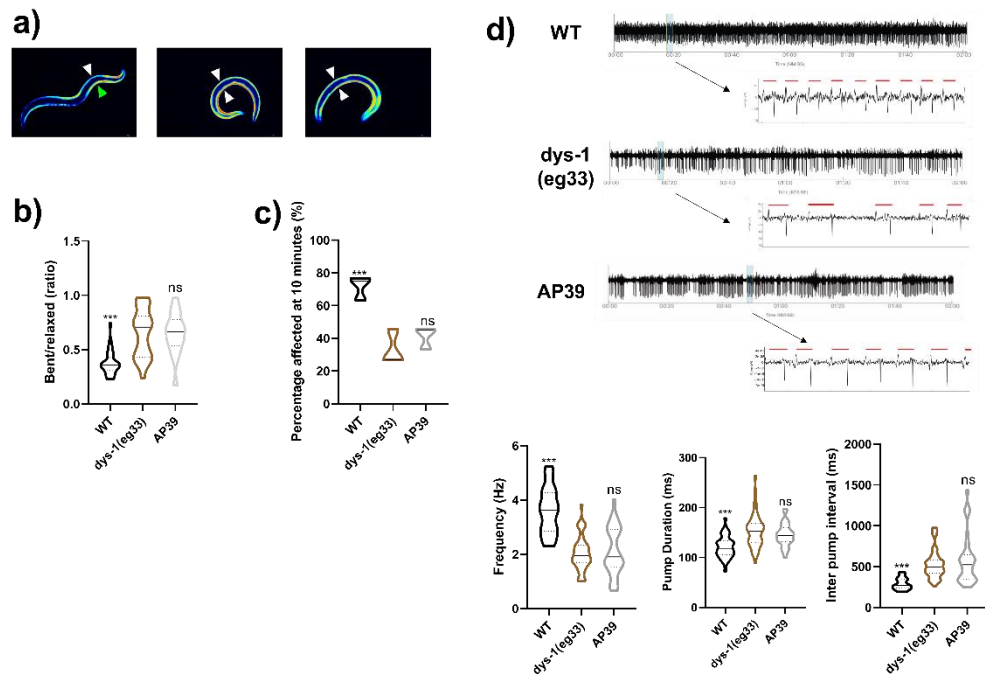
Figure 4.6. AP39 does not improve calcium homeostasis.

a) Representative images of calcium report strain in HBR4 (WT), HBR4xBZ33 (*dys-1(eg33)*)) and HBR4xBZ33 treated with AP39 (100 pm). In WT animals, high levels of calcium can be detected on the contracted side (green arrow) of the body wall muscles with no calcium being detected on the relaxed side (white arrow). In *dys-1(eg33)* animals, high levels of calcium can be detected on both the relaxed and contracted sides. Treatment with AP39 did not alter the *dys-1(eg33)* animals. b) Quantification of the relative ratio of calcium intensity for bent (contracted) side vs relaxed side. The ratio is higher than WT in *dys-1(eg33)* which is not restored by AP39. For all strains and treatments N=20. Scale bar: 30 µm. c) The *dys-1* mutant is resistant to levamisole compared to WT. This is not improved by treatment with AP39. For all strains and treatment N=30 with three independent biological replicates for a total of 90 data points per bar. Significance was analysed using one-way ANOVA. Significance compared to *dys-1(eg33)* ***P<0.005, ns P<0.05. d) Analysis of pharyngeal pumping activity, showing a decline in frequency in the *dys-1(eg33)* mutants compared to WT. AP39 did not significantly improve any of these parameters. Representative traces of EPGs recorded. All traces are two minutes long. The blue bar shows the zoomed-in trace with two second representations of the full trace underneath. The red bars show a single pump. For all strains and treatments, on average N=15 with two biologically independent repeats. Significance was analysed using one-way ANOVA. Significance compared to *dys-1(eg33)* ***P<0.001, ns P>0.05.

4.4 Discussion

4.4.1 Mitochondrial H₂S treated animals show similar improvements to muscle health as sodium GYY4137.

The *C. elegans* DMD model has been utilised greatly for the identification and screening of new compounds, from which the current gold-standard treatment prednisone was identified, providing evidence of the translatability between organisms [44],[109]. In Chapter 3 we demonstrated the potential of using H₂S compounds as a treatment for DMD. We showed that NaGYY, an untargeted slow-releasing H₂S compound, could be used to improve muscle health and this was likely in part due to improvements in mitochondrial health. In chronic diseases where long term use is anticipated, potentially delivering H₂S to a specific cell type could be a way to minimise off-target effects. In the current chapter, we have tested a mitochondrial targeted H₂S donor AP39 and have shown it improves muscle health in the *dys-1(eg33)* model. The improvements shown are like that of NaGYY but whereas NaGYY is given at 100 µM, AP39 can be used at the much lower dose of 100 pM. This is important as beyond a certain concentration, H₂S can become cytotoxic and suppress mitochondrial electron transport by inhibiting Complex IV [212].

The purpose of AP39 is to deliver H₂S to the mitochondria and it achieves this using TPP which is known to accumulate in the mitochondria [213]. The successful delivery of H₂S to the mitochondria through AP39 has been demonstrated previously, so it is likely that the effect we are seeing is due to the H₂S [205]. AP39 has been used successfully in cell and rodent models and has been shown to increase

antioxidants and have other cytoprotective effects under oxidative stress, improves outcomes of kidney transplants, improves neurological outcomes after cardiac arrest, and attenuates cell senescence [205],[214]–[219]. More recently we have also shown that AP39 combats the effects of ageing in *C. elegans* which led us to hypothesise that it may also be beneficial in the DMD model (unpublished).

We first wanted to determine if the beneficial effects we saw with NaGYY also occurred with AP39 as this would indicate that NaGYYs effect was largely mitochondrial as we expected. NaGYY was able to improve strength and movement both chronically and acutely but has no impact on lifespan. As mentioned earlier, AP39 can be used at a much lower dose than NaGYY and the optimal dose determined for the DMD model was 100 pM, although the therapeutic effect could be observed between 1 pM-10 µM (standard dose used in other studies is 100 nM). Movement decline has been demonstrated as a good measure of muscle health [169]. Similar to patients, a movement decline can be detected in the *dys-1(eg33)* model, and this is improved with AP39 (100 pM) treatment (Figure 4.1a-1b). Movement is not restored to WT levels implying that a mitochondrially targeted compound alone is not enough to restore levels back to normal. Furthermore, DMD patients exhibit muscle weakness in early life and so we have used a modified Nemaflex device that allows for muscle strength to be measured in *C. elegans* at earlier time points as well, making it more clinically translatable. Similarly to NaGYY, we saw an improvement in strength beyond that of WT (Figure 4.1c), which supports the previous notion that improvements in

strength is likely mitochondrial based [44]. Like NaGYY, AP39 also did not improve lifespan (Figure 4.1d).

Corticosteroids are the standard treatment given for DMD, but these are often discontinued after a couple of years due to side effects or lack of beneficial effect [220]. In addition, there is no evidence to suggest that there is a benefit to starting steroids in boys who have already lost ambulation [11]. Having shown that AP39 treatment can improve movement and strength chronically, we then wanted to determine whether AP39 could continue to give a beneficial effect in aged animals. Interestingly, we saw that at all ages tested, AP39 was still able to improve movement of the *dys-1(eg33)* animals, but this improvement was better after 48 hours exposure compared to 24 hours (Figure 4.2a-2e). This contrasts with what we see in NaGYY, where the movement increase starts to decline at 48 hours. This implies that AP39 could be a better treatment for long term use, especially coupled with its low dose (100 pM) compared to NaGYY (100 μM) and prednisone (370 μM).

4.4.2 Mechanisms underlying improvement in muscle health with mitochondrial H_2S.

There is increasing evidence to suggest that mitochondrial dysfunction is part of the underlying aetiology of DMD [8]. Tears in the sarcolemma from the absence of dystrophin, causes an increase in intra-cellular and inter-mitochondrial calcium. As mitochondria are calcium buffer systems, this increase in calcium results in swelling of the mitochondria and cell death [6]–[8]. In *dys-1(eg33)* animals, this can be

detected through fragmentation of the mitochondrial network [44]. Previously, we showed that NaGYY (100 µM) could improve mitochondrial structure back to that which resembled WT. Unsurprisingly, AP39 (100 pM) was also able to improve mitochondrial structure back to WT (Figure 4.3a).

Mitochondrial function was further assessed using the mitochondrial dye JC-10, which can be used to assess $\Delta\Psi$m. *dys-1(eg33)* animals have a severely depolarised mitochondrial membrane compared to WT, this is often a characteristic of impaired mitochondrial function [44]. We have shown previously that NaGYY (100µM) does not improve this and similarly, AP39 (100 pM) also does not appear to improve mitochondrial membrane potential either (Figure 4.3b). This suggests that AP39 is preserving mitochondrial integrity via an alternate mechanism. Although that being said, higher concentrations of H_2S have been used previously to normalise the $\Delta\Psi$m [221], so it could be that using a higher concentration here could warrant further investigation.

Mitochondrial membrane potential is generated by proton pumps (complexes I, III, and IV) of the ETC. Depolarisation of the mitochondrial membrane potential implies there is an issue with the transportation of protons down the ETC. If this is the case, we would also expect to see a decline in ATP production [222]. We therefore decided to assess MAPR in isolated mitochondria [207]. MAPR is the determination of the maximal rates of mitochondrial ATP production in response to respiratory substrates and the assessment of respiratory chain function using bioluminescence. It is a good method for assessing and diagnosing

141

disorders with a mitochondrial basis. Different combinations of respiratory substrates were tested to evaluate different aspects of the ETC. GS reports on the overall function of the ETC and provides evidence for maximal activity. GM are used to exclusively provide electron flow through complex I (NADH dehydrogenase). The substrate combination of PalM allows measurement of ATP synthesis from fatty acid β-oxidation. S allows for an assessment of complex II activity. A decline could be detected in GS, GM, and PyM in *dys-1(eg33)* compared to WT (Figure 4.4a). This is the first study to show a decline in ATP production rates in *C. elegans* DMD model, however, the results shown here are consistent with those previously determined in *mdx* mouse skeletal muscle [223]. As AP39 (100 pM) did not improve mitochondrial membrane potential, it seemed unlikely that it would improve overall ATP production rates. This was the case for maximal activity (GS), complex I activity (GM) and ATP synthesis from fatty acid β-oxidation (PalM) but not with complex II activity (S) (Figure 4.4a).

Several biochemical measures have been validated as markers for mitochondrial content instead of using TEM which is the gold-standard [224]. Among these measures is CS activity which we have used in this study to assess mitochondrial content. Mitochondrial content has been shown to decline in ageing [225] and in the DMD *mdx* mouse model [223]. Here we show for the first time a decline in mitochondrial content in the *dys-1(eg33)* model compared to WT (Figure 4.4b). Interestingly, AP39 (100 pM) did not increase mitochondrial content in the *dys-1(eg33)*

model. This is surprising as it restored the mitochondria network but not by increasing content.

AP39 has been shown previously to increase the electron transport at respiratory complex III, so we warranted this as requiring further investigation [193]. There are two points in the ETC where electrons can be fed in. The first is at complex I which uses NADH and NADH dehydrogenase enzymes and the second is at complex II which uses $FADH_2$ and succinate dehydrogenase enzymes. The electrons fed in at complex I go to complex III and V, whereas those from complex II go through complex III and IV [226]. Our previous findings in Figure 4.4a and earlier research, implied that any changes that were occurring in the ETC were likely in the latter pathway. To confirm if this was the case, we utilised the complex I inhibitor rotenone and the complex III inhibitor antimycin A. Previously, inhibition of the mitochondrial ETC caused paralysis and muscle cell damage in WT *C. elegans* [95]. Using these treatments enhanced the mitochondrial dysfunction which could be detected by a decline in movement in the *dys-1(eg33)* animals (Figure 4.5a and 4.5c). *dys-1(eg33)* animals pre-treated with AP39 (100 pM) were not able to improve this movement decline in the presence of rotenone (Figure 4.5a) but could in the presence of antimycin A (Figure 4.5c). This demonstrates that AP39 can reverse hypersensitivity to complex III inhibition and provides additional evidence that is it working intramitochondrial in DMD worms. So, like the previous research [193], AP39 is likely acting by increasing electron transport activity at complex III.

To further explore this, we looked at the expression of specific proteins in complex III, cytochrome C, and complex IV (Figure 4.5b). Although we did not detect a statistically significant decline in complex III or complex IV in *dys-1(eg33)* animals compared to WT, there is a downward trend, and we did detect a decline in cytochrome C (Figure 4.5b). AP39 (100 pM) increased protein expression in complex III, cytochrome C, and complex IV (Figure 4.5b). This strengthens our previous thoughts that AP39 is causing an increase in electron transport at complex III and consequently to cytochrome C and complex IV as well and/or encouraging the use of the substrate succinate through complex II/III/IV. This corresponded with an increase in ATP content with AP39 (100 pM) treatment (Figure 4.5d).

Although it is well-known that DMD shows evidence of oxidative stress [227] and H_2S has been proposed as an antioxidant [133], it is unlikely the beneficial effects of AP39 were due to "oxidant scavenging" or direct "antioxidant" activity. Firstly, the rate constants of reaction of bolus sulfide with physiological oxidants such as $O_2^{\cdot-}$, H_2O_2, ONOO- *in vitro*, even at concentrations several orders of magnitude higher than we have used (e.g. 5 mM NaSH), and in the absence of any competing biological milieu, it is far too slow to be physiologically relevant [228]. Secondly, H_2S generated *via* AP39 (100 pM) [167],[205] is likely to slow and resulting H_2S levels would be insufficient even after complete hydrolysis, to at least partially compensate for unfavourable reaction kinetics even in the absence of competing cellular substates.

4.4.3 Global calcium homeostasis is unaffected by mitochondrial H_2S treatment.

Dysregulated calcium homeostasis is an underlying crucial event in the pathophysiology of DMD. In particular there is an increase in intracellular calcium levels in contracting DMD cells [80],[183]. There is evidence to suggest that sarcoplasmic calcium increase occurs before any other phenotype [81]. Previously, elevated calcium levels have been detected in *C. elegans* DMD model by crossing *dys-1(eg33)* with ZW495 strain [*myo-3p::GCamP2 + lin-15(+)*] [81]. We generated a similar strain by crossing HBR4 with the *dys-1(eg33)* mutants that had GCaMP in the body wall muscles and these displayed elevated calcium levels. AP39 treatment did not reduce the calcium levels (Figure 4.6a-6b).

To evaluate changes in calcium homeostasis in muscle, we explored changes in neuromuscular function. Levamisole is a potent cholinergic agonist of the major subtype of ligand gated Ach receptors present on the postsynaptic side of the NMJ. Previously, *dys-1(eg33)* has been shown to be resistant to levamisole, indicating defects in postsynaptic excitation-contraction coupling [44]. AP39 (100 pM) failed to increase the sensitivity of the mutant, implying it is not improving the postsynaptic defect (Figure 4.6c).

As we did not see any changes with the cholinergic agonist, we decided to take a more in depth look at the electrophysiological readouts of neuromuscular function. The NemaMetrix ScreenChip™ was used to record electrophysiological activity. In brief, it is a microfluidic device that monitors activity of the pharynx producing an EPG. As we stated in

Chapter 3, this pumping action of the pharynx does not only enable us to look at calcium homeostasis but can also be a model for cardiac dysfunction which is one of the main causes of death in DMD patients [10]. DMD animals show a decline in pump frequency and exhibit other irregularities in pumping which is similar to what we see in ageing [211]. AP39 (100 pM) does not appear to be improving any aspects of the EPG traces which likely explains why we were not able to detect significant differences in the calcium sensor strain or levamisole assay (Figure 4.6d).

This is interesting as NaGYY (100 µM) also did not improve levamisole resistance, but it did alter the EPG findings. As shown in Chapter 3, it increased the pump frequency, reduced the pump duration, and reduced the inter pump interval in the *dys-1(eg33)* animals. This implies that NaGYY is not acting purely mitochondrially and is having off target effects (unsurprising as it is not a targeted compound). The *dys-1(eg33)* mutants have a decline in pump frequency and a larger interval between pumps, implying there are issues with the muscle contraction. This could be due to failed initiations of action potentials or more likely issues with depolarisation or repolarisation during an action potential, hence the longer pump duration. H_2S can interact with several different ion channels including ATP-sensitive potassium channels, L- type calcium channels, and large conductance calcium-activated potassium channels [229]. Without further investigation it is difficult to determine what off target effect(s) NaGYY is having to give improvements in the EPG

traces, it seems unlikely to be calcium based given the lack of improvement in the presence of levamisole.

4.4.4 Limitations with biochemical based assays in *C. elegans*

We have used several novel techniques in this chapter that have not been applied to *dys-1(eg33)* mutants previously. As we touched upon briefly in Chapter 3, data obtained from the *dys-1(eg33)* mutants is quite variable hence the need to run large numbers with multiple repeats to obtain statistical significance. The variability within these animals coupled with the variability in the techniques that have been used in this chapter, could explain in part why we are not seeing statistical significance in some of these experiments.

Firstly MAPR, the technique used to measure mitochondrial ATP production, requires intact isolated mitochondria from *C. elegans*. There are a couple of major issues with this technique. The first is starting with a large enough number of worms to obtain ideally 1 mg/ml of mitochondria. Most of the time this meant using multiple plates of worms which can cause variability in itself. The second is successfully isolating intact functional mitochondria, as no confirmation experiments were used (i.e. cytochrome c ELISA or western blot) we cannot be certain of the "quality" of the mitochondria isolated. Another issue is how quickly you must work once the mitochondria has been isolated and keeping everything at 4°C. The longer the experiment takes to run, the less activity of the mitochondria. All this combined can explain for the variability in the results. There is an upward trend in our results with AP39

(100 pM) treatment, if we were able to reduce the variability in this technique then we may see something statistically significant.

The CS assay is another biochemical assay that requires the isolation of mitochondria, but it does not have to be intact as for MAPR. In this case, CS activity was used as a biomarker to determine mitochondrial content but this is not the gold standard which is TEM [224]. We already know that mitochondrial content varies extensively between human subjects [224], so it is unsurprising that we see large variability in our mutants to.

Finally, western blots were used to look at protein expression of complex III, cytochrome C, and complex IV. Despite seeing an increase in expression with AP39 treatment (100 pM), we failed to detect an initial significant decline between WT and *dys-1(eg33)* animals in complex III and IV (Figure 4.5b). Usually, western blots are normalised to protein content to ensure equal loading [230]. However, as we know that *dys-1* mutants have differing levels of protein degradation [105], we did not feel that normalising to protein content was appropriate. Instead, we have normalised to worm number (15 worms per sample), but again as mentioned earlier this will also give us variability due to individual based variation.

4.4.5 Mitochondrial based therapies as potential treatments for DMD.

Currently, there is no cure for DMD, and treatment options are limited. The main approved treatment is the use of glucocorticoid medications, with the most common form prescribed being the corticosteroid, prednisone. Although the specific mechanism of prednisone is not fully known, long-term daily treatment has been shown to improve muscle strength and prolong independent ambulation from six months to two years longer than in those not receiving corticosteroid [13]. As with all steroid usage there are often several undesirable side effects. In the short term, these are likely to be weight gain and mood changes, and in the long-term, side effects include growth suppression, thinning of bones, and diabetes [13]. Our results suggest that compounds with a mitochondrial effect such as prednisone, NaGYY, and AP39, warrant further investigation for their efficacy in treating DMD.

As we touched on briefly in Chapter 3, combined therapies will probably be required in order to optimise treatment for DMD [185]. This will likely mean using a therapy to correct the genetic defect and a second one to manage other underlying pathological features of the disease. Exon skipping therapies have shown promising results [231]–[233] and combining H_2S treatment with one of these other emerging therapies could help to restore dystrophin expression and function. In addition, our data suggests that combining a mitochondrial based treatment with a calcium altering treatment (such as dantrolene or ryanodine) could also provide an enhanced effect in treating DMD.

4.5 Conclusion

The use of a mitochondrial targeted H_2S compound, AP39, has alleviated the loss of muscle strength and ambulation in the *C. elegans* DMD model. This has confirmed our previous speculation that NaGYY was largely acting mitochondrially but has highlighted that it was also having unexplored off target affects. AP39 (100 pM) is used at a much lower dose than NaGYY (100 μM) and prednisone (370 μM), so toxicity is less likely. Our acute experiments also demonstrate that AP39 could be better for long term use as its beneficial effect got better after a longer exposure. These improvements are in a large part due to improvements in mitochondrial integrity and function. We have demonstrated that H_2S is likely working by donating electrons to complex III of the ETC. This data highlights the need for further investigation in alternative models to *C. elegans*. Overall, we provide evidence for the use of H_2S compounds, including those which target H_2S delivery to mitochondria, in the treatment of DMD and raise important questions of the role of H_2S in the onset and progression of DMD pathology.

Chapter 5: The role of hydrogen sulfide and the sulfur amino acids in DMD.

5.1 Introduction

The focus of this thesis has been regarding DMD, its pathogenesis, and the lack of treatment options available. This has been discussed extensively in the earlier chapters but in brief it is a genetic disorder inherited in an X-linked recessive fashion and therefore is mainly associated with live male births [176]. It is well established that DMD is caused by mutations in the dystrophin gene which results in progressive muscle damage and degeneration due to the destabilisation of the DGC [1]. It is also known that the absence of dystrophin results in a loss of calcium homeostasis, mitochondrial dysfunction, and oxidative stress. Sadly, there is no cure for DMD but there are ways to help improve quality of life. These include physical therapy, occupational therapy, use of mobility aids, and medications. The most common therapeutic treatment is the use of steroids in the form of glucocorticoids. Steroids have been shown to increase the child's strength and functional ability and can delay the time to becoming wheelchair dependent. However, prolonged exposure to steroids comes with its own side effects and can only be considered as a palliative treatment [13].

Animal models have proven essential in furthering our understanding of DMD and to test potential treatment options. As demonstrated in Chapter 3 and 4, *C. elegans* is a good model for DMD and displays clinically relevant phenotypes that can be assessed, and the underlying pathophysiology is like that of humans. Chapter 3 and 4

have been focused on two H_2S compounds: NaGYY and the mitochondrial targeted H_2S, AP39. Both of which improved health of DMD animals. As we have discussed H_2S is produced naturally in humans and in *C. elegans* through a combination of the following enzymes: CSE, CBS, and 3-MST. All three of these enzymes partake in pathways associated with sulfur metabolism including the TMP and TSP. L-methionine is converted to L-homocysteine via the TMP using the enzymes SAMS, methyl transferase (PRMT) and s-adenosylhomocysteine hydrolase (AHCY). L-homocysteine can be recycled back to L-methionine via the RMP using the enzyme methionine synthase (METR). CBS and CSE can then catalyse L-homocysteine to homoserine and homolanthionine producing H_2S as a biproduct. L-homocysteine may also be converted to L-cystathionine by CBS and then L-cystathionine is converted to L-cysteine by CSE. L-cysteine is further broken down by the TSP; CBS and CSE catalyse the de-sulfhydration of L-cysteine to produce H_2S and, 3-MST generates H_2S by modifying the action of the CAT enzyme. L-cysteine may also be catalysed to L-glutathione via L-glutathione synthase enzymes and to L-taurine via three other enzymes including cysteine dioxygenase (CDO) [234]–[236]. This can be seen in Figure 1.6.

It has previously been demonstrated that there is a H_2S deficiency in dKO (utrophin/dystrophin) deficient mice and a decline in the protein expression of CSE and 3-MST in these animals [45]. We therefore wanted to determine whether there were alterations in sulfur metabolism in the *C. elegans* model of DMD and if this corresponded with a decline in H_2S

levels. Here we demonstrate that these animals have defects in sulfur metabolism and, there is a decline in global H_2S levels, both factors are improved by supplementation of NaGYY and AP39. To validate the beneficial effects of sulfur, we supplemented the SAA that form the basis of this pathway: L-methionine, L-homocysteine, L-cysteine, L-glutathione, and L-taurine. All the SAA improve health of the DMD animals in a similar but distinct manner to the afore mentioned H_2S compounds. This study provides evidence for the use of SAA as potential therapeutics in DMD.

5.2 Materials and methods

5.2.1 Strains and culture conditions

Strains obtained from the CGC were N2 (WT, wildtype) and BZ33 *(dys-1(eg33).* Mitochondrial network integrity and cell death was assessed using CB5600 [*ccIs4251 (Pmyo-3::Ngfp-lacZ; Pmyo-3::Mtgfp*) I; *him-8 (e1489)* IV] and CC91 [*dys-1(eg33)* I; *ccIs4251* I; *him-8(e1489)* IV] (developed previously in this lab). The calcium sensor strain used was HBR4 {*goeIs3 [myo-3p::GCamP3.35::unc54 39utr + unc-119*(+)]} (kindly donated by Professor Higashitani) and this was crossed in this lab with BZ33 to give the strain HBR4xBZ33. All worms were cultured at 20°C on NGM agar plates seeded with *E. coli* OP50 (*2.1.2*). Animals for the study were age synchronised by washing plates with M9 buffer, and worms at the L1 stage were cultured on plates until adulthood (*2.2.1*).

5.2.2 Pharmacological compounds

NaGYY was synthesised as described previously [164], the compound was dissolved in ddH$_2$O and added to the surface of a 3 cm seeded NGM plate approximately 24 hours before use (*2.3.2*). The concentration used was 100 µM as determined in Chapter 3. AP39 was synthesised as described previously [167], the compound was initially dissolved in DMSO and further diluted in ddH$_2$O before being dispensed onto the surface of a 3 cm seeded NGM plate approximately 24 hours before use (*2.3.3*). The concentration used was 100 pM as determined previously in Chapter 4. All SAA were diluted initially in ddH$_2$O before being added to the surface of a seeded 3 cm NGM agar plate. Optimal

concentrations were determined by thrash assay and are as followed: L-methionine 10 mM, L-homocysteine 10 µM, L-cysteine 10 µM, L-glutathione 100 µM, and L-taurine 10 µM (*2.3.4*).

5.2.3 H$_2$S detection in *C. elegans*

H$_2$S levels were determined through incubation with the fluorogenic probe AzMC. Briefly, 90 Day 1 adults were picked into M9 buffer, and three freeze-thaw cycles were performed in liquid nitrogen. Samples were incubated in 50 µM AzMC for two hours at 20°C and fluorescence read on a BMG fluorostar plate reader. Samples were normalised to protein content determined via the standard Bradford assay [173] (*2.9.1*).

5.2.4 mRNA quantification via RT-qPCR

Total RNA was extracted from Day 1 nematodes using the TRIzol method as previously described [175]. Reverse transcription to cDNA was carried out using oligo(dT) priming according to manufactures protocol (PrimeScript™ RT Reagent Kit, Takara). Real time PCR was performed using TB Green Premix Ex Taq™ II (Takara) on a CFX Connect™ Real-Time PCR Detection System (Bio-Rad). Relative fold change was determined by 2$^{-\Delta\Delta CT}$ method and normalised to the housekeeping gene, *eef-2*. This was selected using the reference gene selector tool on GeNorm. Primer sequences can be found below and were selected from the ORFeome project [237] (*2.9.2*).

Table 5.1: Primers used in RT-qPCR

Gene	Forward primer	Reverse primer
sams-1	TGTCCTCCAAATTCCTTTTCACC	AGTGAGCGATAGCAGATGT
prmt-1	TGAGTACCGAAAACGGGA	AGTGCATGGTGTAGGTGT
ahcy-1	TGGCCCAGTCTAAGCCAGCTTAC	AATATCTGTAGTGGTCTGGCTTGT
metr-1	TGACTCGAAGTAGTCTTTTCGAGG	AATCCGTATCATAGCCAAGAATTGGT
cdo-1	TGATGTTAGTTGTTCAAATTCGTGAAA	AATTGCCATTCTTAGATCCTCTGT
CSE-2	TGGCTACTTTCCCACACT	ATACTTTTGGAATGGCAATCTTCA
3-MST-4	CCTGTCTTTTGCCTGCCTAC	GCAGAACAATTGAAGCGACA
eef-2	TGGTCAACTTCACGGTCGAT	CATCTTGTCGAGATAGTTGTCAAGG

5.2.5 Thrash assay

The motility of *C. elegans* was assessed by picking individual animals into a liquid medium (M9 buffer) and counting the frequency of thrashes (*2.5.2*). For each treatment, movement rates for ten worms were measured with three biologically independent repeats [169].

5.2.6 Mitochondrial and cell death imaging

To assess the mitochondrial network, the CB5600 [*ccls4251 (Pmyo-3::Ngfp-lacZ; Pmyo-3::Mtgfp*) I; *him-8(e1489)* IV] strain and CC91 [*dys-1(eg33)* I; *ccls4251* I; *him-8(e1489)* IV] strain were used for WT imaging and dystrophy imaging respectively. Approximately 20 worms were imaged per strain, having been grown to Day 1 of adulthood either with or without a SAA (*2.7.1*). The same strains were used to evaluate cell death as described previously [46]. Briefly, images were taken on Day 4 and Day 8 of adulthood and after animals were assessed for missing cell nuclei which is a marker of cell death. Approximately 20 animals were assessed per condition (*2.7.1*).

5.2.7 Calcium imaging

The calcium concentration in the body wall muscles of *C. elegans* was determined from HBR4 {*goeIs3 [myo-3p::GCamP3.35::unc54 39utr + unc-119*(+)]} and HBR4xBZ33 animals. Approximately 20 animals per condition were imaged. The intensity of the GFP was quantified using ImageJ software (*2.8.1*).

5.2.8 Levamisole assay

Approximately 30 Day 1 adult worms were picked into 2.5 ml of levamisole hydrochloride at 100 µM in M9 buffer. The percentage of animals paralysed at 30 minutes was recorded. For each experiment there were three biological independent repeats (*2.8.2*).

5.2.9 Development of animals on RNAi

Clones were obtained from the Open Biosystems Vidal Library. Clones used were as follows: *jnk-1*: B0478.1, *skn-1*: T19E7.2 and *daf-16*: R13H8.1. *sir-2.1*: R11A8.4 clone was obtained from the Ahringer library. The RNAi feeding method was utilised in this case, where worms were fed bacteria expressing dsRNA [168]. L1 worms were synchronised as described previously onto RNAi plates containing a bacterial lawn expressing one of the RNAis. Worms were left to develop at 20°C until Day 1 of adulthood where a thrash assay was then carried out (*2.4.2*).

5.2.10 Statistical analysis

Normality was initially assessed using the D'Agostino and Pearson tests, and then the statistical test was selected based on normality. Statistical differences were assessed using either one-way ANOVA, two-way ANOVA, or Kruskal-Wallis test. Significance was determined as $P < 0.05$, and all statistical analyses were completed using GraphPad Prism (USA). Graphs are presented as violin plots.

5.3 Results

5.3.1 C. elegans DMD animals have altered levels of enzymes associated with sulfur metabolism and have reduced H_2S levels.

In a pilot study it was established for the first time that there was a reduction in sulfide levels and in H_2S producing enzymes in dKO DMD mice [45]. In Chapter 3 and 4 we demonstrated that supplementation of the H_2S compounds NaGYY and AP39 could improve health in DMD *C. elegans* implying a deficit was likely in these animals too. To determine if there were alterations in sulfur metabolism in the DMD animals we performed RT-qPCR experiments on several enzymes that form part of the pathways associated with sulfur metabolism. *dys-1(eg33)* animals have increased expression of SAMS (responsible for one of the stages to convert methionine to homocysteine) and reduced expression of CDO (responsible for one of the stages to convert cysteine to taurine) and 3-MST (one of the H_2S generating enzymes) compared to WT (Figure 5.1a). NaGYY and AP39 treatment of *dys-1(eg33)* animals caused an increase in expression of SAMS, CDO, CSE (another H_2S generating enzyme) and 3-MST (Figure 5.1b). No significant differences were observed in PRMT, AHCY, and METR, all of which are part of the TMP and RMP (Figure 5.1a-1b). This data implies that there are alterations in sulfur metabolism in the *dys-1(eg33)* animals as suspected and supplementation of H_2S compounds increased the expression of some of these enzymes. We next wanted to see whether the alterations in sulfur metabolism corresponded with a decline in H_2S levels. We have utilised a method that uses the H_2S fluorgenic probe AzMC to measure H_2S levels in *C. elegans* [174]. There was a decline in global H_2S levels

in the *dys-1(eg33)* animals compared to WT as expected, and supplementation with NaGYY and AP39 increased H_2S levels. In fact, AP39 boosted levels back to WT (Figure 5.1c).
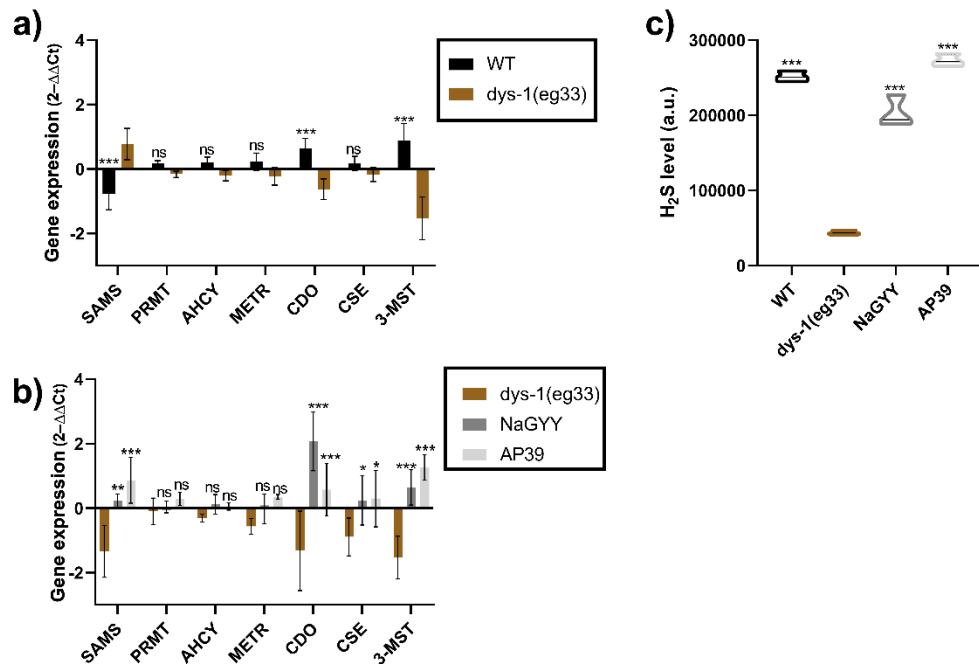
Figure 5.1. DMD animals have alterations in their sulfur metabolism and H_2S levels are reduced.

a) Relative quantification mRNA levels of enzymes associated with sulfur metabolism in WT and *dys-1(eg33)* animals. An increase can be seen in SAMS (s-adenosylmethionine synthetase), and CDO (cysteine dioxygenase) and 3-MST (3-mercaptopyruavate transferase) were declined in *dys-1(eg33)* animals. b) Increased expression can be seen in SAMS, CDO, CSE, (cystathionine-γ-lyase) and 3-MST with NaGYY and AP39 treatment. There were no differences in PRMT (methyl transferase), AHCY, (s-adenosylhomocysteine hydrolase) or METR (methionine synthase). *N*=3 repeated experiments. Results were analysed with a two-way ANOVA. All significance points are compared to *dys-1(eg33)*. ***P<0.0001, **P<0.01, *P<0.05, ns P>0.05. c) Fluorescence intensity of the AzMC signal, normalised to protein content. There is a decline in global H_2S levels in the *dys-1(eg33)* animals compared to WT, this is increased by NaGYY and AP39 treatment. For all strains and treatment group *N*=90 with three biological repeats for a total of 270 data points per violin. Results were analysed with a one-way ANOVA. All significance points are compared to *dys-1(eg33)*. ***P < 0.0001.

5.3.2 Supplementation of sulfur containing amino acids increased H_2S levels and improved functional defects in movement of *dys-1(eg33)* animals.

As we have shown that the sulfur metabolism pathway is altered in the *C. elegans* DMD model, we were interested to see if supplementing the SAA (that are a part of or come off from these pathways) could improve muscle health. As the SAA occur naturally, they could be more tolerable for patients. The five amino acids we assessed were L-methionine, L-homocysteine, L-cysteine, L-glutathione, and L-taurine. We first assessed whether these amino acids could improve movement in the animals (as this is a good indicator of muscle health), and if so, what the optimal concentration was (Figure 5.2). We found that all the amino acids were able to improve movement and, do-so in a dose-dependent fashion. The following concentrations were used throughout the study unless otherwise stated: L-methionine 10 mM (Figure 5.2a), L-homocysteine 10 µM (Figure 5.2b), L-cysteine 10 µM (Figure 5.2c), L-glutathione 100 µM (Figure 5.2d), and L-taurine 10 µM (Figure 5.2e). It is interesting to note that L-methionine was required at a concentration at least 10-fold higher than the other SAA. In addition, as shown in Figure 5.2f, there are no major differences to the degree of how much movement is improved with the various SAA. This implies that any of the SAA could be given, and the same effect would be seen in this model. We also trialled two non-SAA: phenylalanine and lysine. Phenylalanine gave a slight improvement in movement but not to the same levels as the SAA and lysine showed no improvements (Figure 5.2f). This indicates that it is likely the sulfur component that is having the beneficial effect which would correspond with our previous data from NaGYY and AP39. Having

seen this improvement, we also assessed whether the SAA increased global H_2S levels. All the SAA increased H_2S in the *dys-1(eg33)* animals but to different degrees. Unsurprisingly, L-cysteine gave one of the largest improvements as this is the main substrate for the H_2S-generating enzymes (Figure 5.2g).
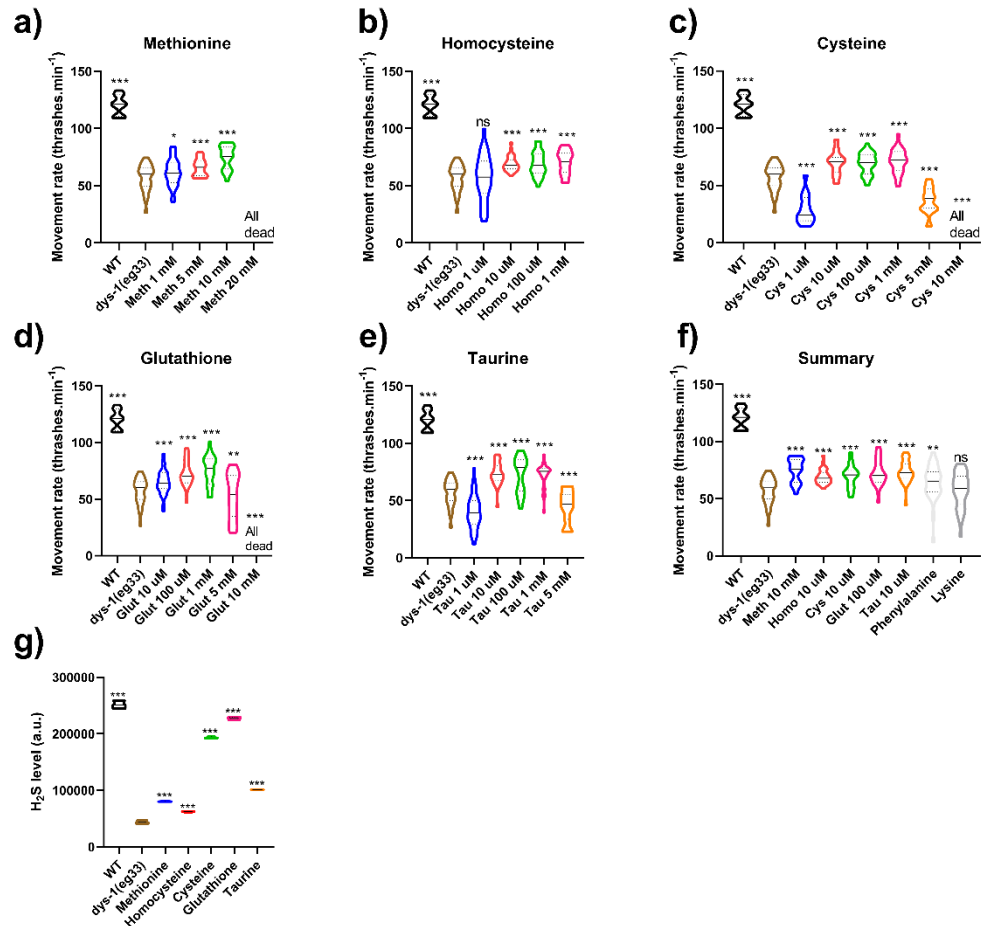
Figure 5.2. Sulfur containing amino acids improve movement and increase H_2S levels in the dys-1(eg33) model.

a) Methionine treatment significantly improved the thrash rate of *dys-1(eg33)* in a dose-dependent manner (1 mM – 10 mM). b) Homocysteine improved movement in *dys-1(eg33)* (10 μM – 1 mM). c) Cysteine significantly improvement thrash rate in *dys-1(eg33)* (10 μM – 5 mM). d) *dys-1(eg33)* movement was improved with L-glutathione treatment (10 μM – 5 mM). e) Taurine treatment also improved thrash rate in *dys-1(eg33)* (10 μM – 5 mM). f) Summary figure of the selected optimum doses for each sulfur containing amino acid, there are no significant differences between amino acids. Phenylalanine improves movement in the *dys-1(eg33)* model but not to the same levels as the sulfur containing amino acids. There is no improvement with lysine treatment. For all strains and treatment N=10 with five replicates with three biological repeats for a total of 150 data points per violin plot. Results were analysed with a two-way ANOVA. All significance points were compared to *dys-1(eg33)* ***P<0.0001, **P<0.005, *P<0.05, ns$P$>0.05. g) Fluorescence intensity of the AzMC signal, normalised to protein content. All the sulfur containing amino acids increased H_2S levels. For all strains and treatment group N=90 with three biological repeats for a total of 270 data points per violin. Results were analysed with a one-way ANOVA. All significance points are compared to *dys-1(eg33)*. ***P < 0.0001.

5.3.3 Sulfur containing amino acid supplementation improves mitochondrial structure and delays the onset of cell death.

One of the key findings from Chapter 3 and 4 is that the health improvements shown from H_2S supplementation are likely mitochondrial based. We therefore decided to determine whether the SAA could also improve the mitochondrial network of the *dys-1(eg33)* animals. Unlike with NaGYY and AP39 treatment, the improvement seen with the SAA was not as stark (Figure 5.3a). We have consequently classified the appearance of the mitochondria from each worm into one of three groups: well networked, moderately well-networked, and disorganised
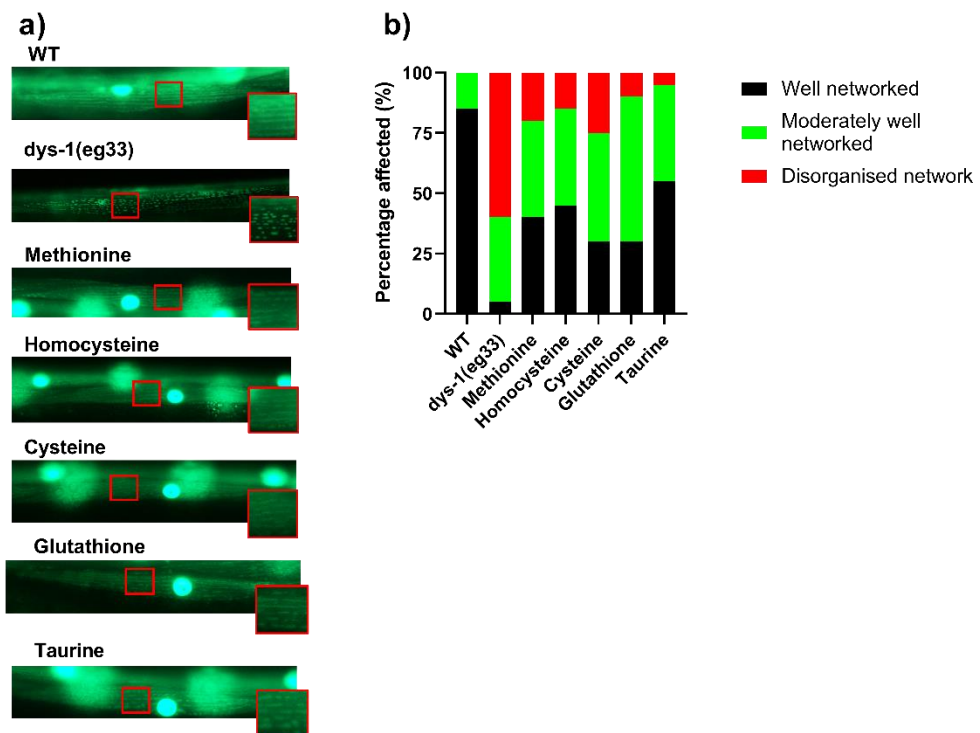
Figure 5.3. The mitochondrial network of dys-1(eg33) animals is improved by the sulfur containing amino acids.

a) Representative images of CB5600 (WT with GFP tagged mitochondria) which displayed a well organised mitochondrial network. CC91 (*dys-1(eg33)* with GFP tagged mitochondria) which showed a severely disorganised mitochondrial network. L-Methionine (10 mM), L-homocysteine (10 µM), L-cysteine (10 µM), L-glutathione (100 µM), and L-taurine (10 µM), all improved the mitochondrial network of the *dys-1(eg33)* animals but not to WT levels. b) A stacked bar graph showing the percentage of well networked, moderately well networked and disorganised network within each group. The sulfur containing amino acids have animals with more well organised networks compared to *dys-1(eg33)*. For all strains and treatments N=20.

network. By doing this we can see that the SAA are in fact improving the mitochondrial network (Figure 5.3b). The well network group contains 85% WT, 5% *dys-1(eg33),* 40% L-methionine, 45% L-homocysteine, 30% L-cysteine, 30% L-glutathione, and 55% L-taurine. This indicates that the mitochondrial network is being improved but not to WT levels.
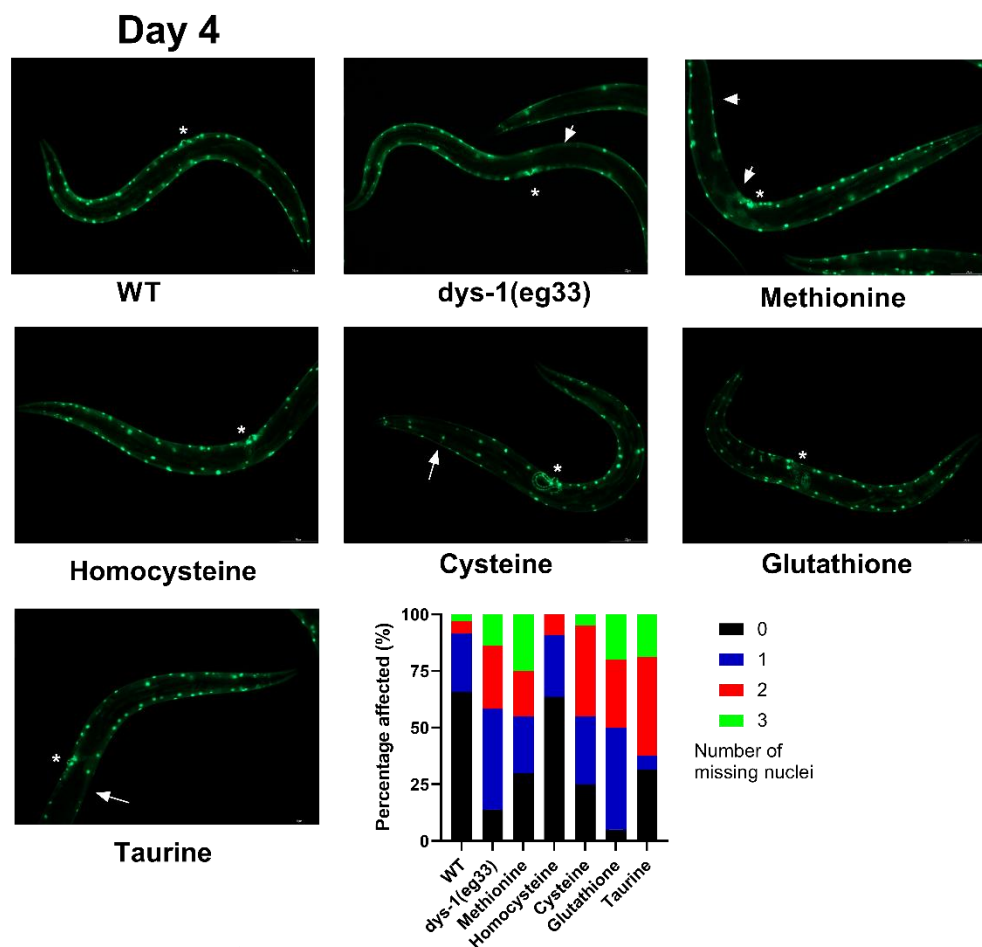
Figure 5.4. Sulfur containing amino acids mildly delay the onset of cell death at day four of adulthood.

Representative images of muscle cell death in CB5600 (WT), CC91 (*dys-1(eg33)*), and CC91 treated with sulfur amino acid compounds: L-Methionine (10 mM), L-homocysteine (10 µM), L-cysteine (10 µM), L-glutathione (100 µM), and L-taurine (10 µM). Muscle cell death (as identified by the absence of muscle nuclei) was more severe in the *dys-1(eg33)* animals compared to WT. The scatter bar graph shows a higher proportion of animals with no missing nuclei when treated with the sulfur amino acid compounds bar glutathione. However, the proportion of animals with 2 or more missing nuclei was similar across all groups bar homocysteine. Vulva is identified by the * and arrows show the missing nuclei. For all strains and treatments *N*=20. Scale bar: 30 µm.

We next wanted to determine whether we could delay the onset of cell death in the *dys-1(eg33)* animals. Muscle cell death can be identified by the absence of muscle nuclei in *C. elegans*. At Day 4 of adulthood, *dys-1(eg33)* starts to display muscle cell death with most worms showing at least one missing muscle nuclei. The SAA treated animals show a slightly higher percentage of animals with no missing
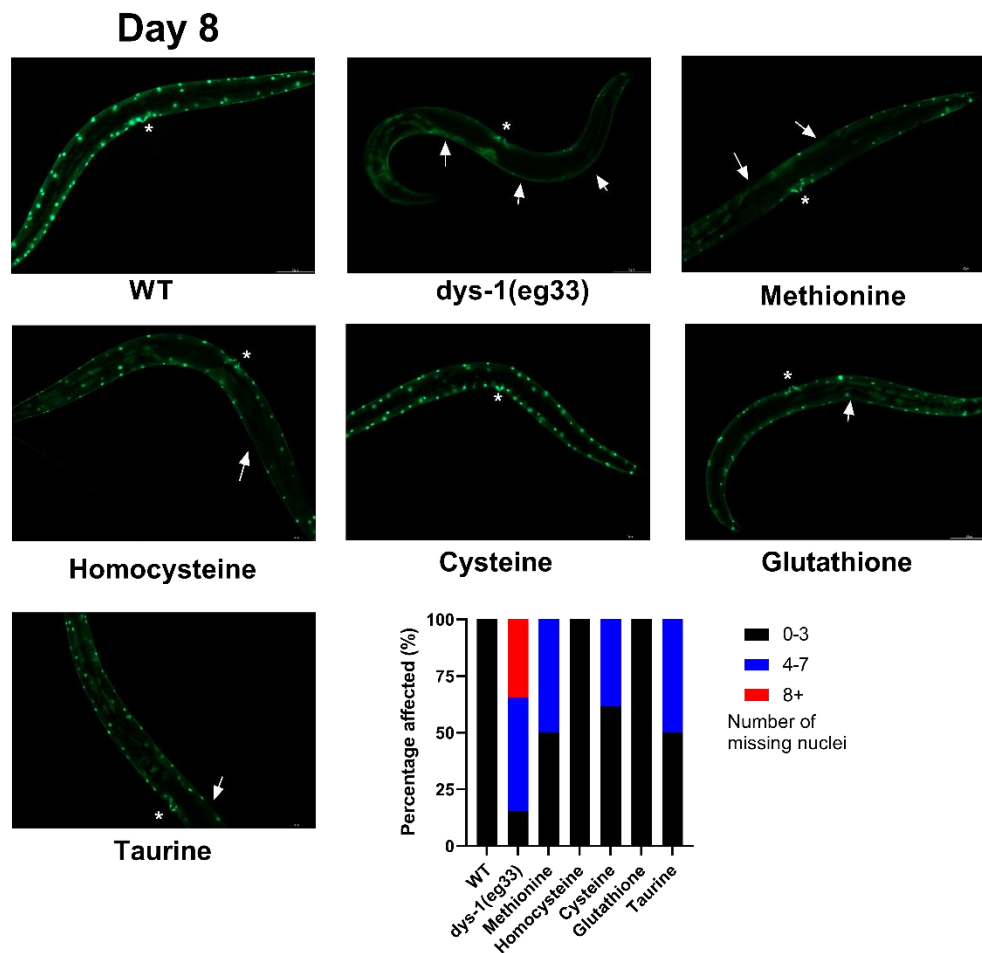
Figure 5.5. Sulfur containing amino acids delays the onset of cell death at Day 8 of adulthood.

Representative images of muscle cell death in CB5600 (WT), CC91 (*dys-1(eg33)*), and CC91 treated with sulfur amino acid compounds: L-methionine (10 mM), L-homocysteine (10 µM), L-cysteine (10 µM), L-glutathione (100 µM), and L-taurine (10 µM). Muscle cell death (as identified by the absence of muscle nuclei) was more severe in the *dys-1(eg33)* animals compared to WT. The scatter bar graph shows a higher proportion of animals with 0-3 missing nuclei when treated with the sulfur amino acid compounds in particular homocysteine and glutathione. Vulva is identified by the * and arrows show the missing nuclei. For all strains and treatments *N*=20. Scale bar: 30 µm.

nuclei compared to untreated *dys-1(eg33)*, however the proportion of animals with two of more missing nuclei was similar across all groups bar L-homocysteine (Figure 5.4).

Having seen little difference at Day 4 of adulthood we then assessed cell death again at Day 8 of adulthood to see if perhaps the SAA may have a longer-term beneficial effect. Once again, we see that the *dys-1(eg33)* animals have more severe muscle cell death compared to WT animals. However, at this time point we can clearly see that all the SAA delay the onset of cell death in particular L-homocysteine and L-glutathione (Figure 5.5).

5.3.4 Calcium handling is improved in the *dys-1(eg33)* animals with treatment from the sulfur containing amino acids.

As discussed previously one of the main underlying pathophysiological events in DMD is mishandling of calcium and calcium overload [5],[183]. We illustrated in Chapter 3 that NaGYY gave mild improvements in calcium handling whereas AP39 in Chapter 4 gave no effect. This was hypothesised to be due to these compounds predominantly affecting the mitochondria. Interestingly, when we tested the SAA a clear improvement in calcium handing could be detected in the *dys-1(eg33)* animals.

To determine this, we crossed HBR4 (a reporter strain which expresses the calcium indicator GCaMP3 in all body wall muscles) with the *dys-1(eg33)* strain. During a muscle contraction a calcium current is necessary and a rise in calcium can be seen on the contracted side in

WT animals and no calcium on the relaxed side (Figure 5.6a, green arrow contracted side, white arrow relaxed side). However, in the dystrophin animals, elevated calcium can be seen on both the contracted and relaxed sides regardless of muscle contraction (Figure 5.6a, both white arrows). When we treated the *dys-1(eg33)* animals with any of the SAA, we saw a restoration of calcium handling, in that there were high levels of calcium on the contracted side of the body wall muscles and the elevated levels of calcium on the relaxed side were no longer as apparent (Figure 5.6a). Quantification of the ratio of the contracted versus the relaxed side confirmed that the SAA supplementation improved calcium handing (Figure 5.6b).

Having seen an improvement with the calcium reporter strains we then looked at levamisole sensitivity. Previously, *dys-1(eg33)* animals have been shown to be resistant to levamisole indicating defects in postsynaptic excitation-contraction coupling [44]. As shown in Chapter 3 and 4, neither NaGYY nor AP39 was able to improve this defect so we were not expecting the SAA to either. However, we did see an improvement with all the SAA, implying that the mechanism(s) of action are slightly different, or the SAA are having a more global effect rather than specifically being targeted to the mitochondria (Figure 5.6c).
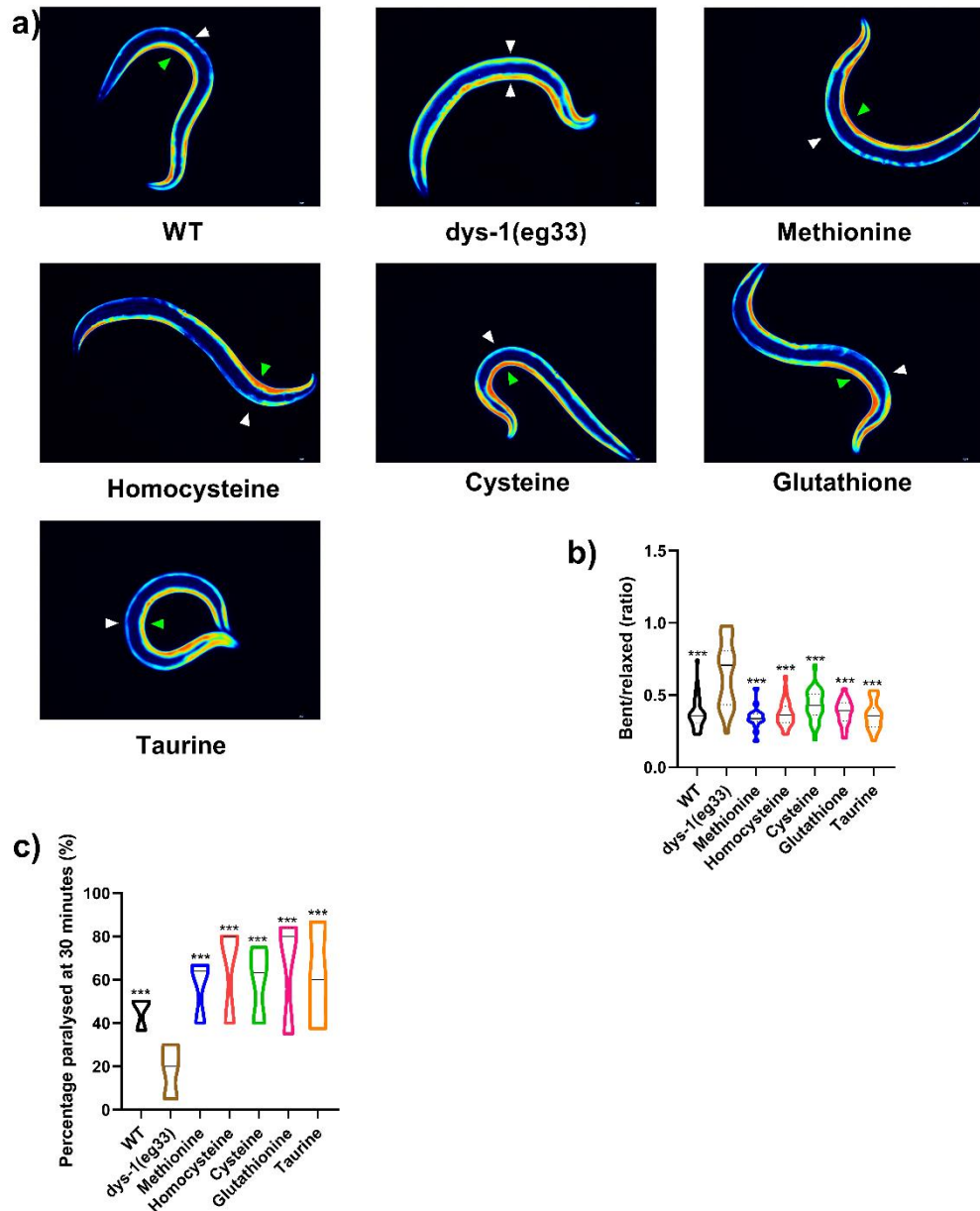
Figure 5.6. Calcium mishandling is improved in the dys-1(eg33) animals with the sulfur containing amino acids but it does not improve anesthesia sensitivity.

a) Representative images of calcium report strain in HBR4 (WT), HBR4xBZ33 (*dys-1(eg33)*), and HBR4xBZ33 treated with sulfur amino acid compounds: L-methionine (10 mM), L-homocysteine (10 µM), L-cysteine (10 µM), L-glutathione (100 µM), and L-taurine (10 µM). In WT animals, high levels of calcium can be detected on the contracted side (green arrow) of the body wall muscles with no calcium being detected on the relaxed side (white arrow). In *dys-1(eg33)* animals, high levels of calcium can be detected on both the relaxed and contracted sides. Treatment with the sulfur containing amino acids restored calcium handling to that which represented WT. b) Quantification of the relative ratio of calcium intensity for bent (contracted) side vs relaxed side. The ratio is higher than WT in *dys-1(eg33)* but is restored by treatment with the sulfur containing amino acids. For all strains and treatments $N=20$. Scale bar: 30 µm. c) *dys-1(eg33)* animals are resistant to levamisole after 30 minutes of exposure compared to WT. This is improved by all sulfur containing amino acids. For all strains and treatments $N=30$ with three independent biological repeats, equating to 90 data points per bar. Results were analysed with a two-way ANOVA. All significance points were compared to *dys-1(eg33)* ***$P<0.0001$.

5.3.5 The mechanisms underlying the beneficial health effects with the sulfur containing amino acids are similar but distinct to the H_2S compounds.

In Chapter 3 and 4 we found that the H_2S compounds were predominantly acting mitochondrially with minimal effects on calcium handling. As we have seen an improvement in both mitochondrial dysfunction and in calcium dysregulation with SAA supplementation, we were interested to see if the genes that have been found to be beneficial for the effect of NaGYY were also required for the SAA. In Chapter 3 we explored whether some of the genes that were found to be required for lifespan extension in ageing worms with NaGYY [155] were also required for NaGYY's effect in the *dys-1(eg33)* model. Like NaGYY, all the SAA required *jnk-1* and *daf-16* for their mechanism of action. This was determined as with *jnk-1* or *daf-16* treatment, there was a decline in movement compared to *dys-1(eg33)* even with additional treatment from the SAA (Figure 5.7a-7e). All the SAA require *sir-2.1* present to give a beneficial effect, however, the decline with L-homocysteine was not significant (Figure 5.7a-7e). Interestingly, unlike NaGYY, although there was a slight movement decline with *skn-1* RNAi, this was not significant with any of the SAA. This implies that *skn-1* is not as necessary for the effect of the SAA (Figure 5.7a-7e). This is particularly striking as *skn-1* is an orthologue for NFE2 and is a regulator of oxidative stress and proteostasis [195]. This may explain why we are not seeing as strong of an effect in the mitochondria as we have with the H_2S compounds.
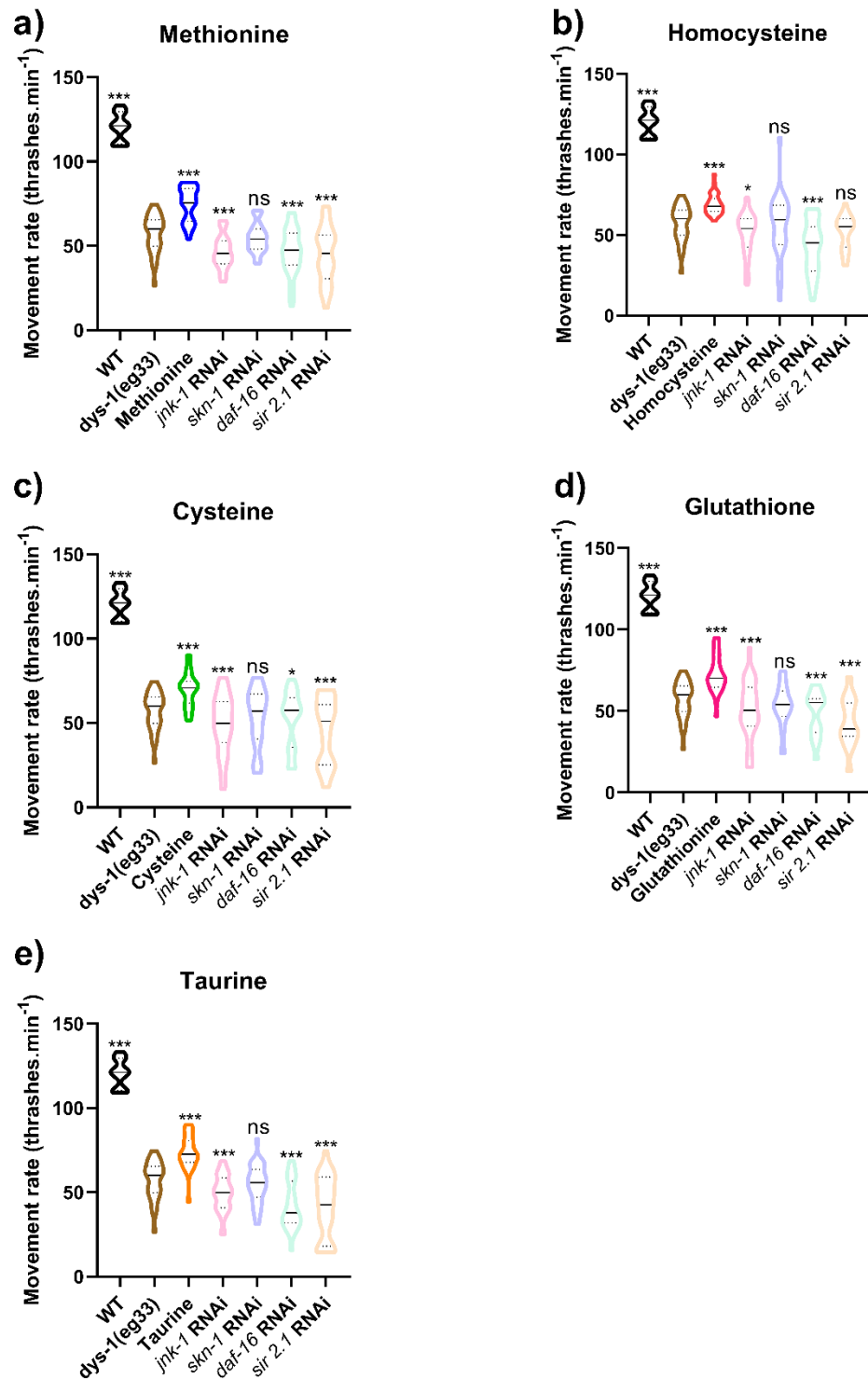
Figure 5.7. The effect of RNAi treatment on ageing and stress related genes, in relation to the mechanism of action of the sulfur containing amino acids.

a) L-methionine requires *jnk-1, daf-16,* and *sir-2.1* to have its beneficial effects, *skn-1* is not. b) *jnk-1* and *daf-16* are required for the beneficial effect of L-homocysteine, but it does not depend on *skn-1* or *sir-2.1*. c) L-cysteine requires all the genes tested bar *skn-1*. d) L-glutathione does not rely on *skn-1* but does need *jnk-1, daf-16,* and *sir-2.1*. e) *jnk-1, daf-16,* and *sir-2.1* are required for L-taurine's beneficial effect but it does not rely heavily on *skn-1*. All strains and conditions *N*=10 with five replicates and three biological independent repeats, equating to 150 points per violin plot. Results were analysed with a two-way ANOVA. ****P*<0.0001, **P*<0.05, ns *P*>0.05.

170

5.4 Discussion

5.4.1 *C. elegans* DMD animals have a H_2S deficit and sulfur metabolism is altered.

H_2S is the third endogenous signalling gasotransmitter to be recognised, after NO and CO. Previously studied for its toxicity, it is now well recognised for its physiological benefits at low levels. H_2S signalling has been linked to several diseases including age-related pathologies, where there is an increase in oxidative stress and the accumulation of ROS in the mitochondria. H_2S has been shown to be an efficient antioxidant and can inhibit ROS [238]. DMD shares this similarity with ageing in that with a deficiency in dystrophin, there is an increase in oxidative stress in skeletal muscle. Chapters 3 and 4 showed that supplementing the H_2S compounds NaGYY and AP39 improved health in the *C. elegans* DMD model. This implied that there were likely issues with sulfur metabolism in the DMD model resulting in a H_2S deficiency.

To further investigate this, we looked at the expression of genes that play a role in the metabolism of sulfur, between DMD *C. elegans* and WT. The DMD animals display an increased expression in SAMS, which is responsible for the breakdown of L-methionine to S-adenosyl methionine. This is part of the TMP responsible for the conversion of L-methionine to L-homocysteine. There was reduced expression in CDO, which forms part of the TSP to produce L-taurine from L-cysteine. In regards to the H_2S generating enzymes, there was a reduction in expression of CSE (although this was not significant) and a reduction in 3-MST. CBS was not measured due to technical difficulties (Figure 5.1a). This confirms that there are likely issues with sulfur metabolism in the *C.*

elegans DMD model. Of the two transcriptomic papers using the *C. elegans* DMD model, one was a microarray study and the other a RNA sequencing study [66],[67]. Although not a focus of their papers, both showed increased expressions of SAMS and the RNA sequencing paper showed a decline in expression of CBS and CSE which corresponds with our RT-qPCR data [66],[67]. A study exploring human primary myoblasts from DMD donors and *mdx* mice, also noted a decline in expression off CSE, 3-MST, and CDO, highlighting the similarities between multiple species [146].

Despite increased interest in the field, obtaining measurements of H_2S has presented some challenges especially across species. Here we have used an AzMC dye to obtain measurements of H_2S levels in *C. elegans* where fluorescence was measured on a plate reader following incubation. This dye has been used previously in *C. elegans* [174] but we obtained more consistent results with our method. We were able to confirm that there is a H_2S deficit in DMD *C. elegans* (Figure 5.1c). Abnormalities of H_2S have been linked to mitochondrial dysfunction, which is also part of DMD's pathophysiology, so taken together this implies that H_2S deficiency could be a part of DMD's pathogenesis.

5.4.2 Sulfur containing amino acids improved muscle health in DMD *C. elegans.*

One of the main benefits of using *C. elegans* is for its high-throughput drug screening capabilities. *C. elegans* have been used previously for large-scale drug screens in the muscular dystrophy model,

with the gold-standard treatment prednisone being identified [109],[129]. Having identified H_2S compounds as being able to improve muscle health in the DMD worm model, we were interested to see whether giving naturally occurring SAA would also improve health of these animals.

The SAA differ to the other amino acids as they contain sulfur, whereas the other amino acids are made from carbon, hydrogen, oxygen, and nitrogen. L-methionine is an essential amino acid obtained from the diet and is the first amino acid during the synthesis of proteins. It is broken down to L-homocysteine (but this can also be recycled back to L-methionine). High levels of homocysteine are associated with a condition called hyperhomocysteinemia, which is present in a wide range of diseases and thought to be caused by a deficiency in CBS [239]. L-homocysteine is then broken down to L-cysteine by the enzymes CBS and CSE, this process is irreversible, so the production of L-cysteine relies on L-methionine (it can be obtained from the diet if there are insufficient levels of L-methionine). The increased expression of SAMS reflects the increased need to metabolise L-methionine down to L-cysteine and the reduced expression in the H_2S generating enzymes suggests that there is insufficient L-cysteine to further metabolise to L-glutathione, L-taurine, and H_2S. L-methionine and L-cysteine are arguably the most important of the SAA as they are directly incorporated into proteins. Sulfur is more electronegative than oxygen and thus makes these amino acids more hydrophobic and all are considered as antioxidants in proteins [240]. Taurine is one of the most abundant amino acids found in animal tissue, accounting for 53% of the amino acids in

173

muscle. It has been shown to have roles as an antioxidant, a membrane stabiliser, and a neurotransmitter [241].

Disorders have been known to develop when SAA are deficient or in excess, highlighting the importance of retaining adequate levels [242]. Methionine and taurine deficiency has been noted previously in the muscles of dystrophic *mdx* mice [145],[146] and studies have commenced looking at taurine supplementation in the *mdx* mouse model [243]. A deficiency in cysteine has also been noted in the *mdx* mouse model and this was linked to the deficiency in taurine [147]. As far as we are aware these is no data available for homocysteine or glutathione levels in muscle in any DMD model. However, there is enough evidence to suggest that supplementing these amino acids could be a viable treatment and warrants further study.

Given that amino acid balance is sensitive, we first wanted to determine two things; if we could detect an improvement in health in the animals and if so, what was the optimal concentration. Starting concentrations were determined from data that showed lifespan extension in *C. elegans* with amino acid supplementation [157]. We saw an improvement in movement with all the SAA. Interestingly, the optimum dose determined for L-methionine was at least ten times higher than the other SAA (Figure 5.2a and 2f). This is unsurprising given our RT-qPCR data and the importance of methionine in protein synthesis. Phenylalanine and lysine were also tested to see if they could improve movement in the dystrophin animals to determine if any amino acid could be beneficial or was this specific to those that contained sulfur. There

was a significant improvement with phenylalanine and no improvement with lysine implying it is likely the sulfur aspect that is important. The improvement in movement seen with the SAA was not as substantial as with NaGYY seen in Chapter 3 but more like those of AP39 in Chapter 4.

5.4.3 Mechanisms underlying sulfur containing amino acids in improved DMD worm health.

One of the key findings associated with the mechanism of action of the H_2S compounds was that the improvement in muscle health was linked to improvements in mitochondrial health and less so calcium homeostasis. It therefore seemed precedent to explore whether the mechanisms underlying the improvement in health in the H_2S compounds was similar or different to those underlying the improvement with the SAA.

Mitochondrial and metabolic dysfunction are phenotypes of DMD. *C. elegans* DMD animals display this phenotype by having a disruption of their mitochondrial integrity and this integrity is restored by prednisone, NaGYY, and AP39 as shown in Chapter 3 and 4. An improvement can be seen in the mitochondrial network with all the SAA as well but not to WT levels. As the SAA are antioxidants it is unsurprising that they can improve mitochondrial health to a degree. In fact, methionine supplementation has been shown to stimulate mitochondrial respiration in yeast [244] and altered mitochondrial gene expression in broilers [245]. Cysteine supplementation has been shown to be beneficial in a small subgroup of mitochondrial translation deficiencies [246] and L-glutathione

deficiency has been linked to impairment of the ETC in mitochondrial disease [247]. Taurine, the most abundant of the SAA, has been demonstrated to enhance mitochondrial function in skeletal muscle [248] which supports the findings of this study, that taurine improves the mitochondrial network to a greater extent than the other SAA.

Dysregulation of calcium homeostasis is an underlying pathophysiology of DMD. The dysregulation of calcium handling and the influx of calcium has been linked to myofiber cell death [249]. As demonstrated previously, *dys-1(eg33)* animals display an increase in muscle cell death over time [46] which is delayed by NaGYY treatment as shown in Chapter 3. We wanted to determine whether the SAA could delay the onset and the extent of the cell death displayed by these animals. The SAA also delay the onset of cell death, but this is more apparent at the later time point (Figure 5.4-5.5). There is limited data looking at the correlation of SAA supplementation and muscle cell death but is has been shown in ageing mice that cysteine supplementation delays loss of muscle mass [250]. Unsurprisingly, most of the available publications are focused on taurine supplementation which has been shown to delay the onset of sarcopenia [160].

The dysregulated calcium homeostasis was largely unaffected with treatment from the H_2S compounds (as shown in Chapter 3 and 4) but having seen a delay in cell death with the SAA we were interested to see whether this was influenced more strongly with these supplements. Calcium levels appeared to return to normal levels with addition of all the SAA (Figure 5.6a-6b). Again, there has been little done to understand

how supplementation of the SAA can modulate calcium levels. However, cysteine has been shown to enhance calcium removal and increase SERCA activity in rats with impaired cardiac calcium homeostasis [251] and taurine is well known for its ability to regulate and reduce intracellular calcium [252].

Dystrophic muscles are already compromised and so they are less adaptive and more susceptible to stress, yet the mechanisms underlying this are incompletely understood [253]. *jnk-1*, *skn-1*, *daf-16*, and *sir-2.1* have all been shown to be required for the beneficial effects of H_2S treatment in ageing [155] and DMD *C. elegans* (Chapter 3). JNK-1 is a homologue of human stress-activated protein kinases (SAPK) and forms part of MAPK pathways which are involved in the cellular stress response. JNK-1 is predominately found in neuronal cells and can cause DAF-16 (a transcription factor for FOXO) to translocate to the nucleus under stressors such as oxidative stress and temperature changes. DAF-16 is then able to upregulate other genes associated with cellular stress [254]. All the SAA required the presence of *jnk-1* and *daf-16* for their beneficial effect (Figure 5.7a-7e), suggesting that like the H_2S compounds, part of their mechanism could be by enhancing stress tolerance. *sir-2.1* (an orthologue for human sirtuin 1), is part of a highly conserved family of NAD+-dependent deacetylase. This has been shown to be a key regulator of ageing and healthspan via regulation of metabolism and the oxidative stress response [199],[255]. The presence of *sir-2.1* was necessary for the positive impact of all the SAA, further highlighting the need for genes which regulate oxidative stress (Figure

5.7a-7e). Interestingly, RNAi against *skn-1* (orthologue of human NFE2), did not cause a decline in movement in the *dys-1* animals with SAA treatment but as there was not an improvement in movement either, it is clearly required for the full effect of the SAA supplementation. *skn-1* is also an important mediator of the oxidative stress response [253].

5.4.4 Modulation of the sulfur metabolism pathway warrants further investigation in the management of DMD therapy.

Several therapies are currently under investigation for the treatment of DMD. These include but are not limited to exon skipping, cellular therapy, and gene therapy. The aim of these therapies is to restore dystrophin and to improve muscle symptoms. By far the most successful have been exon skipping therapies with a handful being given accelerated approval from the FDA these include: Amondys 45 [20], Exondys 51 [18], and Vyondys 53 [19]. These therapies can only be given to patients who have genetic mutations amenable to skipping of exons 45, 51, and 53, and are not a cure. Thus, there is a significant unmet clinical need for effective treatments. Here we have shown there is a H_2S deficit in DMD *C. elegans* and previously in dKO animals as well [45]. This is also met with changes in expression of sulfur metabolism enzymes in *C. elegans*, human myoblasts, and *mdx* mice [146]. Modulation of this pathway with sulfur containing compounds has been proven beneficial in both *C. elegans* and in *mdx* mice [45],[146]. Many DMD patients will take supplements, such as carnitine, green tea, and the amino acids glutamine and arginine, without any evidence showing that they're

effective. Here we have also shown that supplementation of the naturally occurring SAA can bolster muscle health in *C. elegans* DMD. To our knowledge, only taurine supplementation has been investigated in other models and is a current ongoing area of interest [147],[149],[243]. Supplementation studies of the other SAA also warrants further investigation, as do dietary studies. People with DMD are recommended to have a high-protein diet with lots of fibre, therefore including sulfur-rich food (which are usually high-protein as well), such as eggs, fish, whole grains, and certain types of vegetables, should be relatively simple to include. Another potential avenue is to explore whether monitoring H_2S levels could be a biomarker at diagnosis and for disease progression.

5.5 Conclusion

Overall, we have shown that there is a H_2S deficit in the *C. elegans* DMD model. This decline is caused by discrepancies in enzymes associated with the sulfur metabolism pathway and H_2S producing enzymes. Supplementation of SAA alleviated the loss of ambulation in these animals and improved muscle health. The mechanism of action of the SAA is like that of the H_2S compounds, where the health improvements are likely due to improvements in the mitochondrial integrity and through a reduction of oxidative stress. The SAA also amended the calcium dysregulation seen in DMD animals. Altogether this suggests that H_2S deficiency could be a part of the pathophysiology of DMD and further supplementation studies of sulfur containing compounds are necessary.

Chapter 6: General discussion

6.1 Overview of aims

As discussed at the beginning of this thesis, DMD is a rare neuromuscular disorder that despite extensive research, currently has no cure. Treatment options are limited with the main pharmacological therapy being corticosteroids. There have been large advances in exon-skipping therapies with approximately 30% of patients being amenable to exon 51, 53, or 45 skipping [256]. However, alternative pharmacological therapies are still required for corticosteroids as these can only be given for a couple of years due to several detrimental side effects. The study of potential therapies usually occurs in animal models and throughout this thesis this has been in *C. elegans*. A review of the literature as discussed in the introductory chapter, demonstrated the usefulness of using *C. elegans* as a model for DMD and its suitability as a drug screening platform. Some of the methods used in this thesis are novel in this model and add to the clinical relevance of *C. elegans* as a model for DMD. The aims of this thesis were to demonstrate the potential of using H_2S compounds for the treatment of DMD using clinically relevant phenotypes and to understand the mechanisms that may underly the beneficial effects.

6.2 Improving the clinical relevance of the DMD nematode model.

The main symptom of DMD in patients is muscle weakness which results in frequent falls and difficulty with walking and running. Both these phenotypes have been recapitulated in this model throughout this thesis and in previously published articles [44]. In addition, DMD patients are often described as having an "unusual" or "waddling" gait and for the first time we were able to show that the DMD animals also had alterations in their gait as well, using a system called CeleST. CeleST, is a software used to assess multiple parameters associated with swim locomotion, to provide more descriptive measures than looking at movement data alone [170],[178]. It reads out on four morphological parameters and four activity parameters. All of which were altered in the DMD animals bar curling. This provided evidence to suggest that like patients, *C. elegans* DMD also have an altered "gait".

DMD patients have a shortened lifespan with the average life expectancy being late twenties to early thirties. Although DMD animals have been shown to have a shortened lifespan previously [46], we have shown this can also be detected using an automated lifespan machine called the NemaLife [172]. This machine removes several issues associated with doing standard longevity assays on agar plates such as picking and transferring animals. This provides the opportunity in the future to carry out large-scale studies in the dystrophin model.

The most common cause of death in DMD patients is cardio-respiratory failure [10]. *C. elegans* do not have a heart muscle and so it would be reasonable to conclude that alternations in the heart muscle

and cardiac failure cannot be studied in this model. This assumption would be incorrect as the pharynx feeding muscle in *C. elegans* is a rhythmically active muscle pump that resembles the muscle cells in the mammalian heart [184]. We used the NemaMetrix ScreenChip™ to take EPG recordings of stimulated pumping in the *C. elegans* DMD model and demonstrated that there were alterations in the EPG traces compared to WT. Our results raise the possibility of using the worm DMD model to gain greater mechanistic insight into DMD cardiac pathology as well as screening for compounds to ameliorate it.

Finally, mitochondrial dysfunction is part of the underlying pathophysiology of DMD. We have established methods to help further understand this dysfunction in the *C. elegans* DMD model. We have established that the *dys-1(eg33)* animals have a decline in their MAPR, CS activity, (marker of mitochondrial content) and ATP content. They are also hypersensitive to complex I and III inhibition. Taken together these methods have helped to improve the clinical relevance of this model and provide vantage points for future studies.

6.3 Summary of results

Previously H_2S supplementation has been shown to extend lifespan and improve healthspan in ageing *C. elegans* [155]. Due to the similarities in muscle degeneration with age and in DMD, we trialled H_2S supplementation as a potential therapeutic for DMD. The first compound trialled was the slow-release H_2S compound NaGYY. NaGYY was able to improve overall health of the DMD animals including improvements to their movement, strength, and gait. The proposed underlying mechanism for this was by improving the mitochondrial dysfunction that these animals have and partially restoring calcium dysregulation. This mechanism is like that of the current gold-standard treatment prednisone.

To further explore this and to investigate the underlying mechanism(s), we then utilised another H_2S compound, AP39, which is mitochondrially targeted. This compound was used at a 1000 times lower dose than NaGYY. AP39 was also able to improve movement and strength, demonstrating that at least part of the mechanism of action was through correcting the mitochondrial dysfunction. H_2S is a known electron donor and AP39 in particular has been known to increase electron transport at respiratory complex III in the ETC [257]. This possibility was assessed using western blotting and complex inhibitors and it seems likely that this could be the case here as well. To verify this, measures of ATP content were taken and AP39 increased ATP content in the DMD animals.

One thought that had not been addressed until the end of this thesis was, if we are supplementing H_2S is there actually a deficiency in

these animals? We confirmed that these animals do have a deficiency in H_2S, and this is likely caused by alterations in sulfur metabolism and decreased expression of H_2S producing enzymes. We were therefore interested to see if supplementing sulfur via a different method could also be beneficial. We supplemented these animals with naturally occurring SAA which did also improve health of the DMD *C. elegans* but not to the same extent as the H_2S compounds. This had led us to conclude that supplementing sulfur either via H_2S compounds or with SAA is beneficial to worm health and warrants further investigation in other models.

6.4 Future directions

The next obvious steps for H_2S based therapies will be to trial in alternative models. Cell culture experiments in primary human cells would allow us to directly measure H_2S to see if there is a decline in DMD cells compared to a control. It would also allow for ease to measure other parameters that are more difficult and variable in the worms such as direct measure of ETC activity, OCR, and oxidative stress. Proof of principle experiments in rodent models and human subjects showing a decline in H_2S, would provide further evidence to warrant supplementation trials. Prior to the COVID-19 pandemic these translational type studies were going to be completed as part of this thesis. We had obtained some DMD patient cells and obtained ethical approval for the collection of peripheral blood from DMD patients but unfortunately the execution of these experiments was unachievable in the time frame left. The idea behind these studies were to measure H_2S, NAD+, and SAA levels in patient peripheral blood to collect evidence to support future supplementation studies.

Another area that has been touched on throughout this thesis is the promise of combination therapy and the use of a 'therapeutic cocktail'. The H_2S compounds are predominantly acting mitochondrially and as we have demonstrated, not improving calcium dysregulation. This suggests that combining prednisone and/or one of the H_2S compounds with a calcium reducing compound such as dantrolene, could be beneficial. In addition, combining one of these treatments with exon-

skipping therapies could provide an enhanced effect of correcting the genetic defect and the underlying pathophysiology at the same time.

Finally, in regard to the model itself, it is interesting to note that in the worm, animals are genetically identical (i.e. homozygous for the same mutation(s)), yet have variable individual results. It is unclear whether stochastic differences in global gene expression or environmental differences underly the variability. Notably, the response to H_2S supplementation in worms is highly variable at the individual level. This raises the interesting question of whether individual differences in mitochondrial function/homeostasis underlie individual differences in DMD severity.

References

1. Blake, D. J., Weir, A., Newey, S. E. & Davies, K. E. Function and Genetics of Dystrophin and Dystrophin-Related Proteins in Muscle. *Physiol. Rev.* **82**, 291–329 (2015).

2. Koenig, M. *et al.* Complete cloning of the Duchenne muscular dystrophy (DMD) cDNA and preliminary genomic organization of the DMD gene in normal and affected individuals. *Cell.* **50**, 509–517 (1987).

3. Gao, Q. & McNally, E. M. The Dystrophin Complex: structure, function and implications for therapy. *Compr. Physiol.* **5**, 1223–1239 (2015).

4. Moens, P., Baatsen, P. H. & Marechal, G. Increased susceptibility of EDL muscles from mdx mice to damage induced by contractions with stretch. *J. Muscle Res. Cell. Motil.* **14**, 446–451 (1993).

5. Bodeinsteiner, J. B. & Engel, A. G. Intracellular calcium accumulation in Duchenne dystrophy and other myopathies: a study of 567,000 muscle fibers in 114 biopsies. *Neurology.* **28**, 439–446 (1978).

6. Deconinck, N. & Dan, B. Pathophysiology of Duchenne Muscular Dystrophy: Current Hypotheses. *Pediatr. Neurol.* **36**, 1–7 (2007).

7. Millay, D. P. *et al.* Genetic and pharmacologic inhibition of mitochondrial-dependent necrosis attenuates muscular dystrophy. *Nat. Med.* **14**, 442–447 (2008).

8. Kelly-Worden, M. & Thomas, E. Mitochondrial Dysfunction in Duchenne Muscular Dystrophy. *Open J. Endocr. Metab. Dis.* **04**, 211–218 (2014).

9. Emery, A. Population frequencies of inherited neuromuscular diseases--a world survey. *Neuromuscul. Disord.* **1**, 19–29 (1991).

10. Ryder, S. *et al.* The burden, epidemiology, costs and treatment for Duchenne muscular dystrophy: An evidence review. *Orphanet J. Rare Dis.* **12**, 1–21 (2017).

11. Birnkrant, D. J. *et al.* Diagnosis and management of Duchenne muscular dystrophy, part 1: diagnosis, and neuromuscular, rehabilitation, endocrine, and gastrointestinal and nutritional management. *Lancet Neurol.* **17**, 251–267 (2018).

12. Angelini, C. The role of corticosteroids in muscular dystrophy: a critical appraisal. *Muscle Nerve.* **36**, 424–435 (2007).

13. Kim, S., Campbell, K. A., Fox, D. J., Matthews, D. J. & Valdez, R. Corticosteroid Treatments in Males With Duchenne Muscular Dystrophy: Treatment Duration and Time to Loss of Ambulation. *J. Child Neurol.* **30**, 1275–1280 (2015).

14. McDonald, C. M. *et al.* Long-term effects of glucocorticoids on function, quality of life, and survival in patients with Duchenne muscular dystrophy: a prospective cohort study. *Lancet.* **391**, 451–461 (2018).

15. Malik, V., Rodino-Klapac, L. R. & Mendell, J. R. Emerging drugs

for Duchenne muscular dystrophy. *Expert Opin Emerg Drugs.* **17**, 261–277 (2012).

16. Bladen, C. L. *et al.* The TREAT-NMD DMD Global Database : Analysis of More than 7,000 Duchenne Muscular Dystrophy Mutations. *Hum. Mutat.* **36**, 395–402 (2015).

17. Aartsma-Rus, A. & Krieg, A. M. FDA Approves Eteplirsen for Duchenne Muscular Dystrophy: The Next Chapter in the Eteplirsen Saga. *Nucleic Acid Ther.* **27**, 1–3 (2017).

18. McDonald, C. M. *et al.* Open-Label Evaluation of Eteplirsen in Patients with Duchenne Muscular Dystrophy Amenable to Exon 51 Skipping: PROMOVI Trial. *J. Neuromuscul. Dis.* 1–13 (2021).

19. Heo, Y. Golodirsen: First Approval. *Drugs.* **80**, 329–333 (2020).

20. Shirley, M. Casimersen: First Approval. *Drugs.* **81**, 875–879 (2021).

21. Dent, K. M. *et al.* Improved molecular diagnosis of dystrophinopathies in an unselected clinical cohort. *Am J Med Genet A.* **134**, 295–298 (2005).

22. Barton, E. R., Morris, L., Musaro, A., Rosenthal, N. & Sweeney, H. L. Aminoglycoside antibiotics restore dystrophin function to skeletal muscles of *mdx* mice. *J. Cell Biol.* **157**, 137–148 (1999).

23. Wagner, K. R. *et al.* Gentamicin treatment of Duchenne and Becker muscular dystrophy due to nonsense mutations. *Ann. Neurol.* **49**, 706–711 (2001).

24. Welch, E. M. *et al.* PTC124 targets genetic disorders caused by nonsense mutations. *Nature.* **447**, 87–91 (2007).

25. Bushby, K. *et al.* Ataluren treatment of patients with nonsense mutation dystrophinopathy. *Muscle Nerve.* **50**, 477–487 (2014).

26. Jones, D. Duchenne muscular dystrophy awaits gene therapy. *Nat. Biotechnol.* **37**, 335–337 (2019).

27. Bulfield, G., Siller, W. G., Wight, P. A. & Moore, K. J. X chromosome-linked muscular dystrophy (*mdx*) in the mouse. *PNAS.* **81**, 1189–1192 (1984).

28. Sicinski, P. *et al.* The Molecular Basis of Muscular Dystrophy in the *mdx* Mouse: A Point Mutation. *Science.* **244**, 1578–1580 (1989).

29. McGreevy, J. W., Hakim, C. H., Mcintosh, M. A. & Duan, D. Animal models of Duchenne muscular dystrophy : from basic mechanisms to gene therapy. *Dis. Model. Mech.* **8**, 195–213 (2015).

30. Wells, D. J. Tracking progress: an update on animal models for Duchenne muscular dystrophy. *Dis. Model. Mech.* **11**, 1–3 (2018).

31. Sui, T. *et al.* A novel rabbit model of Duchenne muscular dystrophy generated by CRISPR/Cas9. *Dis. Model. Mech.* **11**, 1–9 (2018).

32. Larcher, T. *et al.* Characterization of dystrophin deficient rats: A new model for duchenne muscular dystrophy. *PLoS ONE.* **9**, 1–13 (2014).

33. Nakamura, K. *et al.* Generation of muscular dystrophy model rats with a CRISPR/Cas system. *Sci. Rep.* **4**, 1–6 (2015).

34. Klymiuk, N. *et al.* Dystrophin-deficient pigs provide new insights into the hierarchy of physiological derangements of dystrophic muscle. *Hum. Mol. Genet.* **22**, 4368–4382 (2013).

35. Gaschen, L. *et al.* Cardiomyopathy in Dystrophin-Deficient Hypertrophic Feline Muscular Dystrophy. *J. Vet. Intern. Med.* **13**, 346–356 (1999).

36. Guyon, J. R. *et al.* The dystrophin associated protein complex in zebrafish. *Hum. Mol. Genet.* **12**, 601–615 (2003).

37. Berger, J., Berger, S., Hall, T. E., Lieschke, G. J. & Currie, P. D. Dystrophin-deficient zebrafish feature aspects of the Duchenne muscular dystrophy pathology. *Neuromuscul. Disord.* **20**, 826–832 (2010).

38. Greener, M. J. & Roberts, R. G. Conservation of components of the dystrophin complex in Drosophila. *FEBS Lett.* **482**, 13–18 (2000).

39. Shcherbata, H. R. *et al.* Dissecting muscle and neuronal disorders in a Drosophila model of muscular dystrophy. *EMBO J.* **26**, 481–493 (2007).

40. Blazie, S. M. *et al.* Comparative RNA-Seq analysis reveals pervasive tissue-specific alternative polyadenylation in *Caenorhabditis elegans* intestine and muscles. *BMC Biol.* **13**, 1–20 (2015).

41. Nguyen, F., Cherel, Y., Guigand, L., Goubault-Leroux, I. & Wyers,

M. Muscle lesions associated with dystrophin deficiency in neonatal golden retriever puppies. *J. Comp. Pathol.* **126**, 100–108 (2002).

42. Chambers, S. P. *et al.* Dystrophin in adult zebrafish muscle. *Biochem Biophys Res Commun.* **286**, 478–483 (2001).

43. Grisoni, K., Martin, E., Gieseler, K., Mariol, M. C. & Ségalat, L. Genetic evidence for a dystrophin-glycoprotein complex (DGC) in *Caenorhabditis elegans*. *Gene.* **294**, 77–86 (2002).

44. Hewitt, J. E. *et al.* Muscle strength deficiency and mitochondrial dysfunction in a muscular dystrophy model of *Caenorhabditis elegans* and its functional response to drugs. *Dis. Model. Mech.* **11**, 1–13 (2018).

45. Ellwood, R. A. *et al.* Mitochondrial hydrogen sulfide supplementation improves health in the *C. elegans* Duchenne muscular dystrophy model. *PNAS.* **118**, 1–12 (2021).

46. Oh, K. H. & Kim, H. Reduced IGF signaling prevents muscle cell death in a *Caenorhabditis elegans* model of muscular dystrophy. *PNAS.* **110**, 19024–19029 (2013).

47. Altun, Z. F. & Hall, D. H. Pericellular strctures. *WormAtlas* (2009).

48. Gieseler, K., Qadota, H. & Benian, G. M. Development, structure, and maintenance of *C. elegans* body wall muscle. *WormBook.* 1–59 (2017).

49. Sleigh, J. N. & Sattelle, D. B. *C. elegans* models of neuromuscular

diseases expedite translational research. *Transl. Neurosci.* **1**, 214–227 (2010).

50. *C. elegans* S. Consortium. Genome sequence of the nematode *C. elegans*: a platform for investigating biology. *Science.* **282**, 2012–2018 (1998).

51. Sulston, J. E., White, J. G. & Wood, W. B. *The nematode Caenorhabditis elegans*. (Cold Spring Harbor, New York: Cold Spring Harbor Laboratory, 1988).

52. Murfitt, R. R., Vogel, K. & Sanadi, D. R. Characterization of the mitochondria of the free-living nematode, *Caenorhabditis elegans*. *Comp. Biochem.* **53**, 423–430 (1976).

53. Okimoto, R., Macfarlane, J. L., Clary, D. O. & Wolstenholme, D. R. The mitochondrial genomes of two nematodes, *Caenorhabditis elegans* and *Ascaris suum*. *Genetics.* **130**, 471–498 (1992).

54. Gieseler, K., Abdel-Dayem, M. & Ségalat, L. In vitro interactions of *Caenorhabditis elegans* dystrophin with dystrobrevin and syntrophin. *FEBS Lett.* **461**, 59–62 (1999).

55. Bessou, C., Giugia, J. B., Franks, C. J., Holden-Dye, L. & Ségalat, L. Mutations in the *Caenorhabditis elegans* dystrophin-like gene *dys-1* lead to hyperactivity and suggest a link with cholinergic transmission. *Neurogenetics.* **2**, 61–72 (1998).

56. Chamberlain, J. S. & Benian, G. M. Muscular dystrophy: The worm turns to genetic disease. *Curr. Biol.* **10**, 795–797 (2000).

57. Culetto, E. & Sattelle, D. B. A role for *Caenorhabditis elegans*. *Hum. Mol. Genet.* **9**, 869–878 (2000).

58. Krajacic, P., Shen, X., Purohit, P. K., Arratia, P. & Lamitina, T. Biomechanical profiling of *Caenorhabditis elegans* motility. *Genetics.* **191**, 1015–1021 (2012).

59. Bainbridge, C., Schuler, A. & Vidal-Gadea, A. G. Method for the assessment of neuromuscular integrity and burrowing choice in vermiform animals. *J. Neurosci. Methods.* **264**, 40–46 (2016).

60. Beron, C. *et al.* The burrowing behavior of the nematode *Caenorhabditis elegans*: A new assay for the study of neuromuscular disorders. *Genes, Brain Behav.* **14**, 357–368 (2015).

61. Megeney, L. A., Kablar, B., Garrett, K., Anderson, J. E. & Rudnicki, M. A. MyoD is required for myogenic stem cell function in adult skeletal muscle. *Genes Dev.* **10**, 1173–1183 (1996).

62. Gieseler, K., Grisoni, K. & Segalat, L. Genetic suppression of phenotypes arising from mutations in dystrophin-related genes in *Caenorhabditis elegans*. *Curr. Biol.* **10**, 1092–1097 (2000).

63. Sznitman, J., Purohit, P. K., Krajacic, P., Lamitina, T. & Arratia, P. E. Material Properties of *Caenorhabditis elegans* Swimming at Low Reynolds Number. *Biophysj.* **98**, 617–626 (2010).

64. Scholtes, C. *et al.* DRP-1-mediated apoptosis induces muscle degeneration in dystrophin mutants. *Sci. Rep.* **8**, 1–16 (2018).

65. Hewitt, J. E. *et al.* Multi-environment phenotyping of *C. elegans* for robust evaluation of physical performance. *bioRxiv.* (2020).

66. Hrach, H. C. *et al.* Transcriptome changes during the initiation and progression of Duchenne Muscular Dystrophy in *C. elegans*. *Hum. Mol. Genet.* **29**, 1607–1623 (2020).

67. Towers, P. R. *et al.* Gene expression profiling studies on *Caenorhabditis elegans* dystrophin mutants *dys-1(cx-35)* and *dys-1(cx18)*. *Genomics.* **88**, 642–649 (2006).

68. Kharraz, Y., Guerra, J., Pessina, P., Serrano, A. L. & Muñoz-Cánoves, P. Understanding the Process of Fibrosis in Duchenne Muscular Dystrophy. *Biomed Res. Int.* **2014**, 1–11 (2014).

69. Chen, Y. W., Zhao, P., Borup, R. & Hoffman, E. P. Expression profiling in the muscular dystrophies: Identification of novel aspects of molecular pathophysiology. *J. Cell Biol.* **151**, 1321–1336 (2000).

70. Gieseler, K., Bessou, C. & Ségalat, L. Dystrobrevin- and dystrophin-like mutants display similar phenotypes in the nematode *Caenorhabditis elegans*. *Neurogenetics.* **2**, 87–90 (1999).

71. Johnson, R. P. *C. elegans* dystroglycan DGN-1 functions in epithelia and neurons, but not muscle, and independently of dystrophin. *Development.* **133**, 1911–1921 (2006).

72. Blazie, S. M. *et al.* Alternative Polyadenylation Directs Tissue-Specific miRNA Targeting in *Caenorhabditis elegans* Somatic

Tissues. *Genetics.* **206**, 757–774 (2017).

73. Cuppen, E., van der Linden, A. M., Jansen, G. & Plasterk, R. H. A. Proteins Interacting with *Caenorhabditis elegans* Gα Subunits. *Comp. Funct. Genomics.* **4**, 479–491 (2003).

74. Oh, H. J. *et al.* Interaction of α-catulin with dystrobrevin contributes to integrity of dystrophin complex in muscle. *J. Biol. Chem.* **287**, 21717–21728 (2012).

75. Lecroisey, C. *et al.* ZYX-1, the unique zyxin protein of *Caenorhabditis elegans*, is involved in dystrophin-dependent muscle degeneration. *Mol. Biol. Cell.* **24**, 1232–1249 (2013).

76. Brouilly, N. *et al.* Ultra-structural time-course study in the *C. elegans* model for Duchenne muscular dystrophy highlights a crucial role for sarcomere-anchoring structures and sarcolemma integrity in the earliest steps of the muscle degeneration process. *Hum. Mol. Genet.* **24**, 6428–6445 (2015).

77. Kim, H., Rogers, M. J., Richmond, J. E. & McIntire, S. L. SNF-6 is an acetylcholine transporter interacting with the dystrophin complex in *Caenorhabditis elegans*. *Nature.* **430**, 891–896 (2004).

78. Zhou, S. & Chen, L. Neural integrity is maintained by dystrophin in *C. elegans*. *J Cell Biol.* **192**, 349–363 (2011).

79. Lecroisey, C. *et al.* DYC-1, a Protein Functionally Linked to Dystrophin in *Caenorhabditis elegans* Is Associated with the Dense Body, Where It Interacts with the Muscle LIM Domain

Protein ZYX-1. *Mol. Biol. Cell.* **19**, 785–796 (2008).

80. Vallejo-Illarrameni, A., Toral-Ojeda, I., Aldanondo, G. & Lopez de Munain, A. Dysregulation of calcium homeostasis in muscular dystrophies. *Expert Rev. Mol. Med.* **16**, (2014).

81. Hughes, K. J. *et al.* Physical exertion exacerbates decline in the musculature of an animal model of Duchenne muscular dystrophy. *PNAS.* **116**, 3508–3517 (2019).

82. Carre-Pierrat, M. *et al.* The SLO-1 BK Channel of *Caenorhabditis elegans* is Critical for Muscle Function and is Involved in Dystrophin-dependent Muscle Dystrophy. *J. Mol. Biol.* **358**, 387–395 (2006).

83. Kim, H. *et al.* The dystrophin complex controls BK channel localization and muscle activity in *Caenorhabditis elegans*. *PLoS Genet.* **5**, 1–10 (2009).

84. Chen, B. *et al.* a-Catulin CTN-1 is required for BK channel subcellular localization in *C. elegans* body-wall muscle cells. *EMBO.* **29**, 3184–3195 (2010).

85. Gieseler, K. *et al.* Molecular, Genetic and Physiological Characterisation of Dystrobrevin-like (*dyb-1*) Mutants of *Caenorhabditis elegans*. *J. Mol. Biol.* **307**, 107–117 (2001).

86. Grisoni, K. *et al.* The *stn-1* syntrophin gene of *C. elegans* is functionally related to dystrophin and dystrobrevin. *J. Mol. Biol.* **332**, 1037–1046 (2003).

87. Gieseler, K., Grisoni, K., Mariol, M. C. & Ségalat, L. Overexpression of dystrobrevin delays locomotion defects and muscle degeneration in a dystrophin-deficient *Caenorhabditis elegans*. *Neuromuscul. Disord.* **12**, 371–377 (2002).

88. Jattujan, P., Meemon, K. & Suphamungmee, W. Loss of Dystrobrevin Causes Muscle Degeneration and a Short Lifespan in *Caenorhabditis elegans*. *WJST.* **15**, 659–667 (2018).

89. Mariol, M. C., Martin, E., Chambonnier, L. & Ségalat, L. Dystrophin-dependent muscle degeneration requires a fully functional contractile machinery to occur in *C. elegans*. *Neuromuscul. Disord.* **17**, 56–60 (2007).

90. Karpati, G., Carpenter, S. & Prescott, S. Small-caliber skeletal muscle fibers do not suffer necrosis in *mdx* mouse dystrophy. *Muscle Nerve.* **11**, 795–803 (1988).

91. Mizuno, Y. Prevention of myonecrosis in *mdx* mice: effect of immobilization by the local tetanus method. *Brain Dev.* **14**, 319–322 (1992).

92. Mokhtarian, A., Lefaucheur, J. P., Even, P. C. & Sebille, A. Hindlimb immobilization applied to 21-day-old *mdx* mice prevents the occurrence of muscle degeneration. *J. Appl. Physiol.* **86**, 924–931 (1999).

93. Zhan, H. *et al.* In vivo single-molecule imaging identifies altered dynamics of calcium channels in dystrophin-mutant *C. elegans*. *Nat. Commun.* **5**, 1–12 (2014).

94. Mariol, M. C. & Ségalat, L. Muscular degeneration in the absence of dystrophin is a calcium-dependent process. *Curr. Biol.* **11**, 1691–1694 (2001).

95. Sudevan, S. *et al.* Mitochondrial dysfunction causes Ca^{2+} overload and ECM degradation – mediated muscle damage in *C . elegans*. *FASEB J.* **33**, 9540–9550 (2019).

96. Takagi, A., Kojima, S., Ida, M. & Araki, M. Increased Leakage of Calcium Ion From the Sarcoplasmic Reticulum of the *Mdx* Mouse. *Jounrnal Neurol. Sci.* **110**, 160–164 (1992).

97. Niebroj-Dobosz, I., Kornguth, S., Schutta, H. S. & Siegel, F. L. Elevated calmodulin levels and reduced calmodulin-stimulated calcium-ATPase in Duchenne progressive muscular dystrophy. *Neurology.* **39**, 1610–1614 (1989).

98. Chakkalakal, J. V, Michel, S. A., Chin, E. R., Michel, R. N. & Jasmin, B. J. Targeted inhibition of Ca^{2+}/calmodulin signaling exacerbates the dystrophic phenotype in *mdx* mouse muscle. *Hum. Mol. Genet.* **15**, 1423–1435 (2006).

99. Joyce, P. I., Satija, R., Chen, M. & Kuwabara, P. E. The atypical calpains: Evolutionary analyses and roles in *Caenorhabditis elegans* cellular degeneration. *PLoS Genet.* **8**, 1–16 (2012).

100. Giugia, J. B., Gieseler, K., Arpagaus, M. & Ségalat, L. Mutations in the dystrophin-like *dys-1* gene of *Caenorhabditis elegans* result in reduced acetylcholinesterase activity. *FEBS Lett.* **463**, 270–272 (1999).

101. Ségalat, L. & Anderson, J. E. Duchenne muscular dystrophy: Stalled at the junction? *Eur. J. Hum. Genet.* **13**, 4–5 (2005).

102. Belosludtsev, K. N., Dubinin, M. V, Belosludtsev, N. V & Mironova, G. D. Mitochondrial Ca^{2+} Transport: Mechanisms, Molecular Structures, and Role in Cells. *Biochem.* **84**, 593–607 (2019).

103. Giacomotto, J. *et al.* Chemical genetics unveils a key role of mitochondrial dynamics, cytochrome c release and ip3r activity in muscular dystrophy. *Hum. Mol. Genet.* **22**, 4562–4578 (2013).

104. Lee, I. *et al.* A single gene network accurately predicts phenotypic effects of gene perturbation in *Caenorhabditis elegans*. *Nat. Genet.* **40**, 181–188 (2008).

105. Nyamsuren, O., Faggionato, D., Loch, W., Schulze, E. & Baumeister, R. A mutation in CHN-1/CHIP suppresses muscle degeneration in *Caenorhabditis elegans*. *Dev. Biol.* **312**, 193–202 (2007).

106. Giacomotto, J. *et al.* Evaluation of the therapeutic potential of carbonic anhydrase inhibitors in two animal models of dystrophin deficient muscular dystrophy. *Hum. Mol. Genet.* **18**, 4089–4101 (2009).

107. Lee, A. Y. *et al.* Searching for signaling balance through the identification of genetic interactors of the Rab guanine-nucleotide dissociation inhibitor *gdi-1*. *PLoS ONE.* **5**, 1–16 (2010).

108. O'Reilly, L. P., Luke, C. J., Perlmutter, D. H., Silverman, G. A. &

Pak, S. C. *C. Elegans* in High-Throughput Drug Discovery. *Adv. Drug Deliv. Rev.* **69**–**70**, 247–253 (2013).

109. Gaud, A. *et al.* Prednisone reduces muscle degeneration in dystrophin-deficient *Caenorhabditis elegans*. *Neuromuscul. Disord.* **14**, 365–370 (2004).

110. Carre-Pierrat, M. *et al.* Blocking of striated muscle degeneration by serotonin in *C. elegans*. *J. Muscle Res. Cell Motil.* **27**, 253–258 (2006).

111. Ryu, D. *et al.* NAD+ repletion improves muscle function in muscular dystrophy and counters global PARylation. *Sci. Transl. Med.* **8**, 1–29 (2016).

112. Dubinin, M. V. *et al.* The effect of deflazacort treatment on the functioning of skeletal muscle mitochondria in Duchenne muscular dystrophy. *Int. J. Mol. Sci.* **21**, 1–18 (2020).

113. Manning, J. *et al.* Amitriptyline is efficacious in ameliorating muscle inflammation and depressive symptoms in the *mdx* mouse model of Duchenne muscular dystrophy. *Exp. Physiol.* **99**, 1370–1386 (2014).

114. Waugh, T. A. *et al.* Fluoxetine prevents dystrophic changes in a zebrafish model of Duchenne muscular dystrophy. *Hum. Mol. Genet.* **23**, 4651–4662 (2014).

115. Arora, R. C., Kuncl, R. W., Morgan, J., Cohen, L. & Meltzer, H. Y. Serotonin Uptake in Blood Platelets of Duchenne Muscular

Dystrophy Patients. *Muscle Nerve.* **10**, 359–362 (1987).

116. Murphy, D. L., Mendell, J. R. & Engel, W. K. Serotonin and Platelet Function in Duchenne Muscular Dystrophy. *Arch Neurol.* **28**, 239–242 (1973).

117. Chahbouni, M. *et al.* Melatonin treatment normalizes plasma pro-inflammatory cytokines and nitrosative/oxidative stress in patients suffering from Duchenne muscular dystrophy. *J. Pineal Res.* **48**, 282–289 (2010).

118. Chahbouni, M. *et al.* Melatonin treatment counteracts the hyperoxidative status in erythrocytes of patients suffering from Duchenne muscular dystrophy. *Clin. Biochem.* **44**, 853–858 (2011).

119. Hibaoui, Y., Reutenauer-Patte, J., Patthey-Vuadens, O., Ruegg, U. T. & Dorchies, O. M. Melatonin improves muscle function of the dystrophic *mdx* 5Cv mouse, a model for Duchenne muscular dystrophy. *J. Pineal Res.* **51**, 163–171 (2011).

120. Julie, Y. H., Ophelie, R. P., Ruegg, Patthey, V. & Dorchies, O. M. Melatonin Improves Muscle Function of the Dystrophic *mdx* Mouse, a Model for Duchenne Muscular Dystrophy. *J. Pineal Res.* **123**, 4757–4763 (2018).

121. Talsness, D. M., Belanto, J. J. & Ervasti, J. M. Disease-proportional proteasomal degradation of missense dystrophins. *PNAS.* **112**, 12414–12419 (2015).

122. Assereto, S. *et al.* Pharmacological Rescue of the Dystrophin-Glycoprotein Complex in Duchenne and Becker Skeletal Muscle Explants by Proteasome Inhibitor Treatment. *Am. J. Physiol. Cell Physiol.* **290**, 577–582 (2006).

123. Kumamoto, T., Fujimoto, S., Horinouchi, H., Ueyama, H. & Tsuda, T. Proteasome Expression in the Skeletal Muscles of Patients With Muscular Dystrophy. *Acta Neuropathol.* **100**, 595–602 (2000).

124. Bonuccelli, G. *et al.* Proteasome inhibitor (MG-132) treatment of *mdx* mice rescues the expression and membrane localization of dystrophin and dystrophin-associated proteins. *Am. J. Pathol.* **163**, 1663–1675 (2003).

125. Hollinger, K. & Selsby, J. T. The physiological response of protease inhibition in dystrophic muscle. *Acta Physiol.* **208**, 234–244 (2013).

126. Carter, N. D. *et al.* Carbonic Anhydrase III in Duchenne Muscular Dystrophy. *Clin Chim Acta.* **133**, 201–208 (1983).

127. Ohta, M. *et al.* Carbonic Anhydrase III in Serum in Muscular Dystrophy and Other Neurological Disorders: Relationship With Creatine Kinase. *Clin. Chem.* **37**, 36–39 (1991).

128. Raman, S. V *et al.* Eplerenone for early cardiomyopathy in Duchenne muscular dystrophy: results of a two-year open-label extension trial. *Orphanet J. Rare Dis.* **12**, 1–5 (2017).

129. Giacomotto, J., Ségalat, L., Carre-Pierrat, M. & Gieseler, K.

Caenorhabditis elegans as a chemical screening tool for the study of neuromuscular disorders. Manual and semi-automated methods. *Methods.* **56**, 103–113 (2012).

130. De Luca, A. *et al.* A multidisciplinary evaluation of the effectiveness of cyclosporine A in dystrophic *Mdx* mice. *Am. J. Pathol.* **166**, 477–489 (2005).

131. Kirschner, J. *et al.* Treatment of Duchenne muscular dystrophy with ciclosporin A: A randomised, double-blind, placebo-controlled multicentre trial. *Lancet Neurol.* **9**, 1053–1059 (2010).

132. Valladares, D. *et al.* IP3 receptor blockade restores autophagy and mitochondrial function in skeletal muscle fibers of dystrophic mice. *Biochim. Biophys. Acta - Mol. Basis Dis.* **1864**, 3685–3695 (2018).

133. Zhang, Y. *et al.* Hydrogen Sulfide, the Next Potent Preventive and Therapeutic Agent in Aging and Age-Associated Diseases. *Mol. Cell. Biol.* **33**, 1104–1113 (2013).

134. Yamasaki, H. & Cohen, M. F. Biological consilience of hydrogen sulfide and nitric oxide in plants: Gases of primordial earth linking plant, microbial and animal physiologies. *Nitric Oxide.* **55**–**56**, 91–100 (2016).

135. Filipovic, M. R. Persulfidation (S-sulfhydration) and H_2S. *Handb Exp Pharmacol.* **230**, 29–59 (2015).

136. Qabazard, B. *et al.* Hydrogen Sulfide Is an Endogenous Regulator of Aging in *Caenorhabditis elegans*. *Antioxid. Redox Signal.* **20**,

2621–2630 (2014).

137. Szabo, C. & Papapetropoulos, A. International Union of Basic and Clinical Pharmacology. CII: Pharmacological Modulation of H_2S Levels: H_2S Donors and H_2S Biosynthesis Inhibitors. *Pharmacol Rev.* **69**, 497–564 (2017).

138. Mathew, N. D., Schlipalius, D. I. & Ebert, P. R. Sulfurous Gases As Biological Messengers and Toxins: Comparative Genetics of Their Metabolism in Model Organisms. *J. Toxicol.* 1–14 (2011).

139. Filipovic, M. R., Zivanovic, J., Alvarez, B. & Banerjee, R. Chemical Biology of H_2S Signaling through Persulfidation. *Chem Rev.* **118**, 1253–1337 (2018).

140. Kabil, O. & Banerjee, R. Enzymology of H_2S Biogenesis, Decay and Signaling. *Antioxidants Redox Signal.* **20**, 770–782 (2014).

141. Singh, S., Padovani, D., Leslie, R. A., Chiku, T. & Banerjee, R. Relative contributions of cystathionine beta-synthase and gamma-cystathionase to H_2S biogenesis via alternative trans-sulfuration reactions. *J Biol Chem.* **284**, 22457–22466 (2009).

142. Yadav, P. K., Yamada, K., Chiku, T., Koutmos, M. & Banerjee, R. Structure and kinetic analysis of H_2S production by human mercaptopyruvate sulfurtransferase. *J Biol Chem.* **288**, 20002–20013 (2013).

143. Incecik, F., Avsioglu, G., Erel, O., Neselioglu, S. & Herguner, O. M. Dynamic thiol/disulphide homeostasis in children with Duchenne

muscular dystrophy. *Acta Neurol. Belg.* **119**, 215–218 (2019).

144. Cain, C. *et al.* Prevention and Treatment of Duchenne Cardiomyopathy with Hydrogen Sulfide-Donor Therapy. *FASEB J.* **33**, 831.5 (2019).

145. Martins-Bach, A. B., Bloise, A. C., Vainzof, M. & Rabbani, S. Metabolic profile of dystrophic *mdx* mouse muscles analyzed with in vitro magnetic resonance spectroscopy (MRS). *Magn. Reson. Imaging.* **30**, 1167–1176 (2012).

146. Panza, E. *et al.* Duchenne's muscular dystrophy involves a defective transsulfuration pathway activity. *Redox Biol.* **45**, (2021).

147. Terrill, J. R., Grounds, M. D. & Arthur, P. G. Taurine deficiency, synthesis and transport in the *mdx* mouse model for Duchenne Muscular Dystrophy. *Int J Biochem Cell Biol.* **66**, 141–148 (2015).

148. Burns, D. P. *et al.* N-Acetyl cysteine improves dystrophic (*mdx*) mouse diaphragm muscle quality and strength. *FASEB J.* **33**, 843.12 (2019).

149. Terrill, J. R., Pinniger, G. J., Graves, J. A., Grounds, M. D. & Arthur, P. G. Increasing taurine intake and taurine synthesis improves skeletal muscle function in the *mdx* mouse model for Duchenne muscular dystrophy. *J. Physiol.* **11**, 3095–3110 (2016).

150. Degl'Innocenti, D., Rosati, F., Iantomasi, T., Vincenzini, M. T. & Ramponi, G. GSH system in relation to redox state in dystrophic skin fibroblasts. *Biochimie.* **81**, 1025–1029 (1999).

151. Baron, D. *et al.* Immune response and mitochondrial metabolism are commonly deregulated in DMD and aging skeletal muscle. *PLoS ONE.* **6**, 1–11 (2011).

152. Gaffney, C. J. *et al.* Greater loss of mitochondrial function with ageing is associated with earlier onset of sarcopenia in *C. elegans. Aging.* **10**, 3382–3396 (2018).

153. Miller, D. L. & Roth, M. B. Hydrogen sulfide increases thermotolerance and lifespan in *Caenorhabditis elegans. PNAS.* **104**, 20618–20622 (2007).

154. Chen, Y.-H. *et al.* Endogenous hydrogen sulfide in patients with COPD. *Chest.* **128**, 3205–3211 (2005).

155. Qabazard, B. *et al. C. elegans* aging is modulated by hydrogen sulfide and the sulfhydrylase/cysteine synthase *cysl-2. PLoS ONE.* **8**, 1–12 (2013).

156. Lee, B. C., Kaya, A. & Gladyshev, V. N. Methionine restriction and lifespan control. *Ann N Y Acad Sci.* **1363**, 116–124 (2016).

157. Edwards, C. *et al.* Mechanisms of amino acid-mediated lifespan extension in *Caenorhabditis elegans. BMC Genet.* **16**, 1–24 (2015).

158. Henry, O. R. *et al.* Suppression of Homocysteine Levels by Vitamin B12 and Folates: Age and Gender Dependency in the Jackson Heart Study. *Am. J. Med. Sci.* **344**, 110–115 (2012).

159. Droge, W. Oxidative stress and ageing: is ageing a cysteine

deficiency syndrome? *Phil. Trans. R. Soc. B.* **360**, 2355–2372 (2005).

160. Scicchitano, B. M. & Sica, G. The Beneficial Effects of Taurine to Counteract Sarcopenia. *Curr. Protein Pept. Sci.* **19**, 673–680 (2018).

161. Sekhar, R. V *et al.* Deficient synthesis of glutathione underlies oxidative stress in aging and can be corrected by dietary cysteine and glycine supplementation. *Am. J. Clin. Nutr.* **94**, 847–853 (2011).

162. Brenner, S. The Genetics Of *Caenorhabditis elegans. Genetics.* **77**, 71–94 (1974).

163. Byerly, L., Cassada, R. C. & Russell, R. L. The life cycle of the nematode *Caenorhabditis elegans*: I. Wild-type growth and reproduction. *Dev. Biol.* **51**, 23–33 (1976).

164. Alexander, B. E. *et al.* Investigating the generation of hydrogen sulfide from the phosphonamidodithioate slow-release donor GYY4137. *Med Chem Comm.* **6**, 1649–1655 (2015).

165. Banjoko, S. O., Sridhar Mynapello, K. C., Ogunkola, I. O. & Masheyi, O. O. Methylene chloride exposure and carboxyhemoglobin levels in cabinetmakers. *Indian J Occup Env. Med.* **11**, 56–60 (2007).

166. Fagin, J., Bradley, J. & Williams, D. Carbon monoxide poisoning secondary to inhaling methylene chloride. *Br Med J.* **281**, 1461

(1980).

167. Le Trionnaire, S. *et al.* The synthesis and functional evaluation of a mitochondria-targeted hydrogen sulfide donor, (10-oxo-10-(4-(3-thioxo-3H-1,2-dithiol-5-yl)- phenoxy)decyl)triphenylphosphonium bromide (AP39). *Med Chem Comm.Comm* **5**, 728–736 (2014).

168. Lisa, T., Donald, L. C. & Andrew, F. Ingestion of bacterially expressed dsRNAs can produce specific and potent genetic interference in *Caenorhabditis elegans*. *Gene.* **263**, 103–112 (2001).

169. Gaffney, C. J., Bass, J. J., Barratt, T. F. & Szewczyk, N. J. Methods to Assess Subcellular Compartments of Muscle in *C. elegans*. *J. Vis. Exp.* 1–12 (2014).

170. Restif, C. *et al.* CeleST: Computer Vision Software for Quantitative Analysis of *C. elegans* Swim Behavior Reveals Novel Features of Locomotion. *PLoS Comput. Biol.* **10**, 1–12 (2014).

171. Rahman, M. *et al.* NemaFlex: A microfluidics-based technology for standardized measurement of muscular strength of *C. elegans*. *Lab chip.* **18**, 2187–2201 (2018).

172. Rahman, M. *et al.* NemaLife chip: a micropillar-based microfluidic culture device optimized for aging studies in crawling *C. elegans*. *Sci. Rep.* **10**, 1–19 (2020).

173. Bradford, M. M. A rapid and sensitive method for the quantitation of microgram quantities of protein utilizing the principle of protein-

dye binding. *Anal. Biochem.* **7**, 248–254 (1976).

174. Ng, L. T. *et al.* Lifespan and healthspan benefits of exogenous H_2S in *C. elegans* are independent from effects downstream of *eat-2* mutation. *Aging Mech. Dis.* **6**, 1–14 (2020).

175. Rio, D. C., Ares Jr, M., Hannon, G. J. & Nilsen, T. W. Purification of RNA Using TRIzol (TRI Reagent). *Cold Spring Harb. Protoc.* (2010).

176. Rumeur, E. Le. Dystrophin and the two related genetic diseases, Duchenne and Becker muscular dystrophies. *Bosn. J. Basic Med. Sci.* **15**, 14–20 (2015).

177. Timpani, C. A., Hayes, A. & Rybalka, E. Revisiting the dystrophin-ATP connection: How half a century of research still implicates mitochondrial dysfunction in Duchenne Muscular Dystrophy aetiology. *Med. Hypotheses.* **85**, 1021–1033 (2015).

178. Ibáñez-Ventoso, C., Herrera, C., Chen, E., Motto, D. & Driscoll, M. Automated Analysis of *C. elegans* Swim Behavior Using CeleST Software. *J. Vis. Exp.* 1–9 (2016) doi:10.3791/54359.

179. Etheridge, T. *et al.* The integrin-adhesome is required to maintain muscle structure, mitochondrial ATP production, and movement forces in *Caenorhabditis elegans*. *FASEB J.* **29**, 1235–1246 (2015).

180. Thomas, S. S. *et al.* Classification of the Gait Patterns of Boys With Duchenne Muscular Dystrophy and Their Relationship to Function.

J. Child Neurol. **25**, 1103–1109 (2013).

181. D'Angelo, M. G. *et al.* Gait pattern in Duchenne muscular dystrophy. *Gait Posture.* **29**, 36–41 (2009).

182. Etheridge, T. *et al.* Mitochondria-targeting hydrogen sulfide donors prolong healthspan: lifespan ratio in *Caenorhabditis elegans. Free Radic. Biol. Med.* **112**, 51 (2017).

183. Imbert, N., Cognard, C., Duport, G., Guillou, C. & Raymond, G. Abnormal calcium homeostasis in Duchenne muscular dystrophy myotubes contracting in vitro. *Cell Calcium.* **18**, 177–186 (1995).

184. Lockery, S. R. *et al.* A microfluidic device for whole-animal drug screening using electrophysiological measures in the nematode *C. elegans. Lab chip.* **12**, 2211–2220 (2012).

185. Cordova, G., Negroni, E., Cabello-Verrugio, C., Mouly, V. & Trollet, C. Combined therapies for Duchenne muscular dystrophy to optimize treatment efficacy. *Front. Genet.* **9**, 1–8 (2018).

186. Ciafaloni, E. *et al.* Age at onset of first signs or symptoms predicts age at loss of ambulation in Duchenne and Becker Muscular Dystrophy: Data from the MD STAR net. *J. Pediatr. Rehabil. Med.* **9**, 5–11 (2016).

187. Dillin, A., Crawford, D. K. & Kenyon, C. Timing Requirements for Insulin/IGF-1 Signaling in *C. elegans. Science.* **298**, 830–834 (2002).

188. Kimura, H., Shibuya, N. & Kimura, Y. Hydrogen Sulfide Is a

Signaling Molecule and a Cytoprotectant. *Antioxid. Redox Signal.* **17**, 45–57 (2012).

189. Contreras, L., Drago, I., Zampese, E. & Pozzan, T. Mitochondria : The calcium connection. *BBA - Bioenerg.* **1797**, 607–618 (2010).

190. Frederick, D. W. *et al.* Complementary NAD+ replacement strategies fail to functionally protect dystrophin-deficient muscle. *Skelet. Muscle.* **10**, 1–14 (2020).

191. Sanner, B. M., Meder, U., Zidek, W. & Tepel, M. Effects of glucocorticoids on generation of reactive oxygen species in platelets. *Steroids.* **67**, 715–719 (2002).

192. Fedotcheva, T. A. *et al.* Effect of steroid hormones on production of reactive oxygen species in mitochondria. *Biofizika.* **57**, 1014–1019 (2012).

193. Gero, D. *et al.* The novel mitochondria-targeted hydrogen sulfide (H2S) donors AP123 and AP39 protect against hyperglycemic injury inmicrovascular endothelial cells in vitro. *Pharmacol. Res.* **113**, 186–198 (2016).

194. Oh, S. W. *et al.* JNK regulates lifespan in *Caenorhabiditis elegans* by modulating nuclear translocation of forkhead transcription factor/DAF-16. *PNAS.* **102**, 4494–4499 (2005).

195. Blackwell, T. K., Steinbaugh, M. J., Hourihan, J. M., Ewald, C. Y. & Isik, M. SKN-1/Nrf, stress responses, and aging in *Caenorhabditis elegans*. *Free Radic. Biol. Med.* **88**, 290–301

(2015).

196. Sun, X., Chen, W. D. & Wang, Y. D. DAF-16/FOXO transcription factor in aging and longevity. *Front. Pharmacol.* **8**, 1–8 (2017).

197. Rafacho, A., Ortsäter, H., Nadal, A. & Quesada, I. Glucocorticoid treatment and endocrine pancreas function: Implications for glucose homeostasis, insulin resistance and diabetes. *J. Endocrinol.* **223**, R49–R62 (2014).

198. Tamez-Pérez, H. E. Steroid hyperglycemia: Prevalence, early detection and therapeutic recommendations: A narrative review. *World J. Diabetes.* **6**, 1073 (2015).

199. Bamps, S., Wirtz, J., Savory, F. R., Lake, D. & Hope, I. A. The *Caenorhabditis elegans* sirtuin gene, *sir-2.1*, is widely expressed and induced upon caloric restriction. *Mech. Ageing Dev.* **130**, 762–770 (2009).

200. Polhemus, D. J. *et al.* A Novel Hydrogen Sulfide Prodrug, SG1002, Promotes Hydrogen Sulfide and Nitric Oxide Bioavailability in Heart Failure Patients. *Cardiovasc. Ther.* **33**, 216–226 (2015).

201. Wallace, J. L. *et al.* A proof-of-concept, Phase 2 clinical trial of the gastrointestinal safety of a hydrogen sulfide-releasing anti-inflammatory drug. *Br. J. Pharmacol.* **177**, 769–777 (2020).

202. Wang, P., Zhang, G., Wondimu, T., Ross, B. & Wang, R. Hydrogen sulfide and asthma. *Exp. Physiol.* **96**, 847–852 (2011).

203. Fu, M. *et al.* Hydrogen sulfide (H_2S) metabolism in mitochondria

and its regulatory role in energy production. *PNAS.* **109**, 2943–2948 (2012).

204. Markaki, M. & Tavernarakis, N. Modeling human diseases in *Caenorhabditis elegans. Biotechnol J.* **5**, 1261–1276 (2010).

205. Szczesny, B. *et al.* AP39 [10-oxo-10-(4-(3-thioxo-3H-1,2-dithiol-5yl)phenoxy)decyl) triphenylphosphonium bromide], a mitochondrially targeted hydrogen sulfide donor, stimulates cellular bioenergetics, exerts cytoprotective effects and protects against the loss of mitochondria. *Nitric Oxide.* **41**, 120–130 (2014).

206. Petrillo, S. *et al.* Oxidative stress in Duchenne muscular dystrophy : focus on the NRF2 redox pathway. *Hum. Mol. Genet.* **26**, 2781–2790 (2017).

207. Wibom, R., Hagenfeldt, L. & Von Döbeln, U. Measurement of ATP production and respiratory chain enzyme activities in mitochondria isolated from small muscle biopsy samples. *Anal. Biochem.* **311**, 139–151 (2002).

208. Hueston, J. L. & Suprenant, K. A. Loss of dystrophin and the microtubule-binding protein ELP-1 causes progressive paralysis and death of adult *C. elegans. Dev. Dyn.* **238**, 1878–1886 (2008).

209. Dai, L. *et al.* Hydrogen sulfide inhibited L-type calcium channels (CaV1.2) via up-regulation of the channel sulfhydration in vascular smooth muscle cells. *Eur. J. Physiol.* **858**, 1–10 (2019).

210. Munaron, L., Avanzato, D., Moccia, F. & Mancardi, D. Hydrogen

sulfide as a regulator of calcium channels. *Cell Calcium.* **53**, 77–84 (2013).

211. Russell, J. C. *et al.* Electrophysiological Measures of Aging Pharynx Function in *C. elegans* Reveal Enhanced Organ Functionality in Older , Long-lived Mutants. *J Gerontol A Biol Sci Med Sci.* **74**, 1173–1179 (2019).

212. Szabo, C. *et al.* Regulation of mitochondrial bioenergetic function by hydrogen sulfide. Part I. Biochemical and physiological mechanisms. *Br. J. Pharmacol.* **171**, 2099–2122 (2014).

213. Smith, R. A., Hartley, R. C. & P, M. M. Mitochondria-targeted small molecule therapeutics and probes. *Antioxid. Redox Signal.* **15**, 3021–3038 (2011).

214. Zhu, C. *et al.* Supplementing preservation solution with mitochondria - targeted H_2S donor AP39 protects cardiac grafts from prolonged cold ischemia – reperfusion injury in heart transplantation. *Am. J. Transplant.* **19**, 3139–3148 (2019).

215. Juriasingani, S., Akbari, M., Yh, J., Whiteman, M. & Sener, A. H_2S supplementation : A novel method for successful organ preservation at subnormothermic temperatures. *Nitric Oxide.* **81**, 57–66 (2018).

216. Lobb, I. *et al.* Hydrogen Sulfide Protects Renal Grafts Against Prolonged Cold Ischemia – Reperfusion Injury via Specific Mitochondrial Actions. *Am. J. Transplant.* **17**, 341–352 (2017).

217. Ikeda, K. *et al.* Mitochondria-targeted hydrogen sulfide donor AP39 improves neurological outcomes after cardiac arrest in mice. *Nitric Oxide.* **49**, 90–96 (2018).

218. Latorre, E., Torregrossa, R., Wood, M. E., Whiteman, M. & Harries, L. W. Mitochondria-targeted hydrogen sulfide attenuates endothelial senescence by selective induction of splicing factors HNRNPD and SRSF2. *Aging.* **10**, 1666–1681 (2018).

219. Karwi, Q. G. *et al.* AP39 , a mitochondria-targeting hydrogen sulfide (H_2S) donor , protects against myocardial reperfusion injury independently of salvage kinase signalling. *Br. J. Pharmacol.* **174**, 287–301 (2017).

220. Mendell, J. R. *et al.* Randomized, double-blind six-month trial of prednisone in Duchenne's muscular dystrophy. *N. Engl. J. Med.* **320**, 1592–1597 (1989).

221. Suzuki, K. *et al.* Hydrogen sulfide replacement therapy protects the vascular endothelium in hyperglycemia by preserving mitochondrial function. *PNAS.* **108**, 13829–13834 (2011).

222. Zorova, L. D. *et al.* Mitochondrial Membrane Potential. *Anal. Biochem.* **552**, 50–59 (2018).

223. Rybalka, E., Timpani, C. A. & Cooke, M. B. Defects in Mitochondrial ATP Synthesis in Dystrophin-Deficient *Mdx* Skeletal Muscles May Be Caused by Complex I Insufficiency. *PLoS ONE.* 1–16 (2014).

224. Larsen, S. *et al.* Biomarkers of mitochondrial content in skeletal muscle of healthy young human subjects. *J. Physiol.* **14**, 3349–3360 (2012).

225. Short, K. R. *et al.* Decline in skeletal muscle mitochondrial function with aging in humans. *PNAS.* **102**, 5618–5623 (2005).

226. Zhao, R.-Z., Jiang, S., Zhang, L. & Yu, Z.-B. Mitochondrial electron transport chain, ROS generation and uncoupling. *Int. J. Mol. Med.* **44**, 3–15 (2019).

227. Grounds, M. D. *et al.* Biomarkers for Duchenne muscular dystrophy: myonecrosis, inflammation and oxidative stress. *Dis. Model. Mech.* **13**, (2020).

228. Carballal, S. *et al.* Reactivity of hydrogen sulfide with peroxynitrite and other oxidants of biological interest. *Free Radic. Biol. Med.* **50**, 196–205 (2011).

229. Tang, G., Wu, L. & Wang, R. Interaction of hydrogen sulfide with ion channels. *Clin Exp Pharmacol Physiol.* **37**, 753–763 (2010).

230. Bass, J. J. *et al.* An overview of technical considerations for Western blotting applications to physiological research. *Scand. J. Med. Sci. Sport.* **27**, 4–25 (2016).

231. Echevarría, L., Aupy, P. & Goyenvalle, A. Exon-skipping advances for Duchenne muscular dystrophy. *Hum. Mol. Genet.* **27**, R163–R172 (2018).

232. U.S. National Library of Medicine. Study of SRP-4045 and SRP-

4053 in DMD Patients (ESSENCE). (2019).

233. Nippon Shinyaku Co. LTD. Marketing authorization in Japan of VILTEPSO intravenous infusion 250 mg for the treatment of Duchenne muscular dystrophy. (2020).

234. Cao, X. *et al.* A Review of Hydrogen Sulfide Synthesis, Metabolism, and Measurement: Is Modulation of Hydrogen Sulfide a Novel Therapeutic for Cancer? *Antioxid. Redox Signal.* **31**, (2019).

235. Stipanuk, M. H. Sulfur amino acid metabolism: pathways for production and removal of homocysteine and cysteine. *Annu. Rev. Nutr.* **24**, 538–577 (2004).

236. Sbodio, J. I., Snyder, S. H. & Paul, B. D. Regulators of the transsulfuration pathway. *Br. J. Pharmacol.* **176**, 583–593 (2018).

237. Reboul, J. *et al. C. elegans* ORFeome version 1.1: Experimental verification of the genome annotation and resource for proteomescale protein expression. *Nat. Genet.* **34**, 35–41 (2003).

238. Perridon, B. W., Leuvenink, H. G. D., Hillebrands, J.-L., van Goor, H. & Bos, E. M. The role of hydrogen sulfide in aging and age-related pathologies. *Aging (Albany. NY).* **8**, 2264–2289 (2016).

239. Veeranki, S., Gandhapudi, S. K. & Tyagi, S. C. Interactions of hyperhomocysteinemia and T cell immunity in causation of hypertension. *Can J Physiol Pharmacol.* **95**, 239–246 (2017).

240. Levine, R. L., Mosoni, L., Berlett, B. S. & Stadtman, E. R.

Methionine residues as endogenous antioxidants in proteins. *PNAS.* **93**, 15036–15040 (1996).

241. Brosnan, J. T. & Brosnan, M. E. The Sulfur-Containing Amino Acids: An Overview. *Am. Soc. Nutr.* **136**, 1636S-1640S (2006).

242. Townsend, D. M., Tew, K. D. & Tapiero, H. Sulfur containing amino acids and human disease. *Biomed Pharmacother.* **58**, 47–55 (2004).

243. Terrill, J. R., Webb, S. M., Arthur, P. G. & Hackett, M. J. Investigation of the effect of taurine supplementation on muscle taurine content in the *mdx* mouse model of Duchenne muscular dystrophy using chemically specific synchrotron imaging. *Analyst.* **145**, 7242–7251 (2020).

244. Tripodi, F. *et al.* Methionine supplementation stimulates mitochondrial respiration. *Biochim. Biophys. Acta - Mol. Cell Res.* **1865**, 1901–1913 (2018).

245. Del Vesco, A. P. *et al.* Effect of methionine supplementation on mitochondrial genes expression in the breast muscle and liver of broilers. *Livest. Sci.* **151**, 284–291 (2013).

246. Bartsakoulia, M. *et al.* Cysteine Supplementation May be Beneficial in a Subgroup of Mitochondrial Translation Deficiencies. *J. Neuromuscul. Dis.* **3**, 363–379 (2016).

247. Hargreaves, I. P., Sheena, Y., Land, J. M. & Heales, S. J. R. Glutathione deficiency in patients with mitochondrial disease:

Implications for pathogenesis and treatment. *J. Inherit. Metab. Dis.* **28**, 81–88 (2005).

248. Ommati, M. M., Farshad, O., Jamshidzadeh, A. & Heidari, R. Taurine enhances skeletal muscle mitochondrial function in a rat model of resistance training. *PharmaNutrition.* **9**, 100161 (2019).

249. Burr, A. R. & Molkentin, J. D. Genetic evidence in the mouse solidifies the calcium hypothesis of myofiber death in muscular dystrophy. *Cell Death Differ.* **22**, 1402–1412 (2015).

250. Sinha-Hikim, I. *et al.* Long-term supplementation with a cystine-based antioxidant delays loss of muscle mass in aging. *Journals Gerontol. - Ser. A Biol. Sci. Med. Sci.* **68**, 749–759 (2013).

251. Wongjaikam, S., Kumfu, S., Khamseekaew, J., Chattipakorn, S. C. & Chattipakorn, N. Restoring the impaired cardiac calcium homeostasis and cardiac function in iron overload rats by the combined deferiprone and N-acetyl cysteine. *Sci. Rep.* **7**, 1–12 (2017).

252. Foos, T. M. & Wu, J. The role of taurine in the central nervous system and the modulation of intracellular calcium homeostasis. *Neurochem. Res.* **27**, 21–26 (2002).

253. Mensch, A. & Zierz, S. Cellular Stress in the Pathogenesis of Muscular Disorders—From Cause to Consequence. *Int. J. Mol. Sci.* **21**, 1–28 (2020).

254. Wolf, M., Nunes, F., Henkel, A., Heinick, A. & Paul, R. J. The MAP

kinase JNK-1 of *Caenorhabditis elegans*: Location, activation, and influences over temperature-dependent insulin-like signaling, stress responses, and fitness. *J. Cell. Physiol.* **214**, 721–729 (2007).

255. Chang, H. C. & Guarente, L. SIRT1 and other sirtuins in metabolism. *Trends Endocrinol. Metab.* **25**, 138–145 (2014).

256. Beckers, P. *et al.* Newborn screening of Duchenne muscular dystrophy specifically targeting deletions amenable to exon-skipping therapy. *Sci. Rep.* **11**, 1–9 (2021).

257. Gero, D. *et al.* The novel mitochondria-targeted hydrogen sulfide (H$_2$S) donors AP123 and AP39 protect against hyperglycemic injury in microvascular endothelial cells in vitro. *Pharmacol. Res.* **113**, 186–198 (2016).